RICE UNIVERSITY

Optimization of GN&C Performance Requirements for Cislunar Applications

by

Damon O. Kirkpatrick

A Thesis Submitted
in Partial Fulfillment of the
Requirements for the Degree
Master of Science

Approved, Thesis Committee:

Pol D. Spanos, Chair
L. B. Ryon Professor of Mechanical Engineering

Fathi H. Ghorbel
Professor of Mechanical Engineering

Pedram Hassanzadeh
Assistant Professor of Mechanical Engineering

David C. Woffinden
GN&C Autonomous Flight Systems,
NASA Johnson Space Center

Stephen R. Steffes
Senior Member of the Technical Staff,
Charles Stark Draper Laboratory

Houston, Texas
April, 2018

ABSTRACT

Optimization of GN&C Performance Requirements for Cislunar Applications

by

Damon O. Kirkpatrick

For cislunar applications, the performance requirements for a guidance, navigation, and control (GN&C) system can be derived optimally using a systematic approach. GN&C space systems continue to increase in complexity and support a variety of demanding mission objectives. The multifaceted interactions inherent in a GN&C system make deriving performance requirements a challenging and laborious task. For decades allocating these GN&C specific requirements has been a time-consuming, ad hoc, and iterative process that relies on engineering heuristics, flight experience, and judgment. This thesis demonstrates an alternate approach that determines GN&C performance requirements in a systematic, optimal, and consistent manner. The versatility of this approach is demonstrated by calculating the GN&C performance requirements for two cislunar trajectories given multiple mission requirements and performance constraints, different optimization criteria, and varying phases in the design process.

Acknowledgments

First and foremost, I must thank my God and my family for this opportunity and supporting me through it. I give special thanks to my father, Doug Kirkpatrick, who always offered an ear to listen to what was going on with my graduate work, has inspired me to get as much education as possible, and has offered his technical expertise and advice throughout my research. I am indebted to two classmates in particular, Troy Dennis and Clay Higginson, who were always optimistic and gave me invaluable help in my graduate education. I really could not have gotten to this point without my advisor Dave Woffinden who was always, always ready to help, teach, and offer guidance. I would also like to thank my advisors Stephen Steffes and Dr. Pol Spanos for their continued support and having my back. I would not be where I am today without the support of these people and many more not mentioned here, whom I will not soon forget.

Contents

Abstract iii

List of Illustrations ix

List of Tables xi

1 Introduction 1

1.1 Background 3

1.1.1 Top-Level Mission Requirements 3

1.1.2 GN&C System Requirements 5

1.1.3 GN&C System Requirement Generation 5

1.1.4 Navigation Sensor Suite Selection 7

1.1.5 Navigation Sensor Selection 8

1.2 Thesis Outline 11

2 GN&C Performance Modeling 12

2.1 GN&C System Modeling 13

2.1.1 Guidance/Targeting 13

2.1.2 Control 15

2.1.3 Navigation 15

2.2 GN&C Performance Metrics 16

2.3 GN&C Requirements Modeling 19

2.3.1 Navigation Requirements 20

2.3.2 Initial Trajectory Dispersion Requirements 20

2.3.3 System Process Noise Requirements 20

2.3.4 Maneuver Execution Error Requirements 21

2.4 Navigation Performance Modeling 22
2.4.1 Initializing 22
2.4.2 Propagating 23
2.4.3 Updating 25
2.4.4 Correcting 27
2.4.5 Overview 28

3 Optimal GN&C Requirement Generation 30

3.1 Performance Requirement Representation 30
3.2 Scaling GN&C Performance Metrics 32
3.2.1 Sensitivity Analysis Scaling 32
3.2.2 Single Scaling Factor Derivation 34
3.3 Optimizing GN&C Performance Metrics 39
3.3.1 Lower and Upper Bounds 39
3.3.2 Optimal Weights Generation 40

4 Optimal Cislunar GN&C Requirement 48

4.1 Cisunar Trajectories 48
4.1.1 Lunar Outbound Trajectory 48
4.1.2 Lunar Return Trajectory 49
4.2 Cislunar Mission Performance Requirements 50
4.2.1 B-Plane Requirements 50
4.2.2 Entry Interface Requirements 51
4.2.3 $|\Delta \mathbf{V}|$ Dispersion 54
4.3 Cislunar Analysis Assumptions 54
4.4 Lunar Outbound Scenario 56
4.4.1 Lunar Outbound - Baseline 59
4.4.2 Lunar Outbound - Survivability Altered 63
4.4.3 Lunar Outbound - Flight Readiness Altered 65

4.4.4 Lunar Outbound - Cost Function Altered 68

4.4.5 Lunar Outbound - Summary 71

4.5 Lunar Return Scenario 73

4.5.1 Lunar Return - Baseline 77

4.5.2 Lunar Return - Survivability Altered 79

4.5.3 Lunar Return - Flight Readiness Altered 81

4.5.4 Lunar Return - Cost Function Altered 83

4.5.5 Lunar Return - Summary 85

5 Concluding Remarks 87

5.1 Overview 87

5.2 Potential for Future Work 87

5.3 Additional Cases Run for Reference 89

5.3.1 Lunar Outbound Scenario 89

5.3.2 Lunar Return Scenario 97

Bibliography 105

Illustrations

1.1 **Systems Engineering Process**[1] 4

2.1 **Closed-loop GN&C System Diagram**[24] 14
2.2 **Defining Navigation Uncertainty**[2] 16

3.1 **Performance Ellipse Scaling to Meet Mission Requirements**[29] 36

4.1 **EM1 Trajectory**[29] 49
4.2 **B-Plane Visualization** 50
4.3 **LVLH Coordinate System** 52
4.4 **Downtrack versus Crosstrack Position Relative in Space**[17] . . 53
4.5 **Outbound Maneuvers** 56
4.6 **Lunar B-Plane** 58
4.7 **Outbound Sensitivity Analysis Results** 59
4.8 **Outbound Trajectory - Baseline** 62
4.9 **Outbound Trajectory - Survivability Requirements Altered** . 64
4.10 **Outbound Trajectory - Flight Readiness Altered** 67
4.11 **Outbound Trajectory - Cost Function Altered** 70
4.12 **Return Trajectory** 73
4.13 **Return Sensitivity Analysis Results 1 of 2** 75
4.14 **Return Sensitivity Analysis Results 2 of 2** 76
4.15 **Return Trajectory - Baseline** 78

4.16 **Return Trajectory - Survivability Altered** 80

4.17 **Return Trajectory - Flight Readiness Altered** 82

4.18 **Return Trajectory - Cost Function Altered** 84

5.1 **Outbound Trajectory - Surv and FR Altered** 90

5.2 **Outbound Trajectory - Surv and CF Altered** 92

5.3 **Outbound Trajectory - FR and CF Altered** 94

5.4 **Outbound Trajectory - Surv, FR, and CF Altered** 96

5.5 **Return Trajectory - Surv and FR Altered** 98

5.6 **Return Trajectory - Surv and CF Altered** 100

5.7 **Return Trajectory - FR and CF Altered** 102

5.8 **Return Trajectory - Surv, FR, and CF Altered** 104

Tables

2.1 **Summary of Implementing Stochastic Navigation within a LinCov Analysis** 28

4.1 **B-Plane Top-Level Mission Requirements** 57

4.2 **Baseline GN&C Subsystem Requirements - Outbound** 60

4.3 **Surv Altered GN&C Subsystem Requirements - Outbound** . 63

4.4 **FR Altered GN&C Subsystem Requirements - Outbound** . . 66

4.5 **CF Altered GN&C Subsystem Requirements - Outbound** . . 69

4.6 **Outbound Trajectory Summary Table 1 of 2** 71

4.7 **Outbound Trajectory Summary Table 2 of 2** 72

4.8 **EI Top-Level Mission Requirements** 74

4.9 **Correlation Coefficients for Performance Constraints** 74

4.10 **Baseline GN&C Subsystem Requirements - Return** 77

4.11 **Survivability Altered GN&C Subsystem Requirements - Return** 79

4.12 **Flight Readiness Altered GN&C Subsystem Requirements - Return** 81

4.13 **Cost Function Altered GN&C Subsystem Requirements - Return** 83

4.14 **Return Trajectory Summary Table 1 of 2** 85

4.15 **Return Trajectory Summary Table 2 of 2** 86

5.1 **Surv and FR Altered GN&C Subsystem Requirements - Outbound** 89
5.2 **Surv and CF Altered GN&C Subsystem Requirements - Outbound** 91
5.3 **FR and CF Altered GN&C Subsystem Requirements - Outbound** 93
5.4 **Surv, FR, and CF Altered GN&C Subsystem Requirements - Outbound** 95
5.5 **Surv and FR Altered GN&C Subsystem Requirements - Return** 97
5.6 **Surv and CF Altered GN&C Subsystem Requirements - Return** 99
5.7 **FR and CF Altered GN&C Subsystem Requirements - Return** 101
5.8 **Surv, FR, and CF Altered GN&C Subsystem Requirements - Return** 103

Chapter 1

Introduction

This thesis applies a novel and systematic approach for deriving optimal guidance, navigation, and control (GN&C) subsystem performance requirements for both a lunar outbound and a lunar return flight segment. The primary objective is to establish the versatility of this new requirement generation process for a cislunar application. More specifically, this research shows that the same approach for deriving optimal performance requirements can be applied 1) to different flight phases, 2) with multiple top-level requirements and multiple performance constraints, 3) using different optimization criteria, and 4) throughout the entire design process from concept generation to flight.

The capabilities that a GN&C system provide are of increasing interest in modern vehicles. Whether on the land, on the sea, or in the air, vehicles typically require and rely upon a GN&C system to fully function. Currently there exists a growing effort to make vehicles capable of navigating autonomously. This is particularly true with regards to space travel and deep space exploration. As missions continue to expand in scope and capability, both the spacecraft GN&C system and autonomous navigation will play a critical role in their success.

The complexity of a GN&C system makes the process of defining navigation and other GN&C subsystem performance requirements rather challenging and abstract. Each mission has top-level requirements to help ensure mission success, but breaking down top-level mission requirements into system performance requirements is not straightforward. Larson et al. observe that "[t]his translation [from customer expectations to technical system requirements] is often the weakest link in the implementation of systems engineering principles."[1] Although the heritage of the space program has laid a foundation for allocating navigation and GN&C subsystem performance requirements, this process is usually customized for each mission and typically relies on engineering judgment, empirical data, and experience gleaned from past missions.

While programs often resort to using "engineering heuristics, intuition, experience, and rough calculations"[2] to initially derive GN&C subsystem requirements, recently more methodological approaches are being formulated that use Monte Carlo methods and linear covariance (LinCov) analysis. This research expands upon these emerging techniques and outlines a novel approach to systematically and optimally derive navigation and other GN&C performance requirements. These concepts are demonstrated by deriving these requirements for the first exploration mission of the National Aeronautics and Space Administration's (NASA's) Orion Crew Exploration Vehicle (CEV) and highlights the potential to use these techniques from the preliminary design phase through day-of-flight mission planning.

It is important to understand where allocating the GN&C performance requirements takes place in the process of creating and executing a mission. With this understanding, a deeper appreciation of the essential role they play is gained, and the shareholder's desire for optimizing them becomes apparent. Ultimately, a program is interested in purchasing sensors for a GN&C system that will perform sufficiently so that the vehicle meets mission requirements. In general, there are two approaches for choosing a set of sensors that will yield the desired system performance. One method uses the derived performance requirements. First, customers define mission requirements and objectives. Second, engineers determine and allocate performance requirements. Third, system designers use the performance requirements to choose an appropriate collection of sensors that provides the desired performance. An alternative, bottom-up approach to ensure a GN&C system can meet mission requirements uses simulations to analyze the performance of different sensor suite configurations. Their performance is directly compared to top-level mission requirements to ensure mission requirements can be met. The remainder of this chapter details each approach.

1.1 Background

Deep space exploration encompasses a breadth of mission scenarios such as interstellar, interplanetary, rendezvous, asteroid, descent and landing, as well as cislunar missions. Defining GN&C subsystem performance requirements, especially navigation requirements, becomes an essential component to adequately support these discovery missions. Deriving these lower-level requirements also plays a key role in the systems engineering process following the initial conceptual formulation of a mission.[3] The process for deriving these performance constraints depends on the mission, the established practices of a particular organization, the experience of the engineers, or the available pertinent information and resources from heritage flights. The goal of this thesis is to demonstrate that a consistent, well-defined method to derive GN&C subsystem performance requirements is available for a variety of general applications, and in particular deep space exploration.

1.1.1 Top-Level Mission Requirements

Before deriving performance requirements, customers and shareholders must define the top-level mission requirements. In NASA's Systems Engineering Handbook, this is the first step in the process of planning a mission and is depicted in Fig 1.1.

In the systems engineering process, these requirements are usually well-defined, quantitatively.[4] Top-level requirements answer the question: What does success look like for this mission? In the context of GN&C space travel, mission requirements are as diverse as the missions themselves. Generally, they describe critical flight phases where the position, velocity, attitude, and other performance parameters of the spacecraft will largely determine the successful completion of the mission.

In conjunction with requirements, constraints limit the realm of possible outcomes

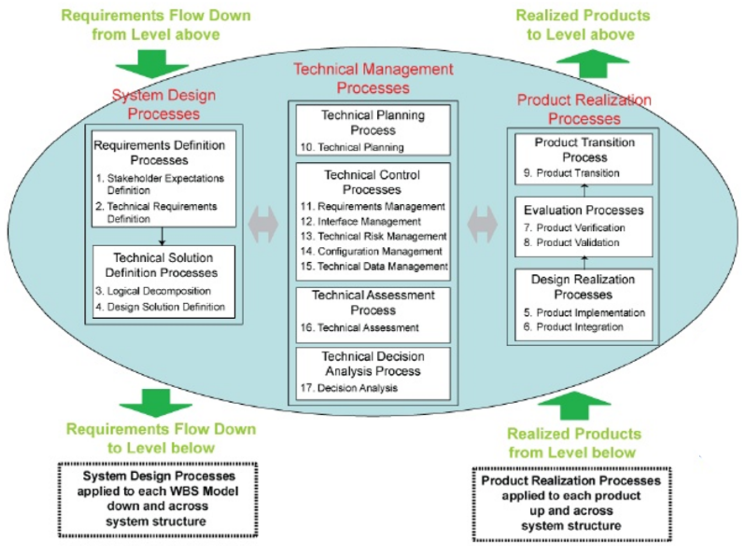

Figure 1.1 : Systems Engineering Process[1]

for mission planning. Constraints typically fit in the categories of cost, schedule, and performance.[3] Each program has an allocated budget with limitations in time for planning, preparing, and executing the mission, and must operate within the scope of current technology and other resources at the program's disposal. A program also encounters political, economic, and physical constraints.[3]

For many space applications, failure to accomplish top-level mission requirements leads to significant and sometimes catastrophic losses personally, financially, and politically. The space systems often cost several million dollars to build, launch, and operate in addition to the time and manpower invested in the development, construction, and execution of these systems. Mission requirements provide boundaries to ensure mission success by constraining deviations so that the spacecraft adequately follows the desired trajectory profile or does not exceed its structural limitations. While losing a vehicle is devastating to a program because of its great financial cost, a space system with people onboard cannot be assigned a price. For this reason, mission requirements play a vital role and receive significant attention. Therefore, the next question shareholders and engineers ask is: How can the system design ensure that the planned trajectory will meet and not violate top-level requirements?

1.1.2 GN&C System Requirements

Defining GN&C system performance requirements helps the system meet mission requirements. This is the second step in the systems engineering process according to Fig 1.1. Generally, engineers allocate navigation and other GN&C subsystem performance requirements in space mission planning. The process for breaking down customers' needs, goals, and objectives into executable technical requirements is often a time-consuming, iterative process, that frequently looks back at the shareholders' requirements and mission constraints.[1]

For GN&C systems, one of the main deliverables from deriving performance requirements are the navigation requirements. They describe how accurately the navigation system must perform in estimating the state of the vehicle (i.e. position, velocity, attitude, angular rate) at different flight phases or navigation regions to ultimately meet mission requirements. Engineers also derive other GN&C subsystem performance requirements to determine the requisite system performance. Should any of the vehicle states or other subsystem parameters exceed the specified requirements, the vehicle may be placed in jeopardy or the intended purpose of the mission could ultimately be frustrated. For this reason, deriving and understanding the GN&C performance requirements in context of the closed-loop system that will achieve the top-level mission requirements are essential.

1.1.3 GN&C System Requirement Generation

Historically and especially at NASA, engineers have allocated these requirements by looking at past missions and using their intuition and best judgment to translate data collected from heritage flights to the current mission. NASA's Apollo, Shuttle, and Orion missions have relied heavily on this heuristic approach for initially allocating lower-level requirements.

Heritage and Heuristics

In the 1960s, the U.S. government was determined to send Americans to the Moon and return them safely to Earth.[5] The Apollo missions were designed to accomplish this goal. Due to the novelty of human space travel, there were many unknowns in determining how to adequately accomplish what the Apollo missions had set out to do. NASA therefore designed a series of missions to test the capabilities and limitations of human space flight. The Gemini program was the precursor to the Apollo missions. According to Goodman et al., the Gemini missions "established an experience base of operational techniques and mission planning for Apollo."[6] The lessons learned from Project Gemini translated directly to Apollo mission planning and even applied to Space Shuttle missions after Apollo.[6] The experience gained from the Apollo missions were just as useful to the Shuttle program as the Gemini missions were to Apollo, as each mission improved upon the last.

Engineers have generally allocated GN&C subsystem performance requirements to specific flight profiles using basic systems engineering practices. Typical practices are outlined by Larson et al.[1] and involve modeling, simulation, prototyping, and optimization; all of which count on creativity, engineering judgment, and domain knowledge, supported by tradeoffs and analyses.

NASA is working to expand human spaceflight missions beyond the Moon in the coming decades. NASA's Orion CEV is one example of a spacecraft that will depend heavily on autonomous GN&C,[7] especially for its eventual deep space mission to Mars.[8] Though in the early stages of development and flight test, the Orion spacecraft promises to be on the cutting edge of GN&C capabilities, with its need for navigation extending outside Low Earth Orbit (LEO) and cislunar space. Keeping with common practice, the Orion program looked to the Apollo and Shuttle programs for initial mission planning, especially with regards to navigation.[7] As opposed to the more focused and relatively specialized Apollo and Shuttle missions, the Orion vehicle has to be able to perform in a variety of flight phases and missions. According to NASA engineers, these include "pre-launch, powered ascent, including aborts, automatic and piloted rendezvous and docking with multiple vehicles in lunar or low Earth orbit, trans-lunar, lunar orbit, and trans-Earth coast, and direct or skip reentry ... culminating in a parachute landing."[7] These mission phases also must account for cargo and crewed missions.[7]

Systematic Approach

The recent development of a general, systematic approach for deriving optimal navigation requirements has the potential to supplement traditional heuristic approaches for deriving and allocating these requirements during mission planning. Woffinden and Breger[2] and Mand[18] use this systematic approach in their respective works. The process involves using Monte Carlo and LinCov techniques to derive performance requirements. The method is limited to analyzing one top-level mission requirement at a time and can only derive navigation requirements. Additionally, this process relies on an iterative, bi-sectional search method to derive optimal navigation requirements.[18] These navigation requirements are subsequently used to select a set of sensors that yield the desired GN&C system performance.

1.1.4 Navigation Sensor Suite Selection

Determining the specific combination of sensors or a system's sensor suite for a given vehicle and mission has historically been an ad hoc process, relying largely on engineering judgment, even for modern day missions.[2] Space programs strive to balance the sensor performance and the corresponding cost. The sensor suite chosen for a mission must provide the requisite precision in navigation to ensure top-level mission requirements are met, however, different navigation sensor suites have different costs associated with them, both financially, in availability, risk, mass, power, and volume.

First, there is a financial cost to be considered. More precise and accurate instruments tend to be more expensive. Sensors that use new technology can also increase the cost of a program. The payload cost associated with adding mass to the spacecraft must also be considered. A heavier system requires more propellant to send it out of Earth's atmosphere and can quickly increase the cost of the mission. This consideration is so important that the Orion program decided to forgo a two fault tolerance requirement for system navigation in order to decrease the weight of the vehicle, for example.[7] Therefore, every mission must determine the optimal combination of sensors for a vehicle that will meet the requirements within cost constraints. If the mission requirements are very lenient and allow relatively large dispersions, errors, and overall uncertainty, then it may not be necessary to include certain instruments, take specific measurements, or use the most advanced equipment, often saving costs.

1.1.5 Navigation Sensor Selection

Once the GN&C system performance requirements are derived that ensure mission objectives can be met, the next step is to identify the navigation sensors that provide the required accuracy in state estimation. Although it is not a focus of this thesis, a brief discussion on sensor selection is included to provide context for trade studies to support autonomous navigation for deep space exploration.

Sensors provide both continuous and discrete measurements to a navigation filter to estimate a spacecraft's translational and rotational state. With current technology, sensors for determining the translational state for deep space exploration generally fall within one of three categories; ground based tracking, visual navigation, and inertial navigation. Derived navigation system requirements are valid regardless of what navigation method is used.

Ground Based Tracking

For deep space exploration, a common and robust method for navigation currently depends on the external infrastructure of the Deep Space Network (DSN). It has been in use for over fifty years and consists of a network of three antennas located at specific locations around the globe (Canberra, Australia; Madrid, Spain; and Goldstone, California, USA).[9] The antennas are strategically placed to receive and transmit signals, providing global coverage. The disadvantages of the DSN are that it is costly to use and is constrained in the number of missions it can support at a given time. Many space operations from minor missions like CubeSats[10] to more prominent missions use the DSN, and therefore it is in high demand for its limited capacity.

Visual Navigation

With the advent and ever increasing capabilities of cameras, computers, and sensors, visual navigation has developed from hand-held sextants like those operated by astronauts during the Apollo missions, to fully autonomous navigation with onboard cameras linked to ephemeris data. Instruments like startrackers, sun sensors, and feature tracking cameras[11] have been used for deep space navigation in the past. Despite the different designs for visual navigation instruments, the basic mathematics behind the state determination is the same. The camera captures images of the spacecraft's surroundings, and the computer identifies known constellations of stars or other celestial bodies in the image. A variety of methods and many different combinations of measurements use the camera to accurately estimate the vehicle's state. For example, measuring the angle between the lines of sight of a known, reference constellation and a second identifiable celestial body or constellation can help calculate the spacecraft's relative position, velocity, and orientation.[12] Multiple sensors and multiple measurements, such as including a measurement of the apparent angular diameter of a nearby celestial body, generally will increase the accuracy of the estimate[12]

Inertial Navigation

Inertial navigation generally uses sensors to measure the accelerations of a vehicle. This navigation method receives continuous measurement inputs from an onboard Inertial Measurement Unit (IMU) using gyros and accelerometers to measure accelerations.[14] The accelerations are integrated to derive spacecraft velocity, and the spacecraft velocity is integrated to calculate its position.[13] The orientation of the vehicle can also be determined by measuring and integrating angular accelerations.[13] Often a navigation filter is used in this process to update the vehicle state by incorporating the estimated state from knowledge of the state dynamics of the vehicle and its environment.[16] This method does not rely on external infrastructure to estimate the vehicle state.

Alternative Approach

Instead of using derived GN&C subsystem performance requirements, a common, alternative approach derives sensor suites directly from top-level mission requirements. This approach to sensor suite selection often involves trade studies. Kremer,[17] Velez,[10] Mand,[18] and D'Souza et al.[19] used this method to identify appropriate sensor suites for the missions of their respective studies. They ran simulations, modeling an exhaustive list of possible sensor combinations and reported the resultant systems' performances. A mission planner could then use that information to choose a sensor suite that yields the desired performance. This method allows the mission planner to determine if a system equipped with certain sensors can meet top-level mission requirements. The disadvantage of this trade study approach is that it is an ad hoc, iterative, and time-consuming process. Currently, there is no systematic way to optimally derive the sensor requirements or an optimal sensor suite from the mission requirements.

The systematic approach to deriving navigation and other GN&C subsystem performance requirements used in this research in effect reverses this process by providing the optimal performance requirements for the mission planner who then decides which sensor suite can perform within the requirements. An optimal sensor suite for a mission can be derived using this new approach. Additionally, this new process improves upon the current method for deriving optimal navigation requirements. It can take into consideration multiple top-level mission requirements and multiple performance constraints and optimally derive other GN&C subsystem performance requirements in addition to navigation requirements.

1.2 Thesis Outline

This research covers the details behind the methods used to derive optimal navigation and other GN&C subsystem performance requirements. The optimal performance requirements for two cislunar trajectories are presented. These GN&C subsystem performance requirements set a performance boundary for the onboard navigation system to estimate the vehicle's state at points along a defined trajectory.

Chapter 2 outlines GN&C performance and requirements modeling used for this research. It details the key processes for navigation performance modeling including a discussion on the implementation of stochastic navigation within LinCov. The details for deriving optimal GN&C lower-level technical requirements are provided in Chapter 3. A description of the selected mission profiles and the database of selected data are presented in Chapter 4 accompanied by a discussion of the results. Chapter 5 contains the conclusions and considerations for future work. Although this thesis is centered on only two cislunar cases, the applications for the method described are widespread. The pattern established in this research can be applied to a variety of missions where the vehicle incorporates a closed-loop GN&C system.

Chapter 2

GN&C Performance Modeling

To ensure that a GN&C system can meet top-level mission requirements, it is necessary to have the capability to analyze its performance. Two approaches are currently used to analyze the performance of a GN&C system. First, Monte Carlo methods are a common way to detemine the statistical performance of physical events that account for random processes. For a Monte Carlo simulation, the algorithm commonly uses a set of pseudo-random numbers sampled from a Gaussian probability density function[20] to account for the effects of random physical phenomena that are not otherwise accounted for in the mathematical models. By evaluating the performance results for hundreds or thousands of simulation runs, each perturbing the various random parameters, the statistical information, namely the mean and standard deviation can be obtained.[21] For a GN&C system, the process calculates the statistical information that characterizes its performance as it follows a reference trajectory. The drawback of Monte Carlo analysis is that it can be computationally demanding to run the required number of simulations to reduce uncertainty[22] and obtain significant statistical information. Sometimes hundreds, thousands, or even tens of thousands of runs may be necessary, depending on the application. Therefore a faster, more economic method is desirable for preliminary analysis.

A second approach for analyzing GN&C system performance uses linear covariance analysis, or LinCov. A LinCov analysis can derive similar statistical information for a system in a single run.[23] The main assumption to be made is that the system can be linearized about a known reference trajectory.[15] The user must ensure the assumption of linearization is valid for the particular application. For many space applications, this has proven to be a valid assumption.[2,11,15,18] Therefore, LinCov is used in this work to provide the statistical analysis data needed for optimizing GN&C subsystem performance requirements.

2.1 GN&C System Modeling

It is important to understand the workings of a GN&C system and how each segment of GN&C operates jointly along a planned trajectory to reach a destination. An understanding of the interactions of the guidance, navigation, and controls systems provides the needed perspective to analyze the GN&C system as a whole.

2.1.1 Guidance/Targeting

Guidance

The guidance system uses physical models of the vehicle and how it reacts in its environment and to external forces to follow a nominal trajectory. A diagram of how guidance interplays with navigation and control is provided in Fig 2.1. Knowing the vehicle's dynamics and the dynamics of environmental factors and forces, gives a clear idea of how the vehicle is to follow its trajectory. Using the estimated state from the navigation system, the guidance system computes the desired vehicle states. Often the roles played by the path planning/guidance and the controllers, shown in Fig 2.1 as separate functions, are executed together, in practice. Therefore, the guidance system often outputs actuator commands as well.

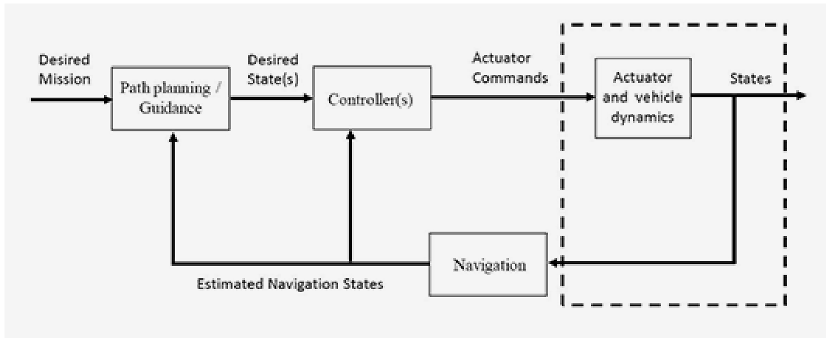

Figure 2.1 : Closed-loop GN&C System Diagram[24]

Targeting

An important, supplemental function of guidance is targeting. Marchand et al. state that targeting "refers to the numerical process of identifying feasible solutions to a problem that is subject to both path and control input constraints."[25] A vehicle's targeting algorithm typically computes the necessary instantaneous velocity change (ΔV) required to transfer a spacecraft from its current state to a desired location given a specified transfer time. There are multiple, commonly used targeting routines. The targeting algorithm utilized for this research investigating the lunar outbound and lunar return scenarios uses a technique called two-level targeting. This aptly-named method consists of two steps or levels to increase accuracy. This method optimizes the current trajectory to hit specific points or patch points.[25]

The level-I process is fairly straightforward. It involves breaking up the trajectory into segments with targeted points called patch states at the end of each segment. The algorithm then places instantaneous maneuver corrections at these patch states to ensure the continuity of the position vectors from one segment to the next.[25] The level-II process ensures the continuity of the velocity at the patch states. As the algorithm works to zero out the velocity discontinuities, the location of the patch states will change slightly, which consequently alters the shape of the trajectory.[26] The level-I process is iterative as it determines the optimal patch states. The two-level targeting algorithm as a whole is iterative. Therefore, the process returns to level-I after the level-II process is complete until an optimal solution is found.[27]

2.1.2 Control

With reference to Fig 2.1, the control system executes the actuator command from the guidance system.[3] In the context of space travel the actuators may include thrusters, momentum wheels, and control surfaces. In short, control is the system's ability to respond to correction inputs and make adjustments to maintain the nominal trajectory via actuation.

2.1.3 Navigation

As the vehicle moves along the desired path, it is necessary to determine its state. The process of estimating the vehicle's state is called navigation. Most commonly, it is estimated with the help of a navigation filter which combines estimation inputs from the process of predicting the vehicle state based on the system dynamics and simultaneously incorporating both continuous and discrete sensor measurements.[18] Navigation is key to effectually implementing guidance and adequately executing control. It closes the loop for a GN&C system (see Fig 2.1). For preliminary analysis, rather than implementing a navigation filter and modeling an assortment of potential sensors that are either unknown or not developed early in the design process, it is helpful to have another way of representing the navigation performance. Stochastic navigation provides this capability and models the effects of a navigation system on the overall performance of the GN&C system.[18] To familiarize the reader with the process of implementing stochastic navigation in a linear covariance analysis, a brief explanation is also developed.

2.2 GN&C Performance Metrics

In the same way that top speed, acceleration, and handling describe the performance of an automobile, there are parameters that measure the performance of a GN&C system. Fig 2.2 introduces key terms that describe the deviations from the nominal and navigation state; dispersions and errors. These deviations are used to calculate the GN&C performance metrics. This section formally defines the GN&C performance metrics and how they are obtained using LinCov analysis techniques. The discussion that follows is regenerated using papers written by Woffinden and Breger[2] and Mand.[18]

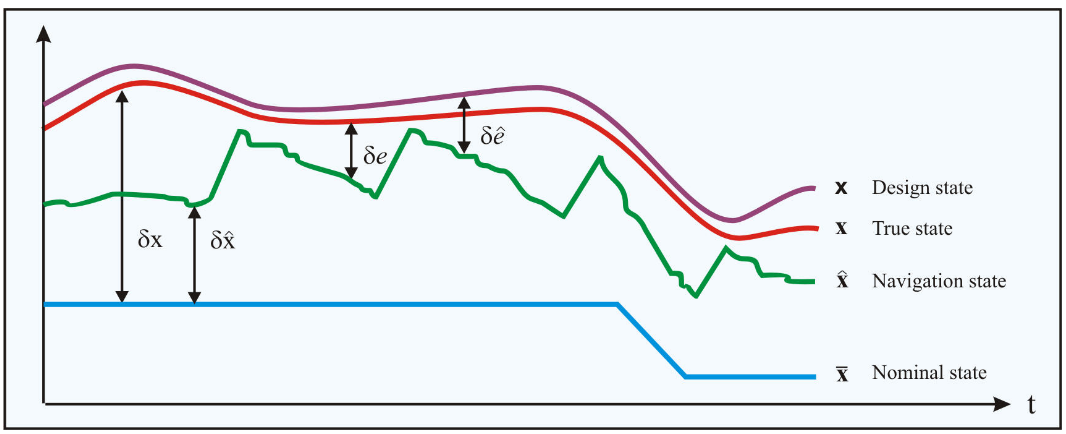

Figure 2.2 : Defining Navigation Uncertainty[2]

The environment dispersions, $\delta\mathbf{x}$, describe how much the vehicle has deviated from the desired, nominal state or trajectory. This relationship is outlined by

$$\delta\mathbf{x} \triangleq \mathbf{x} - \bar{\mathbf{x}}. \tag{2.1}$$

Note that variables related to the true state, $\mathbf{x}$, do not have any additional markings over the variable while all variables related to the nominal state, $\bar{\mathbf{x}}$, are designated as such with a horizontal bar overhead.

The environment dispersions are used to calculate the covariance matrix of the environment dispersions, $\mathbf{D}$,

$$\mathbf{D} = E[\delta\mathbf{x}\delta\mathbf{x}^T]. \tag{2.2}$$

This covariance matrix is one of the performance metrics for a GN&C system and represents how well the system follows the desired trajectory.

The difference between the navigation state and the nominal state, in Fig 2.2 constitutes the navigation dispersions, $\delta\hat{\mathbf{x}}$,described by the equation

$$\delta\hat{\mathbf{x}} \triangleq \hat{\mathbf{x}} - \mathbf{N}\bar{\mathbf{x}}. \tag{2.3}$$

The matrix, $\mathbf{N}$, is merely an $(\hat{n} \times n)$ mapping matrix that is used to allow the nominal and navigation states to be compared in the case that the number of navigation states that make up the $\hat{\mathbf{x}}$ vector does not equal the number of nominal states in the $\bar{\mathbf{x}}$ vector, $\hat{n} \neq \bar{n}$. The navigation state, $\hat{\mathbf{x}}$, is the estimated state output by the onboard navigation system, and $\bar{\mathbf{x}}$ represents where the vehicle should be if it had followed the nominal trajectory. Therefore the covariance matrix of the navigation dispersions,

$$\hat{\mathbf{D}} = E[\delta\hat{\mathbf{x}}\delta\hat{\mathbf{x}}^T], \tag{2.4}$$

reflects how well the onboard navigation system thinks it has followed the reference trajectory.

With reference to Fig 2.2, the navigation error, $\delta\mathbf{e}$, is

$$\delta\mathbf{e} \triangleq \mathbf{N}\mathbf{x} - \hat{\mathbf{x}} = \mathbf{N}\delta\mathbf{x} - \delta\hat{\mathbf{x}}. \tag{2.5}$$

The navigation system will rarely, if ever, determine the state of the spacecraft perfectly. There is therefore a difference between where the vehicle is ($\mathbf{x}$) and where the navigation system thinks it is ($\hat{\mathbf{x}}$). Eqn 2.5 also reveals that the navigation error can be and is most practically derived by taking the difference between the environment and navigation dispersions. The navigation error covariance matrix, $\mathbf{P}$, is expressed as

$$\mathbf{P} = E[\delta\mathbf{e}\delta\mathbf{e}^T] \tag{2.6}$$

and defines how well the navigation system can estimate the vehicle's true state.

The final GN&C performance metric is the onboard navigation error covariance matrix, $\hat{\mathbf{P}}$. This metric, calculated as

$$\hat{\mathbf{P}} = E[\delta\hat{\mathbf{e}}\delta\hat{\mathbf{e}}^T], \tag{2.7}$$

essentially describes how well the navigation system thinks it is following the nominal trajectory. It is re-calculated at each time step by the onboard navigation filter[18] and is derived from the onboard navigation error, defined in the equation

$$\delta\hat{\mathbf{e}} \triangleq \mathrm{x} - \hat{\mathbf{x}}, \tag{2.8}$$

where x is the design state.

The augmented state vector, $\delta\mathbf{X}$, and the augmented state covariance matrix, $\mathbf{C}$ are introduced by the equations

$$\delta\mathbf{X} = \begin{bmatrix} \delta\mathbf{x} \\ \delta\hat{\mathbf{x}} \end{bmatrix} \tag{2.9}$$

and

$$\mathbf{C} = E[\delta\mathbf{X}\delta\mathbf{X}^T]. \tag{2.10}$$

The augmented state covariance matrix is of critical importance in a LinCov analysis. This covariance matrix stores the majority of the relevant statistical information regarding the vehicle states. Three out of the four GN&C system performance metrics can be derived from the augmented state covariance matrix. Note how the environment dispersion covariance matrix, $\mathbf{D}$, the navigation dispersion covariance matrix, $\hat{\mathbf{D}}$, and the navigation error covariance matrix, $\mathbf{P}$, are related to the augmented state covariance matrix, $\mathbf{C}$, as the appropriate terms are turned on or canceled by pre- and post-multiplying the augmented state covariance matrix, $\mathbf{C}$, by coordinated zero and identity matrices,

$$\mathbf{D} = [\mathbf{I}_{n\times n}, \mathbf{0}_{n\times\hat{n}}]\mathbf{C}[\mathbf{I}_{n\times n}, \mathbf{0}_{n\times\hat{n}}]^T, \tag{2.11}$$

$$\hat{\mathbf{D}} = [\mathbf{0}_{\hat{n}\times n}, \mathbf{I}_{\hat{n}\times\hat{n}}]\mathbf{C}[\mathbf{0}_{\hat{n}\times n}, \mathbf{I}_{\hat{n}\times\hat{n}}]^T, \tag{2.12}$$

$$\mathbf{P} = [\mathbf{I}_{\hat{n}\times n}, -\mathbf{I}_{\hat{n}\times\hat{n}}]\mathbf{C}[\mathbf{I}_{\hat{n}\times n}, -\mathbf{I}_{\hat{n}\times\hat{n}}]^T. \tag{2.13}$$

This unique relationship means that only the augmented state covariance matrix and the onboard navigation error covariance matrix, $\hat{\mathbf{P}}$, are initialized, propagated, updated, and corrected. Although the LinCov tool used for this analysis only takes these two covariance matrices as inputs, the expressions for initializing, propagating, updating, and correcting the states are also included in the explanation of applying stochastic navigation within LinCov for completeness.

2.3 GN&C Requirements Modeling

In addition to modeling the performance of the GN&C system, the GN&C requirements that will be optimized are also modeled to determine their impacts on the performance of the GN&C system.[29] The GN&C subsystem performance requirements consist of navigation, initial trajectory dispersion, system process noise, and maneuver execution error requirements. The description of GN&C subsystem requirements in this section follows the same topic outlined in a paper by Woffinden et al.[29]

2.3.1 Navigation Requirements

Stochastic navigation is essential to modeling navigation requirements. The performance of the navigation system is represented by

$$\hat{\mathbf{x}} = \mathbf{N}\mathbf{x} + \delta\bar{\mathbf{e}}, \tag{2.14}$$

where the navigation state is given by the true state perturbed by the navigation error, $\delta\bar{\mathbf{e}}$.[29] The navigation error covariance matrix,

$$\mathbf{P} = E[\delta\mathbf{e}\delta\mathbf{e}^T], \tag{2.15}$$

is an important metric for GN&C systems, and is also used to derive navigation requirements. Navigation requirements describe how accurately the navigation system must perform at any given point on the trajectory to meet mission requirements.

2.3.2 Initial Trajectory Dispersion Requirements

The allowable initial trajectory dispersions, $\delta\bar{\mathbf{x}}_0$, assumed for a particular flight regime are used to define the initial state ($\mathbf{x}_0$)

$$\mathbf{x}_0 = \bar{\mathbf{x}}_0 + \delta\bar{\mathbf{x}}_0, \tag{2.16}$$

as it deviates from the initial nominal trajectory, $\bar{\mathbf{x}}_0$. The initial trajectory dispersion requirements are described by the covariance matrix

$$\mathbf{P}_{\delta\bar{x}} = E[\delta\bar{\mathbf{x}}_0\delta\bar{\mathbf{x}}_0^T]. \tag{2.17}$$

2.3.3 System Process Noise Requirements

The system process noise term accounts for magnetic field disturbances, solar radiation pressure, and gravity gradient among other unmodeled accelerations and torques.[3] It can even account for the motion of astronauts onboard the vehicle, or other random events that are not modeled otherwise. The expression for the true state as it changes over time,

$$\dot{\mathbf{x}} = \mathbf{f}(\mathbf{x}, \mathbf{u}) + \delta\bar{\boldsymbol{\eta}}, \tag{2.18}$$

uses the process noise, $\delta\bar{\boldsymbol{\eta}}$, to capture the errors that are not modeled explicitly. The process noise requirement is modeled by the covariance matrix

$$\mathbf{P}_{\delta\bar{\eta}} = E[\delta\bar{\boldsymbol{\eta}}\delta\bar{\boldsymbol{\eta}}^T]. \tag{2.19}$$

This requirement indicates to what degree the disturbance accelerations can be tolerated in the system.

2.3.4 Maneuver Execution Error Requirements

A simple model for the maneuver execution error requirements for a preliminary analysis of a GN&C system can be characterized by the covariance matrix

$$\mathbf{P}_{\delta\bar{u}} = E[\delta\bar{\mathbf{u}}\delta\bar{\mathbf{u}}^T], \tag{2.20}$$

where $\delta\bar{\mathbf{u}}$ represents the combined maneuver execution errors caused by the guidance and control algorithm and the actuators.[29] This same error is added to the commanded control input, $\hat{\mathbf{u}}$, to yield the actual control input, $\mathbf{u}$:

$$\mathbf{u} = \hat{\mathbf{u}} + \delta\bar{\mathbf{u}}. \tag{2.21}$$

These requirements essentially describe how precisely the maneuvers must be performed for the system to ultimately meet top-level mission requirements.

2.4 Navigation Performance Modeling

Stochastic navigation is a useful error model in a preliminary analysis of a GN&C system, because it simply, yet effectively models the performance of a navigation system without modeling sensors or navigation filters.[18] It is implemented within the LinCov analysis as the statistical information stored in the augmented state and onboard navigation error covariance matrices that characterizes the GN&C system performance is initialized, propagated, updated, and corrected. A full explanation and derivation of LinCov can be found in the works written by Maybeck[23] or Geller.[15]

2.4.1 Initializing

The first step in the analysis is to initialize the augmented state covariance matrix, $\mathbf{C}_0$. To do this, the initial covariance matrix of the environment dispersions, represented by

$$\mathbf{D}_0 = E[\delta\mathbf{x}_0 \delta\mathbf{x}_0^T], \tag{2.22}$$

is determined by the user, based on empirical data or engineering judgment.

The covariance matrix of the desired navigation error is also chosen by the user and is represented by the expression

$$\bar{\mathbf{P}}_0 = E[\delta\bar{\mathbf{e}}_0 \delta\bar{\mathbf{e}}_0^T], \tag{2.23}$$

with the initial navigation error defined as

$$\delta\bar{\mathbf{e}}_0 = \mathbf{N}\delta\mathbf{x}_0 - \delta\hat{\mathbf{x}}_0. \tag{2.24}$$

The initialized augmented state vector

$$\delta\mathbf{X}_0 = \begin{bmatrix} \delta\mathbf{x}_0 \\ \delta\hat{\mathbf{x}}_0 \end{bmatrix} = \begin{bmatrix} \delta\mathbf{x}_0 \\ (\mathbf{N}\delta\mathbf{x}_0 - \delta\bar{\mathbf{e}}_0) \end{bmatrix}, \tag{2.25}$$

contains the initial environment and navigation dispersions and is used to create the initialized augmented state covariance matrix, $\mathbf{C}_0$

$$\mathbf{C}_0 = \begin{bmatrix} E[\delta\mathbf{x}_0\delta\mathbf{x}_0^T] & E[\delta\mathbf{x}_0\delta\mathbf{x}_0^T]\mathbf{N}^T \\ \mathbf{N}E[\delta\mathbf{x}_0\delta\mathbf{x}_0^T] & \mathbf{N}E[\delta\mathbf{x}_0\delta\mathbf{x}_0^T]\mathbf{N}^T + E[\delta\bar{\mathbf{e}}_0\delta\bar{\mathbf{e}}_0^T] \end{bmatrix}, \tag{2.26}$$

which can be expressed in terms of the matrices $\mathbf{D}_0$ and $\bar{\mathbf{P}}_0$ as shown by

$$\mathbf{C}_0 = \begin{bmatrix} \mathbf{D}_0 & \mathbf{D}_0\mathbf{N}^T \\ \mathbf{N}\mathbf{D}_0 & \mathbf{N}\mathbf{D}_0\mathbf{N}^T + \bar{\mathbf{P}}_0 \end{bmatrix}. \tag{2.27}$$

The initial onboard navigation error covariance matrix ($\hat{\mathbf{P}}_0$) is simply set equal to the initial covariance matrix of the desired navigation error

$$\hat{\mathbf{P}}_0 = \bar{\mathbf{P}}_0. \tag{2.28}$$

2.4.2 Propagating

The covariance matrices are then propagated through time. Generally, the change of the navigation error of the states over time, $\delta\dot{\bar{\mathbf{e}}}$, is captured by the equation

$$\delta\dot{\bar{\mathbf{e}}} = (\mathbf{I} - \mathbf{H})\delta\dot{\mathbf{e}}, \tag{2.29}$$

where $\mathbf{H}$ is a selector matrix which selects the states affected by stochastic navigation. For example, if all the states were to be modeled by stochastic navigation, $\mathbf{H}$ would become the identity matrix, $\mathbf{I}$. Thus $\delta\dot{\bar{\mathbf{e}}} = \mathbf{0}$, which indicates that the navigation error would not change as the system is propagated through time and is a defining characteristic of stochastic navigation.[18] With stochastic navigation, the navigation error remains constant over time, and will only potentially change to a different constant value at different segments of the trajectory called navigation regions. The augmented state matrix is therefore propagated (as indicated by the dot above the variable) according to the equation

$$\delta\dot{\mathbf{X}} = \begin{bmatrix} \delta\dot{\mathbf{x}} \\ \delta\dot{\hat{\mathbf{x}}} \end{bmatrix} = \begin{bmatrix} \delta\dot{\mathbf{x}} \\ \mathbf{N}\delta\dot{\mathbf{x}} - (\mathbf{I} - \mathbf{H})\delta\dot{\mathbf{e}} \end{bmatrix}. \tag{2.30}$$

The augmented state and navigation error dynamics of a system during propagation are described by the equations

$$\delta\dot{\mathbf{X}} = \mathbf{A}\delta\dot{\mathbf{X}} \tag{2.31}$$

and

$$\delta\dot{\hat{\mathbf{e}}} = \hat{\mathbf{A}}\delta\dot{\hat{\mathbf{e}}}. \tag{2.32}$$

The $\mathbf{A}$ matrix,

$$\mathbf{A} = \begin{bmatrix} \mathbf{I} & \mathbf{0} \\ \mathbf{HN} & (\mathbf{I} - \mathbf{H}) \end{bmatrix}, \tag{2.33}$$

is referred to as the augmented navigation reset matrix. Further, the matrix

$$\hat{\mathbf{A}} = (\mathbf{I} - \mathbf{H}), \tag{2.34}$$

is called the onboard navigation reset matrix. They use the selector matrix, $\mathbf{H}$, to set the derivative of the navigation states that are to be modeled by stochastic navigation to zero (i.e. they do not change and are not propagated), while allowing the other states to be propagated.

These matrices are therefore also used to properly propagate the augmented state covariance and onboard state covariance matrices through time according to the equations

$$\dot{\mathbf{C}} = \mathbf{A}\dot{\mathbf{C}}\mathbf{A}^T, \tag{2.35}$$

and

$$\dot{\hat{\mathbf{P}}} = \hat{\mathbf{A}}\dot{\hat{\mathbf{P}}}\hat{\mathbf{A}}^T. \tag{2.36}$$

2.4.3 Updating

The update step of the stochastic navigation process is only realized if there is an instantaneous change in the navigation requirements or navigation performance from one time step to another as the covariances are propagated along the trajectory.[2] This change most commonly occurs when the spacecraft enters a different navigation region of the trajectory. Therefore, the navigation error is updated to a new value, indicated by the superscript $^+$ as

$$\delta\bar{\mathbf{e}}^+ = \delta\bar{\mathbf{e}}, \tag{2.37}$$

where $\delta\bar{\mathbf{e}}$ is a prescribed navigation error associated with the new navigation region and is determined a priori. This new term is then used to derive the covariance matrix,

$$\bar{\mathbf{P}} = E[\delta\bar{\mathbf{e}}^+\delta\bar{\mathbf{e}}^{+T}], \tag{2.38}$$

and is subsequently incorporated with the existing augmented state covariance and onboard navigation error matrices.

The state covariance matrix and onboard navigation error are updated using the equations

$$\delta\mathbf{X}^+ = \begin{bmatrix} \delta\mathbf{x}^+ \\ \delta\hat{\mathbf{x}}^+ \end{bmatrix} = \begin{bmatrix} \delta\mathbf{x}^- \\ (\delta\hat{\mathbf{x}} - \mathbf{H}\delta\hat{\mathbf{x}}^-) + (\mathbf{H}\mathbf{N}\delta\mathbf{x}^- - \mathbf{H}\delta\bar{\mathbf{e}}) \end{bmatrix} \tag{2.39}$$

and

$$\delta\hat{\mathbf{e}}^+ = (\delta\hat{\mathbf{e}}^- - \mathbf{H}\delta\hat{\mathbf{e}}^-) + \mathbf{H}\delta\bar{\mathbf{e}}, \tag{2.40}$$

respectively. The environment dispersions are unchanged and therefore take on the value at the previous time step, and the selector matrix, $\mathbf{H}$, makes it so that only the states affected by stochastic navigation are updated with the new navigation error.

The augmented navigation reset and onboard navigation reset matrices ($\mathbf{A}$ and $\hat{\mathbf{A}}$) are used again to reset the previous states

$$\delta\mathbf{X}^{+} = \mathbf{A}\delta\mathbf{X}^{-} + \mathbf{B}\delta\bar{\mathbf{e}}, \tag{2.41}$$

$$\delta\hat{\mathbf{e}}^{+} = \hat{\mathbf{A}}\delta\hat{\mathbf{e}}^{-} + \hat{\mathbf{B}}\delta\bar{\mathbf{e}}. \tag{2.42}$$

Two matrices, the augmented navigation inclusion matrix

$$\mathbf{B} = \begin{bmatrix} \mathbf{0} \\ -\mathbf{H} \end{bmatrix} \tag{2.43}$$

and the onboard navigation inclusion matrix

$$\hat{\mathbf{B}} = \mathbf{H}, \tag{2.44}$$

are introduced in this step to incorporate the updated errors into the previous states.

Finally, the augmented state and onboard navigation covariance matrices are updated using the equations

$$\mathbf{C}^{+} = \mathbf{A}\mathbf{C}^{-}\mathbf{A}^{T} + \mathbf{B}\bar{\mathbf{P}}\mathbf{B}^{T} \tag{2.45}$$

and

$$\hat{\mathbf{P}}^{+} = \hat{\mathbf{A}}\hat{\mathbf{P}}^{-}\hat{\mathbf{A}}^{T} + \hat{\mathbf{B}}\bar{\mathbf{P}}\hat{\mathbf{B}}^{T}, \tag{2.46}$$

ensuring the correct values of the state from the previous time step ($\mathbf{C}^{-}$ and $\hat{\mathbf{P}}^{-}$) appropriately combine with the updated navigation error values stored in $\bar{\mathbf{P}}$.

2.4.4 Correcting

The correction step is needed whenever a maneuver is performed. A trajectory correction burn, for example, will generally alter the dispersions and navigation errors. While the true dispersions do change, the navigation errors do not change using stochastic navigation and must be corrected to their values at the previous time step. The augmented state matrix is therefore corrected by

$$\delta \mathbf{X}^{+c} = \begin{bmatrix} \delta \mathbf{x}^{+c} \\ \delta \hat{\mathbf{x}}^{+c} \end{bmatrix} = \begin{bmatrix} \delta \mathbf{x}^{+c} \\ (\delta \hat{\mathbf{x}}^{+c} - \mathbf{H}\delta \hat{\mathbf{x}}^{+c}) + (\mathbf{HN}\delta \mathbf{x}^{+c} - \mathbf{H}\delta \mathbf{e}^{-c}) \end{bmatrix}. \tag{2.47}$$

The superscripts $^+$ or $^-$ indicate the values at the next or previous time steps, and the superscript ^{c} indicates a corrected value. The equation,

$$\delta \hat{\mathbf{e}}^{+c} = \delta \hat{\mathbf{e}}^{-c}, \tag{2.48}$$

reveals that the navigation error at the new time step, $\delta \hat{\mathbf{e}}^{+c}$, is reset to adopt the same value as the previous time step, and the navigation error at the previous time step, $\delta \hat{\mathbf{e}}^{-c}$, in turn, is given by the expression

$$\delta \hat{\mathbf{e}}^{-c} = \mathbf{N}\delta \mathbf{x}^{-c} - \delta \hat{\mathbf{x}}^{-c}. \tag{2.49}$$

In Eqn 2.49, $\delta \mathbf{x}^{-c}$ is the environment dispersions, and $\delta \hat{\mathbf{x}}^{-c}$ is the navigation dispersion; both before the maneuver. This redefined value of navigation error is substituted into Eqn 2.47 to yield

$$\delta \mathbf{X}^{+c} = \mathbf{A}\delta \mathbf{X}^{+c} + \mathbf{F}\delta \mathbf{X}^{-c}, \tag{2.50}$$

where $\mathbf{F}$ is given by

$$\mathbf{F} = \begin{bmatrix} \mathbf{0} & \mathbf{0}\mathbf{N}^T \\ -\mathbf{HN} & \mathbf{H} \end{bmatrix}. \tag{2.51}$$

This augmented covariance maneuver nulling matrix ($\mathbf{F}$) effectively leaves the navigation error untouched by the effects of the maneuver on the system. The expressions for the corrected augmented state covariance matrix and onboard navigation covariance matrix are given by

$$\mathbf{C}^{+c} = \mathbf{A}\mathbf{C}^{-c}\mathbf{A}^T + \mathbf{F}\mathbf{C}^{-c}\mathbf{F}^T \tag{2.52}$$

and

$$\hat{\mathbf{P}}^{+c} = \hat{\mathbf{P}}^{-c}. \tag{2.53}$$

The LinCov tool uses this process of initializing, propagating, updating, and correcting the augmented state covariance matrix from $\mathbf{C}_0$ to $\mathbf{C}^{+c}$ and the onboard navigation covariance matrix from $\hat{\mathbf{P}}_0$ to $\hat{\mathbf{P}}^{+c}$ to simulate via stochastic navigation how the navigation system would perform as it follows the nominal trajectory. This process is essential to deriving the performance requirements for this research.

2.4.5 Overview

Table 2.1 provides an abbreviated review of the LinCov analysis. It focuses on the augmented state covariance matrix, $\mathbf{C}$, and the onboard navigation error covariance matrix, $\hat{\mathbf{P}}$, because they are the two matrices that are initialized, propagated, updated, and corrected in the LinCov tool.

Step	$\mathbf{C}$	$\hat{\mathbf{P}}$
Initialize	$\mathbf{C}_0 = \begin{bmatrix} \mathbf{D}_0 & \mathbf{D}_0\mathbf{N}^T \\ \mathbf{N}\mathbf{D}_0 & \mathbf{N}\mathbf{D}_0\mathbf{N}^T + \bar{\mathbf{P}}_0 \end{bmatrix}$	$\hat{\mathbf{P}}_0 = \bar{\mathbf{P}}_0$
Propagate	$\dot{\mathbf{C}} = \mathbf{A}\dot{\mathbf{C}}\mathbf{A}^T$	$\dot{\hat{\mathbf{P}}} = \hat{\mathbf{A}}\dot{\hat{\mathbf{P}}}\hat{\mathbf{A}}^T$
Update	$\mathbf{C}^+ = \mathbf{A}\mathbf{C}^-\mathbf{A}^T + \mathbf{B}\bar{\mathbf{P}}\mathbf{B}^T$	$\hat{\mathbf{P}}^+ = \hat{\mathbf{A}}\hat{\mathbf{P}}^-\hat{\mathbf{A}}^T + \hat{\mathbf{B}}\bar{\mathbf{P}}\hat{\mathbf{B}}^T$
Correct	$\mathbf{C}^{+c} = \mathbf{A}\mathbf{C}^{-c}\mathbf{A}^T + \mathbf{F}\mathbf{C}^{-c}\mathbf{F}^T$	$\hat{\mathbf{P}}^{+c} = \hat{\mathbf{P}}^{-c}$

Table 2.1 : Summary of Implementing Stochastic Navigation within a LinCov Analysis

First, $\mathbf{C}_0$ and $\hat{\mathbf{P}}_0$ are initialized using the covariance matrices of the initial environment dispersions and navigation errors which are determined by the user beforehand. Both matrices are then propagated to the next time step, and the $\mathbf{A}$ and $\hat{\mathbf{A}}$ matrices only allow the states affected by stochastic navigation to be propagated. When the system arrives at a time step that indicates a different navigation region, the states are updated with the new navigation error associated with the new navigation region. Finally, when the system executes a maneuver, the matrices are corrected so that the navigation error remains unchanged by the maneuver.

Chapter 3

Optimal GN&C Requirement Generation

3.1 Performance Requirement Representation

There are several methods for optimizing GN&C subsystem performance requirements. The focus of this thesis is to derive an optimal set of performance requirements for the cislunar missions that allow the GN&C system to meet top-level mission requirements. The method for deriving the optimal performance requirements accounting for multiple top-level mission requirements is outlined in this chapter. The optimization involves multiple, often correlated, variables represented by ellipses.

GN&C subsystem performance requirements characterize the level of uncertainty that can be tolerated in the estimation of the vehicle states and other GN&C performance parameters. The constraints on these performance requirements ultimately are the top-level mission requirements. In most cases, the mission requirements are determined a priori, as is the case for the scenarios analyzed in this research. Multivariate or correlated performance requirements that form the bi-variate case can be represented geometrically as an ellipse. Two-dimensional (2-D) ellipses, defined with two performance parameters that are often correlated, may also be described by 2×2 matrices, and correspondingly, n-dimensional ellipsoids, defined with n performance parameters, can be described by $n \times n$ matrices.

It is noted for clarity that the terms ellipse and matrix are used interchangeably, because in this context, the ellipses are represented by matrices and vice versa. In the case that more than two correlated variables are being analyzed at a time, the terms n-dimensional ellipsoid and $n \times n$ matrix best describe the data, however the terms ellipse and matrix are used throughout for simplicity and consistency. Additionally, multiple terms are used to refer to the total performance uncertainty ellipse. These terms include: the performance ellipse, the total error ellipse, and the RSS ellipse of all error sources. As the results of the current analysis are presented as 2-D ellipses, this form is developed further.

A 2-D requirement ellipse in matrix form is generalized by

$$\begin{bmatrix} \sigma_{\bar{p}_1}^2 & \rho\sigma_{\bar{p}_1}\sigma_{\bar{p}_2} \\ \rho\sigma_{\bar{p}_2}\sigma_{\bar{p}_1} & \sigma_{\bar{p}_2}^2 \end{bmatrix}, \tag{3.1}$$

where $\sigma_{\bar{p}_1}^2$ and $\sigma_{\bar{p}_2}^2$ represent the total variances of the two performance parameter that define the specific requirement, and ρ is the correlation coefficient of the parameters.

A 2-D error source ellipse is shown in matrix form by

$$\begin{bmatrix} \sigma_{\delta i_1}^2 & \rho\sigma_{\delta i_1}\sigma_{\delta i_2} \\ \rho\sigma_{\delta i_2}\sigma_{\delta i_1} & \sigma_{\delta i_2}^2 \end{bmatrix}, \tag{3.2}$$

where $\sigma_{\delta i_1}^2$ and $\sigma_{\delta i_2}^2$ are the variances of the contribution of the individual error source (δ_i) to the two performance parameters of interest, and ρ is the corresponding correlation coefficient. It is important to note the physical or geometric meaning of the information that is stored in the matrices. Primordially, the square root of the eigenvalues of the requirement or error source matrices are the lengths of the semi-major and semi-minor axes. For example, in the case of the 2×2 error source matrix from Eqn 3.2, if the variables are not correlated ($\rho = 0$), then the variances $\sigma_{\delta i_1}^2$ and $\sigma_{\delta i_2}^2$ are the eigenvalues of the matrix, and $\sigma_{\delta i_1}$ and $\sigma_{\delta i_2}$ represent the semi-major and semi-minor axes of the 1-σ ellipse.[30] Typically the requirement and error source ellipses are represented using three standard deviation (3-σ) statistics to capture the performance of the system with 99.7% confidence.[28] The eigenvectors of the matrix describe the orientation of the ellipse as it is rotated from the principal axes.

3.2 Scaling GN&C Performance Metrics

The total performance ellipse is made up of multiple error source ellipses. The error source ellipses represent the contributions of navigation error, initial trajectory dispersions, system process noise, and maneuver execution error to the total performance uncertainty. Because of the linearity of the error variables, the individual error ellipses can be added together to form an ellipse of all the error components. The performance metric can be expanded or reduced until it meets the mission requirements. This process may not be completely intuitive considering the potential differences in orientation and shape of the requirement and performance ellipses, therefore the method for scaling is outlined in this section, beginning with a brief discussion on the fundamental concept of sensitivity analysis.

3.2.1 Sensitivity Analysis Scaling

Sensitivity analysis takes advantage of the fact that in a linear process, where the error sources are independent, the sum of each individual error source equals the total error

$$\sigma_p^2 = \sum \sigma_{p|\delta_i}^2. \tag{3.3}$$

In other words, the total variance of a specific GN&C requirement parameter such as downtrack position, flight path angle, or crosstrack velocity, represented by σ_p^2, equals the sum total of each individual error source's contribution, i, to the variance of the parameter of interest, p, represented by $\sigma_{p|\delta_i}^2$.[29] A sensitivity study determines the individual contributions of each error source to the GN&C system top-level requirement parameters. One by one, each error source is evaluated as if it were the only source contributing to the overall uncertainty. To calculate the total uncertainty, the individual components are linearly combined. As a result of analyzing each error source individually, they can be plotted separately, which allows the user to quickly determine visually how each error source contributes to overall uncertainty.

Sensitivity studies are essential for deriving navigation and other GN&C subsystem performance requirements. Consider first a scalar case, looking at the total uncertainty for a given performance parameter, σ_p^2. Expanding Eqn 3.3 to

$$\sigma_p^2 = \sigma_{p|\delta_1}^2 + \sigma_{p|\delta_2}^2 + \cdots + \sigma_{p|\delta_n}^2, \tag{3.4}$$

a scaling factor, α^2, is then applied to each error source contribution that will yield an increased ($\alpha^2 > 1$) or reduced ($\alpha^2 < 1$) total variance of the performance parameter ($\sigma_{p^*}^2$)

$$\sigma_{p^*}^2 = \alpha^2(\sigma_{p|\delta_1}^2 + \sigma_{p|\delta_2}^2 + \cdots + \sigma_{p|\delta_n}^2). \tag{3.5}$$

Distributing the scaling factor to each error source term yields the expression

$$\sigma_{p^*}^2 = \alpha^2\sigma_{p|\delta_1}^2 + \alpha^2\sigma_{p|\delta_2}^2 + \cdots + \alpha^2\sigma_{p|\delta_n}^2. \tag{3.6}$$

Scaling all the error sources by a single scaling factor can be useful, however, each error source contribution is linearly independent, therefore each error source can be scaled by a unique value or weight, w_k^2. Individual weights are applied to each error source term in Eqn 3.5 as expressed in the equation

$$\sigma_{p^*}^2 = \alpha^2(w_1^2\sigma_{p|\delta_1}^2 + w_2^2\sigma_{p|\delta_2}^2 + \cdots + w_n^2\sigma_{p|\delta_n}^2). \tag{3.7}$$

The scaling factor, α^2, is distributed to each error source term. A new weighting term, $w_{k^*}^2$, is defined as

$$w_{k^*}^2 = \alpha^2 w_k^2, \tag{3.8}$$

and Eqn 3.7 becomes

$$\sigma_{p^*}^2 = w_{1^*}^2\sigma_{p|\delta_1}^2 + w_{2^*}^2\sigma_{p|\delta_2}^2 + \cdots + w_{n^*}^2\sigma_{p|\delta_n}^2. \tag{3.9}$$

Ultimately, the goal is to ensure the total variance of a given performance parameter is less than or equal to the maximum allowable dispersions of the performance parameter that constitutes the top-level mission requirement

$$\sigma_p^2 \leq \sigma_{\bar{p}}^2. \tag{3.10}$$

Weighting the individual error sources to yield a new total variance for a performance parameter, $\sigma_{p^*}^2$, that can optimally meet the mission requirements, $\sigma_{\bar{p}}^2$, is possible. With the scalar case developed, the case for optimally scaling and weighting ellipses via linear manipulation of 2×2 matrix manipulation is considered.

3.2.2 Single Scaling Factor Derivation

The optimal weighting method that forms the crux of this investigation branches from the derivation for a single scaling factor for uncorrelated scalar requirements. The full derivation has been completed previously by Woffinden et al.[29]

The mission requirement $(n \times n)$ ellipse is represented by the covariance matrix, $\mathbf{\Sigma}_{\bar{p}}$, defined in Eqn 3.11 with $\delta\mathbf{x}_{\bar{p}}$ representing the maximum dispersions and errors allowed by the mission requirement

$$\mathbf{\Sigma}_{\bar{p}} = E[\delta\mathbf{x}_{\bar{p}}\delta\mathbf{x}_{\bar{p}}^T]. \tag{3.11}$$

$\mathbf{\Sigma}_{\bar{p}}$ can be decomposed to the diagonal matrix of its eigenvalues, $\bar{\mathbf{D}}$, then pre- and post-multiplied by its rotation matrix, consisting of its eigenvector, $\bar{\mathbf{V}}$, as detailed in the equation

$$\mathbf{\Sigma}_{\bar{p}} = \bar{\mathbf{V}}\bar{\mathbf{D}}\bar{\mathbf{V}}^T. \tag{3.12}$$

The requirement ellipse is then transformed[32] to a new, unit circle coordinate space by pre- and post-multiplying by a transformation matrix, $\bar{\mathbf{T}}$. This transformation is an affine transformation[32] and is linear, therefore the effects and results of the processes accomplished in this coordinate space also affect the ellipses in the original coordinate space.[33] Generally, for an affine coordinate transformation, the two coordinate systems can be defined by translation of the axes' origins, a rotation of the axes, and a scale factor.[31] The transformation matrix is formed by taking the inverse square root of the diagonal eigenvalue matrix of the mission requirement ellipse, $\bar{\mathbf{D}}^{-\frac{1}{2}}$, and multiplying it by the rotation matrix, $\bar{\mathbf{V}}$

$$\bar{\mathbf{T}} = \bar{\mathbf{D}}^{-\frac{1}{2}}\bar{\mathbf{V}}. \tag{3.13}$$

This transformation, which makes the requirement ellipse a unit circle in the transformed space, $\mathbf{\Sigma}_{\bar{u}}$, (see Eqn 3.16) is visualized step-wise following the solid yellow line from Figs 3.1a - 3.1b.

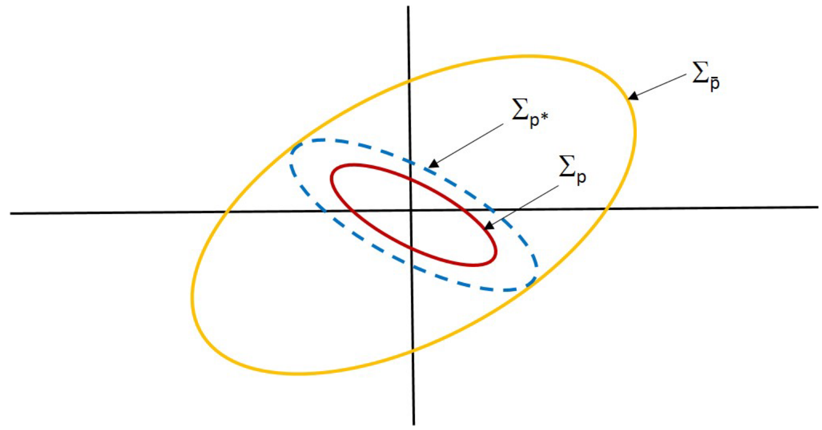

(a) Mission Requirement and Performance Ellipses

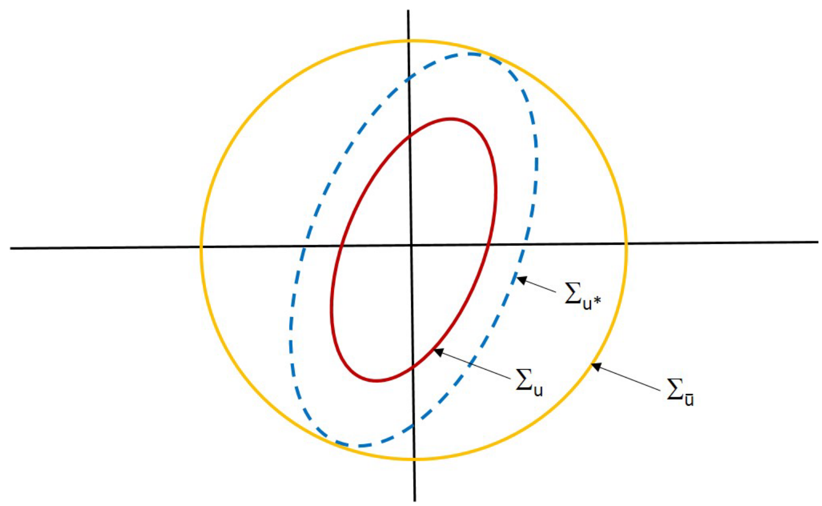

(b) Transformed Ellipses in Unit Circle Space

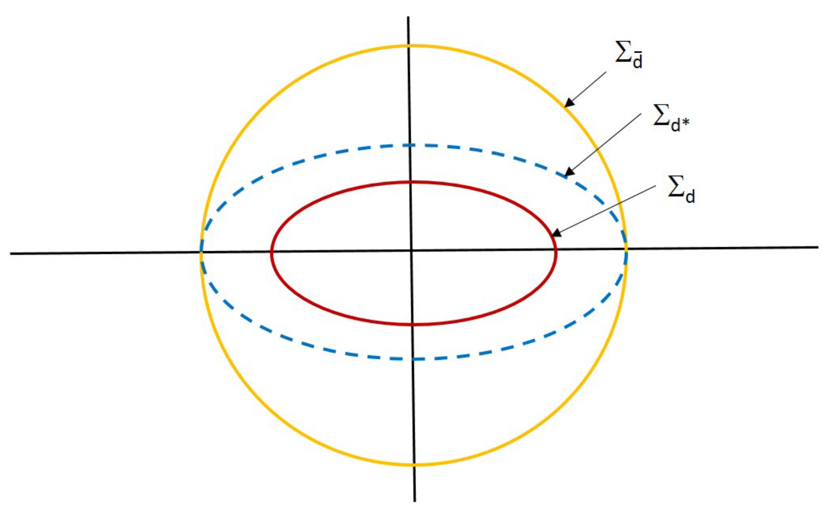

(c) Transformed Ellipses Rotated to Principal Axes

Figure 3.1 : Performance Ellipse Scaling to Meet Mission Requirements[29]

The transformation of the requirement ellipse is also described step by step by

$$\mathbf{\Sigma}_{\bar{u}} = \bar{\mathbf{T}}\bar{\mathbf{P}}\bar{\mathbf{T}}^T, \tag{3.14}$$

$$\mathbf{\Sigma}_{\bar{u}} = \bar{\mathbf{D}}^{-\frac{1}{2}}\bar{\mathbf{V}}(\bar{\mathbf{V}}\bar{\mathbf{D}}\bar{\mathbf{V}}^T)\bar{\mathbf{V}}^T\bar{\mathbf{D}}^{T-\frac{1}{2}}, \tag{3.15}$$

and

$$\mathbf{\Sigma}_{\bar{u}} = \mathbf{I}. \tag{3.16}$$

The next step in deriving the optimal navigation requirements is transforming the performance ellipse, $\mathbf{\Sigma}_p$. This ellipse consists of the RSS of all the error sources,

$$\mathbf{\Sigma}_p = E[\delta\mathbf{x}_p\delta\mathbf{x}_p^T], \tag{3.17}$$

and can be expressed in matrix decomposed form in the expression,

$$\mathbf{\Sigma}_p = \mathbf{V}\mathbf{D}\mathbf{V}^T. \tag{3.18}$$

This ellipse will be scaled to hit the requirements, but first, it is also transformed to the new coordinate space by pre- and post-multiplying by the same transformation matrix derived from the requirement ellipse, $\bar{\mathbf{T}}$. Unlike the requirement ellipse-turned unit circle, the total error ellipse remains an ellipse; now with a different orientation and/or shape (see the red ellipse from Figs 3.1a - 3.1b), and the resultant transformation yields a new performance ellipse, $\mathbf{\Sigma}_u$, defined by Eqns 3.19 and 3.20, often located within the unit circle ($\mathbf{\Sigma}_{\bar{u}}$),

$$\mathbf{\Sigma}_u = \bar{\mathbf{T}}\mathbf{P}\bar{\mathbf{T}}^T, \tag{3.19}$$

$$\mathbf{\Sigma}_u = \bar{\mathbf{D}}^{-\frac{1}{2}}\bar{\mathbf{V}}(\mathbf{V}\mathbf{D}\mathbf{V}^T)\bar{\mathbf{V}}^T\bar{\mathbf{D}}^{-\frac{1}{2}T}. \tag{3.20}$$

Comparing the solid red ellipse to the solid yellow ellipse in Fig 3.1b, the transformed performance ellipse does not yet meet the requirement unit circle and can be scaled until it hits the requirement.

The final step in the process is to rotate all the terms of interest so that the semi-major and semi-minor axes are aligned with the principal axes (see Figs 3.1b-3.1c). To do this, the matrices of the ellipses of interest (the transformed requirement and performance matrices) are pre- and post-multiplied by the transpose of the rotation matrix of the performance ellipse, $\mathbf{V}_u^T$ expressed in the equations

$$\boldsymbol{\Sigma}_{\bar{d}} = \mathbf{V}_u^T \boldsymbol{\Sigma}_{\bar{u}} \mathbf{V}_u \tag{3.21}$$

and

$$\boldsymbol{\Sigma}_d = \mathbf{V}_u^T \boldsymbol{\Sigma}_u \mathbf{V}_u. \tag{3.22}$$

The rotation of the transformed requirement ellipse is trivial, because it is a unit circle.

Finally, at this point the scaling problem — solving for α^2 — is straightforward and the optimal weighting problem becomes feasible. The scaling factor, α^2, is the ratio between the semi-major axis of the transformed requirement ellipse, which is 1 because the transformed ellipse is a unit circle, and the semi-major axis of the transformed total error ellipse,

$$\alpha^2 = \frac{1}{(\text{eig}\,[\boldsymbol{\Sigma}_d])_{max}}. \tag{3.23}$$

The semi-major axis of the transformed performance ellipse is determined by calculating the maximum eigenvalue of its corresponding $n \times n$ matrix. Unity, derived from the unit circle, is divided by the largest eigenvalue to calculate the scaling term, α^2. The downside to this method is that because the performance ellipse, which consists of the RSS of all the error sources, is scaled all together, the same scale factor, α^2, is applied to each error source ellipse of which the performance ellipse is made.

This result is not very practical in almost all applications and therefore is not very useful. For example, the scaling term could be 2.0 which indicates that all the dispersions and errors can increase by a factor of 2.0, and the mission requirements are still met. However, it is possible that increasing an individual error source contribution by a factor of 2.0 is not desirable.

The current investigation uses a method detailed in a text by Woffinden et al.[29] and regenerated here, which builds on the foundation of this method of scaling by calculating optimal weights for individual error sources, thus allowing for optimization and realistic scaling, ultimately deriving optimal GN&C subsystem performance requirements.

3.3 Optimizing GN&C Performance Metrics

3.3.1 Lower and Upper Bounds

Every scenario requires the user to determine the initial value of a given error source and the upper and lower bounds of the scaling terms, now referred to as weights, for each error source variable unique to the mission. Currently no automated way is available for choosing the initial value nor appropriate upper and lower bounds, depending on the scenario. Therefore, the user is wont to use best practices, engineering judgment, and previous empirical data to make these decisions. A straightforward approach is to analyze each of the dispersions and errors individually, determine a realistic minimum and maximum value for that variable given the current trajectory and mission, then divide the minimum and maximum values individually by the initialized value for that error source to yield the lower and upper bounds for the weights, respectively. This procedure is detailed in Eqns 3.24 - 3.27, where σ_{δ_k} represents the initial value of the error source of interest (the subscript k indicating which individual error source is currently under consideration), w_k^2 represents the lower bound (lb) and upper bound (ub) values of the weights for which the equations solve, and $\left[\sigma_{\delta_k}^2\right]$ represents the minimum (min) and maximum (max) values the given error source can realistically take on in the scenario with

$$\sigma_{\delta_k}^2 w_{k_{lb}}^2 = \left[\sigma_{\delta_k}^2\right]_{min}, \tag{3.24}$$

$$w_{k_{lb}}^2 = \frac{\left[\sigma_{\delta_k}^2\right]_{min}}{\sigma_{\delta_k}}, \tag{3.25}$$

$$\sigma_{\delta_k} w_{k_{ub}}^2 = \left[\sigma_{\delta_k}^2\right]_{max}, \tag{3.26}$$

and

$$w_{k_{ub}}^2 = \frac{\left[\sigma_{\delta_k}^2\right]_{max}}{\sigma_{\delta_k}}. \tag{3.27}$$

3.3.2 Optimal Weights Generation

The optimal weights can be solved simply through linear programming. The following steps are taken previous to optimizing the weights.[29] The procedure for transformation and rotation of the requirement ellipse is the same, and will not be repeated here.

The total error matrix,

$$\mathbf{\Sigma}_p = \sum (\mathbf{\Sigma}_{p|\delta_j}), \tag{3.28}$$

is formed by adding together the contributions of each individual error source. This is the ellipse that is to be weighted and scaled in such a manner that it hits the mission requirements. The mission planner may not want to weight or scale every error source for every scenario. For example, it may already be determined which thrusters will be used for the mission, and therefore the maneuver execution error will already be known and should not change. To account for these quantities that will not be weighted, Eqn 3.29 breaks the summation into variables that will be scaled, annotated with the subscript k, and variables that will not be scaled, annotated with the subscript j

$$\mathbf{\Sigma}_{p^*} = \sum (w_k^2 \mathbf{\Sigma}_{p|\delta_k}) + \sum (\mathbf{\Sigma}_{p|\delta_j}). \tag{3.29}$$

Transformation

Mirroring the same procedure outlined previously, the performance ellipse is mapped to the unit circle space. The ellipse is now transformed and is designated as $\mathbf{\Sigma}_{u^*}$,

$$\mathbf{\Sigma}_{u^*} = \bar{\mathbf{T}} \mathbf{\Sigma}_{p^*} \bar{\mathbf{T}}^T. \tag{3.30}$$

Rotation

The next step involves aligning the semi-major and semi-minor axes with the principal axes of the unitized space. This step is accomplished by decomposing the total performance matrix and pre- and post-multiplying it by the transpose of its rotation matrix, $\mathbf{V}_u^T$. The rotated, transformed performance matrix becomes $\mathbf{\Sigma}_{d^*}$,

$$\mathbf{\Sigma}_{d^*} = \mathbf{V}_u^T \mathbf{\Sigma}_{u^*} \mathbf{V}_u. \tag{3.31}$$

An expanded view detailing all the processes involved in transforming and rotating the ellipse is given by

$$\mathbf{\Sigma}_{d^*} = \sum (w_k^2 \mathbf{V}_u^T \mathbf{T} \mathbf{\Sigma}_{p|\delta_k} \mathbf{T}^T \mathbf{V}_u) + \sum (\mathbf{V}_u^T \mathbf{T} \mathbf{\Sigma}_{p|\delta_j} \mathbf{T}^T \mathbf{V}_u). \tag{3.32}$$

Substituting $\mathbf{\Sigma}_{d|\delta_k} = \mathbf{V}_u^T \mathbf{T} \mathbf{\Sigma}_{p|\delta_k} \mathbf{T}^T \mathbf{V}_u$ and $\mathbf{\Sigma}_{d|\delta_j} = \mathbf{V}_u^T \mathbf{T} \mathbf{\Sigma}_{p|\delta_j} \mathbf{T}^T \mathbf{V}_u$, Eqn 3.32 becomes

$$\mathbf{\Sigma}_{d^*} = \sum (w_k^2 \mathbf{\Sigma}_{d|\delta_k}) + \sum (\mathbf{\Sigma}_{d|\delta_j}). \tag{3.33}$$

Setting Up a Linear Problem

Ideally this approach for optimizing the weights of the contributions of individual error sources would use the eigenvalues of $\mathbf{\Sigma}_{d^*}$,

$$\sigma_{d^*}^2 = \text{eig}\left[\sum (w_k^2 \mathbf{\Sigma}_{u|\delta_k}) + \sum (\mathbf{\Sigma}_{u|\delta_j})\right], \tag{3.34}$$

however, doing so introduces non-linearities to the problem, and consequently, linear programming is no longer a viable resource for solving for the optimal weights. This study therefore uses the main diagonals of the rotated matrix, $\mathbf{\Sigma}_{d^*}$, to make a close approximation

$$\sigma_{d^*}^2 = \text{diag}\left[\mathbf{\Sigma}_{d^*}\right]. \tag{3.35}$$

These values stored in the vector, $\sigma_{d^*}^2$, represent the magnitude of the individual error sources in the direction of the principal axes. Although the total performance ellipse has its semi-major and semi-minor axes aligned with the principal axes, each individual error source ellipse does not necessarily line up with the principal axes; although more often than not, the rotation very nearly aligns the ellipses along them. In the rare event that this is not the case, the correction process will account for the minor deviations that occasion this problem. The main diagonals therefore fit the equality

$$\sigma_{d^*}^2 = \sum (w_k^2 \sigma_{d|\delta_k}^2) + \sum (\sigma_{d|\delta_j}^2), \tag{3.36}$$

which brings the equation to a point where the weights can be isolated and each one can be solved for via optimization/linear programming,

The constraint is the top-level requirements. It is desirable for the performance ellipse to hit, but never exceed, the requirement ellipse. This is expressed mathematically with

$$\sum (w_k^2 \sigma_{d|\delta_k}^2) + \sum (\sigma_{d|\delta_j}^2) \leq (1-m)^2 \mathbf{1}, \tag{3.37}$$

where the right hand side of the equation represents the requirement ellipse still in transformed space, the diagonals of which constitute a vector of ones, $\mathbf{1}$. The expression, $(1-m)^2$, preceeding the $\mathbf{1}$ vector accounts for a margin, m, that the mission planner may include, effectively putting in place a factor of safety with the requirement. The left hand side of the equation, the total, weighted error ellipse must, in all $n-$directions, be less than or equal to the requirement, including the associated margin.

Finally, the scaling terms are isolated by bringing the non-scaling terms to the right hand side of the equation expressed by

$$\sum (w_k^2 \sigma_{d|\delta_k}^2) \leq (1-m)^2 \mathbf{1} - \sum (\sigma_{d|\delta_j}^2). \tag{3.38}$$

With the equation in this format, the weights can be solved for. Eqns 3.25 and 3.27 can combine to become

$$w_{k_{lb}}^2 \leq w_k^2 \leq w_{k_{ub}}^2, \tag{3.39}$$

which ensures the optimal weights are within the bounds specified by the user. Eqn 3.39 can be rewritten as

$$\frac{\left[\sigma_{\bar{\delta}_k}^2\right]_{min}}{\sigma_{\delta_k}^2} \leq w_k^2 \leq \frac{\left[\sigma_{\bar{\delta}_k}^2\right]_{max}}{\sigma_{\delta_k}^2}. \tag{3.40}$$

Optimization - Linear Programming

To solve for the optimal weights, which must fall within the user-specified bounds displayed in Eqn 3.40, an $\mathbf{A}$ matrix and a $\mathbf{b}$ vector must be created. Each construct stores key information needed to optimize a given variable. In this case, the variables to be optimized are the weights applied to the individual error source contributions.

For example, the **A** matrix usually stores the given or initial values of a variable as well as the parameters of a specific cost function. The **b** vector stores the limits or requirements of the optimization. The relationship between the two is an inequality used commonly in general linear programming problems[34] and is described by

$$\mathbf{Ax} \leq \mathbf{b}, \tag{3.41}$$

where the variable, **x**, is a vector of variables for which the optimization is to solve.

For the current investigation, these matrices store the necessary information such as the initial values of the error sources and the cost function parameters in the case of the **A** matrix and the top-level mission requirements and upper and lower bounds for the weights in the **b** vector. A better sense for the contents of each construct can be gleaned from a quick study of the following equations

$$\mathbf{A} = \begin{bmatrix} \sigma^2_{d|\delta_1} & \sigma^2_{d|\delta_2} & \cdots & \sigma^2_{d|\delta_k} \\ -1 & 0 & \cdots & 0 \\ 0 & -1 & \cdots & 0 \\ \vdots & \cdots & \cdots & \vdots \\ 0 & 0 & 0 & -1 \\ 1 & 0 & \cdots & 0 \\ 0 & 1 & \cdots & 0 \\ \vdots & \cdots & \cdots & \vdots \\ 0 & 0 & 0 & 1 \end{bmatrix}, \mathbf{b} = \begin{bmatrix} (1-m)^2\mathbf{1} - \sum\left(\sigma^2_{d|\delta_j}\right) \\ -\left[\sigma^2_{\bar{\delta}_1}\right]_{min} \big/ \sigma^2_{\delta_1} \\ -\left[\sigma^2_{\bar{\delta}_2}\right]_{min} \big/ \sigma^2_{\delta_2} \\ \vdots \\ -\left[\sigma^2_{\bar{\delta}_k}\right]_{min} \big/ \sigma^2_{\delta_k} \\ \left[\sigma^2_{\bar{\delta}_1}\right]_{max} \big/ \sigma^2_{\delta_1} \\ \left[\sigma^2_{\bar{\delta}_2}\right]_{max} \big/ \sigma^2_{\delta_2} \\ \vdots \\ \left[\sigma^2_{\bar{\delta}_k}\right]_{max} \big/ \sigma^2_{\delta_k} \end{bmatrix}. \tag{3.42}$$

A cost function is used in optimization to determine in what way the variables of interest ought to be optimized, or in other words specific to this application, how the weights should be weighted. The three canonical equations[34] that constrain the optimization are

$$\max \mathbf{c}^T\mathbf{x}, \tag{3.43}$$

$$\mathbf{A}\mathbf{x} \leq \mathbf{b}, \tag{3.44}$$

and

$$\mathbf{x} \geq \mathbf{0}, \tag{3.45}$$

where $\mathbf{x}$ is the vector of optimal weights, and $\mathbf{c}$ is the vector of cost function parameters. The vector,

$$\mathbf{c} = [-1 - 1 \cdots - 1], \tag{3.46}$$

is simply a vector of -1s of length k. This individual cost function maximizes the sum of the weights,

$$\max \sum w_k^2. \tag{3.47}$$

Maximizing the sum of the weights is one way to allow the dispersions and errors to be as big as possible before hitting the requirement. Typically, these parameters cause the optimizer to increase the scale of error sources that initially contribute very little to the overall error, and decrease the scale of error sources that initially contribute a lot to the performance error to allow all error sources to scale together in an optimal way.

A second parameter set that is useful in the scenarios of interest is

$$\mathbf{c}_i = -\frac{1}{\max(\mathbf{A}_i)}. \tag{3.48}$$

This parameter set takes the inverse of the maximum value of each column, i, of the $\mathbf{A}$ matrix. As the linear programming algorithm seeks to maximize $\mathbf{c}^T\mathbf{x}$, the effect is to de-weight the error sources that initially contribute very little to the overall error compared to those that have a significant contribution.

The final equation for the weighted performance ellipse is

$$\boldsymbol{\Sigma}_{d^o} = \sum (w_k^2 \boldsymbol{\Sigma}_{d|\delta_k}) + \sum (\boldsymbol{\Sigma}_{d|\delta_j}), \tag{3.49}$$

where the calculated weights from the linear programming optimization are applied, and the ellipse looks more like the dashed blue ellipse, $\boldsymbol{\Sigma}_{p^*}$, in Fig 3.1a in the sense that it closely approaches the requirement ellipse.

Correction

Ideally, the edge of the performance ellipse intersects the requirement ellipse at two points directly opposite each other on the ellipse. However, some of the transformed, rotated individual error ellipses will not align exactly with the principal axes after the rotation. Therefore, when the optimized weights are applied to the individual error source ellipses, the total performance ellipse (no longer transformed nor rotated) may come just short of the requirement or slightly exceed it. Some additional steps should be taken to bring the performance ellipse back within the requirements and ensure it approaches the requirement as closely as possible.

One solution is to iterate the optimization process, using $\boldsymbol{\Sigma}_{d^o}$ from Eqn 3.49 after applying the derived weights as the new performance matrix to be scaled. This solution is ideal if the initial weighting leads the weighted performance matrix to exceed or undershoot the requirement by a large amount (i.e. outside of a 5-10% tolerance).

There is a second, more rudimentary way to deal with this issue that works best with even smaller tolerances. Eqn 3.50 introduces the variable α_a^2, which is used to slightly scale the weighted performance ellipse, $\boldsymbol{\Sigma}_{d^o}$,

$$\alpha_a^2 \sigma_{d^o}^2 \leq (1-m)^2 \mathbf{1}. \tag{3.50}$$

In words, the term α_a^2 is the ratio between the requirement including a margin and the maximum value of the diagonal of the weighted performance ellipse. This ratio is solved for in the equations

$$\alpha_a^2 \max(\sigma_{d^o}^2) \leq (1-m)^2, \tag{3.51}$$

and

$$\alpha_a^2 \leq \frac{(1-m)^2}{\max(\sigma_{d^o}^2)}. \tag{3.52}$$

The weights are then multiplied by α_a^2

$$w_{k^*}^2 = \alpha_a^2 w_k^2. \tag{3.53}$$

The updated weights, $w_{k^*}^2$, are applied to their corresponding error source ellipses and summed as in Eqn 3.49, and when the weights are multiplied by the initial error source values, the optimal performance requirements ($\sigma_{\delta\bar{k}}$) are derived.

$$\sigma_{\delta\bar{k}} = w_{k^*}^2 \sigma_{\delta_k} \tag{3.54}$$

The whole process of deriving the vector of optimal weights culminates in applying them to the original error source contributions to derive the optimal navigation and other GN&C subsystem performance requirements.

Chapter 4

Optimal Cislunar GN&C Requirement

4.1 Cisunar Trajectories

The trajectories for the lunar outbound and lunar return segments utilize NASA's Orion Exploration Mission 1 (EM1) profile, shown in Fig 4.1. Specifically, the outbound leg from the Earth to the Moon and the return leg from the Moon to the Earth are adopted to demonstrate the capability of generating optimal GN&C system requirements in a systematic approach. This chapter describes each trajectory and defines the top-level mission and GN&C subsystem performance requirements pertinent to the mission profiles. The results of the optimal requirement generation are then presented.

4.1.1 Lunar Outbound Trajectory

The analyzed trajectory for the lunar outbound scenario begins an hour before the first translational correction burn, Outbound Trajectory Correction 1 (OTC-1), and ends prior to the Outbound Powered Flyby (OPF) burn. During this simulated portion of flight, there are four trajectory correction burns, OTC-1, OTC-2, OTC-3, and OTC-4,[35] which are marked and labeled in Fig 4.1 by green dots along the white nominal trajectory. OTC-1 takes place 6.8 hours after launch.[19] The second and third maneuvers (OTC-2 and OTC-3) occur 19.0 and 74.8 hours after OTC-1.[19] OTC-4 is the final correction burn before the spacecraft performs the lunar flyby. It occurs 6.0 hours before the critical OPF, near the lunar closest approach.[35]

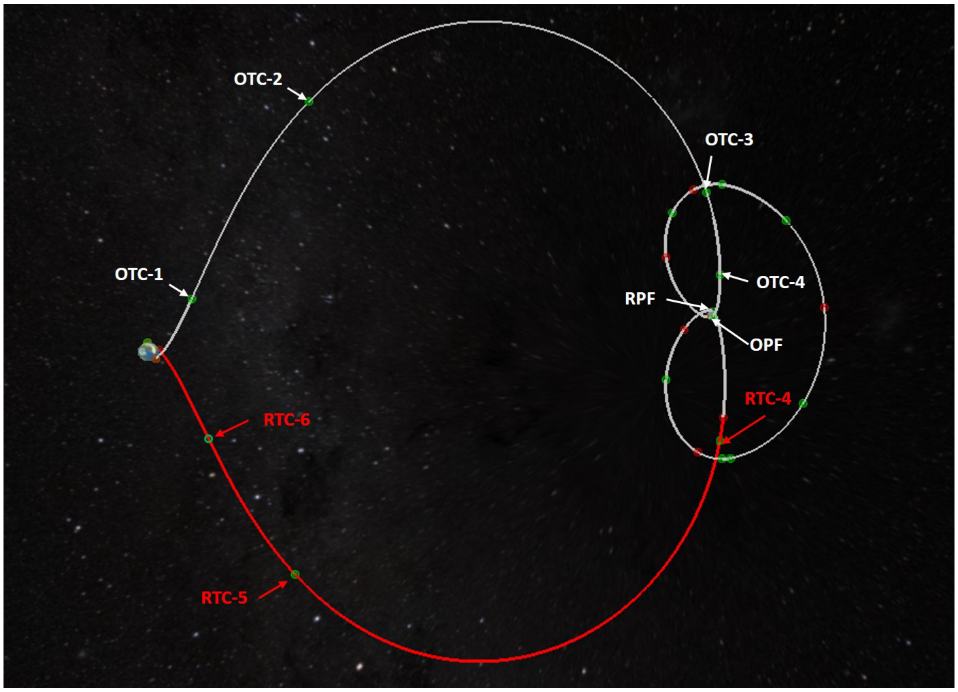

Figure 4.1 : EM1 Trajectory[29]

4.1.2 Lunar Return Trajectory

The lunar return trajectory executes three correction burns as the vehicle transitions from cislunar activities to reentering the Earth's atmosphere at Entry Interface (EI). Figure 4.1 illustrates the return trajectory with the simulated portion highlighted in red. EI is located at approximately 400 kft altitude and is the designated point at which the vehicle begins to reenter the Earth's atmosphere.[29] The return trajectory correction (RTC) burns take place 18.0, 107.4, and 123.4 hours following the Return Powered Flyby (RPF) maneuver.[19] The first burn is referred to as Return Trajectory Correction 4 (RTC-4) with each subsequent burn incrementing sequentially as RTC-5 and RTC-6. The simulation ends at EI. The mission requirements are defined at EI for this flight phase.

4.2 Cislunar Mission Performance Requirements

The GN&C system top-level mission requirements for the Orion EM1 flight profile vary from continuous, time dependent requirements such as $\mathbf{\Delta V}$ dispersions along the trajectory, to requirements specified at certain time epochs such as the moment Orion crosses the B-Plane or at EI.

4.2.1 B-Plane Requirements

The B-Plane is used for targeting when a vehicle is approaching a planet or other celestial body and is defined relative to the celestial body. The unit vectors, $\hat{T}$ and $\hat{R}$, define what is referred to as the B-Plane, which is the plane perpendicular to the incoming hyperbolic trajectory's asymptote (see Figs 4.2a - 4.2b).[36] As shown in Fig 4.2b, $\hat{T}$ and $\hat{R}$ constitute an inertial axis system attached to the celestial body of interest with the origin located at its center of gravity (CG).

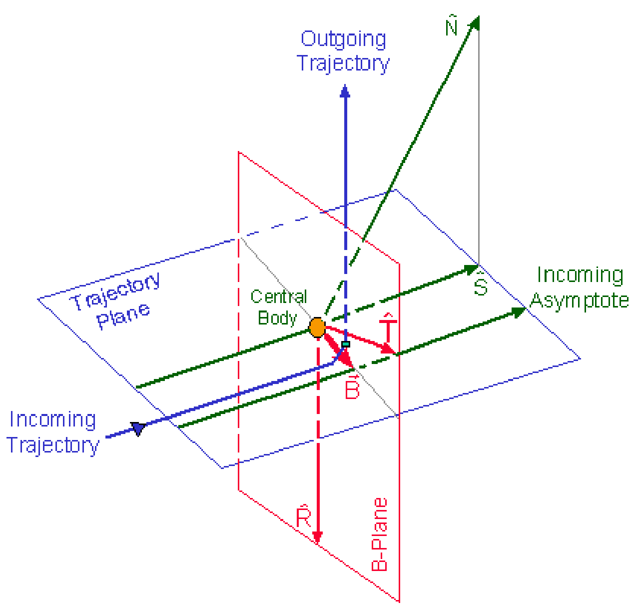

(a) B-Plane Geometry[37]

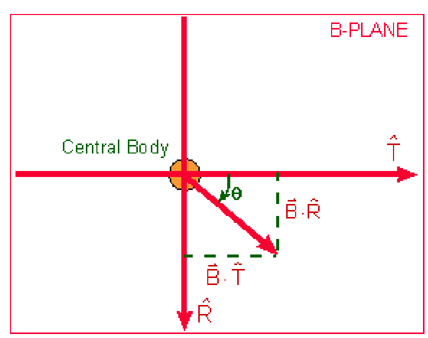

(b) B-Plane Coordinate System[37]

Figure 4.2 : B-Plane Visualization

The unit vector, $\hat{T}$, is orthogonal to the incoming asymptote of the vehicle's hyperbolic path, $\hat{S}$, and the designated north pole of the celestial body, $\hat{N}$,[36]

$$\hat{T} = \frac{\hat{S} \times \hat{N}}{|| \hat{S} \times \hat{N} ||}. \tag{4.1}$$

The unit vector, $\hat{R}$, is orthogonal to the incoming asymptote, $\hat{S}$, and the unit vector, $\hat{T}$,[36]

$$\hat{R} = \hat{S} \times \hat{T}. \tag{4.2}$$

The $\vec{B}$ vector is in the B-Plane and originates at the celestial body's CG and terminates at the intersection of the incoming hyperbolic trajectory and the B-Plane.[36]

Typically, mission requirements specify the accuracy at which the spacecraft intersects the B-Plane which constrains targeting and navigation performance. The end of the $\vec{B}$ vector indicates at what point the vehicle nominally crosses the B-Plane, therefore the $\vec{B}$ vector dispersions often define the mission requirement. The components of the maximum allowable $\vec{B}$ vector dispersions in the $\hat{T}$

$$B_T = \vec{B} \cdot \hat{T}, \tag{4.3}$$

and $\hat{R}$ directions

$$B_R = \vec{B} \cdot \hat{R}, \tag{4.4}$$

constitute a physical corridor in the form of an ellipse projected onto the B-Plane to specify the maximium B-Plane dispersions.[38]

4.2.2 Entry Interface Requirements

The five performance parameters that constitute the top-level mission requirements for EI are the downtrack position, inertial velocity magnitude, inertial flight path angle, crosstrack position, and crosstrack velocity dispersions.[39] These performance metrics are of particular interest in specifying EI corridor requirements because large deviations in these variables can translate to catastrophic mission failure when the vehicle reenters Earth's atmosphere.

Downtrack Position Dispersion

Using Fig 4.3 as a visual reference for the local vertical, local horizontal (LVLH) coordinate system, the spacecraft's downtrack position dispersion is located along the $\hat{\imath}$-direction of a three-dimensional axis system attached to the vehicle with its origin fixed at its CG. The $\hat{\imath}$-direction points along a line tangent to the spacecraft's nominal trajectory, which is nearly aligned with the velocity vector of the spacecraft. The $\hat{k}$-direction is pointed in the direction of a position vector from the CG of the nearest celestial body to the CG of the spacecraft, the radial direction or altitude, and $\hat{\jmath}$ completes the triad, pointing out-of-plane or along the orbital angular velocity vector.

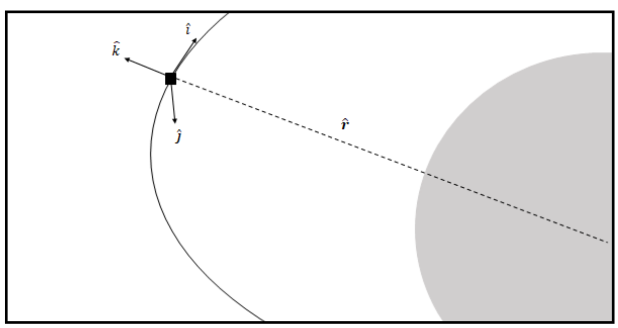

Figure 4.3 : LVLH Coordinate System

Fig 4.4 further develops this inertial reference frame and introduces the crosstrack component, which is orthogonal to the downtrack direction.

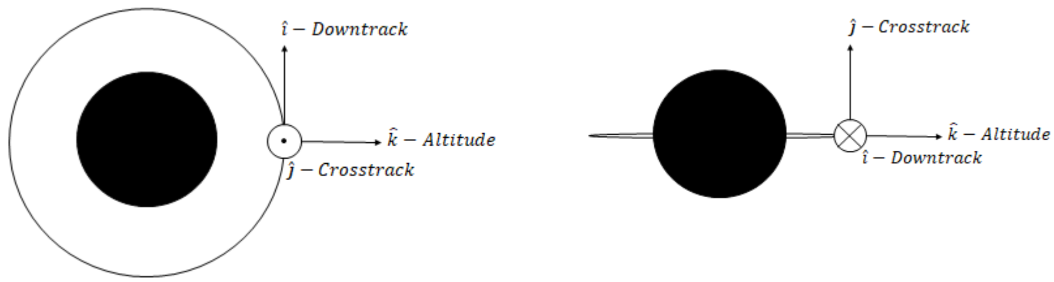

(a) Top View of Orbit

(b) Side View of Orbit

Figure 4.4 : Downtrack versus Crosstrack Position Relative in Space[17]

Inertial Velocity Magnitude Dispersion

The inertial velocity magnitude dispersion is the dispersion of the vehicle's velocity magnitude or speed relative to an inertial reference frame, fixed to the spacecraft's CG.

Inertial Flight Path Angle Dispersion

The inertial flight path angle is the angle between the local horizontal and the inertial velocity vector of the vehicle.[3] Most vehicles are designed for reentry at a specified flight path angle to present the appropriate area of the heat shield to the relative wind.[3] Exceeding the allowable inertial flight path angle dispersions could jeopardize the vehicle, the crew, or the mission. If the flight path angle is too steep, the vehicle could burn up during reentry as a result of excessive exposure. If the flight path angle is too shallow, however, the vehicle could skip off of the atmosphere.

Crosstrack Position Dispersion

Crosstrack position dispersion is orthogonal to downtrack position dispersion and is projected along the $\hat{j}$ direction, as illustrated in Figs 4.3 and 4.4. It describes the out-of-plane dispersions of the vehicle.

Crosstrack Velocity Dispersions

Crosstrack velocity dispersion is the final performance metric for defining EI corridor requirements and is simply the dispersion of the velocity of the spacecraft in the $\hat{k}$ or crosstrack direction.

4.2.3 $|\Delta \mathbf{V}|$ Dispersion

The propellant used represents a key performance parameter to mission planners. A spacecraft has limited capacity, and any additional mass onboard the vehicle increases the launch cost. There is a delicate balance to include sufficient fuel onboard to provide maneuverability and to minimize the overall weight of the spacecraft, to reduce cost. Because propellant usage is directly related to the spacecraft's ability to perform translational maneuvers, $\Delta \mathbf{V}$ is an important performance metric for a GN&C system.

A GN&C system performance requirement for propellant usage is the magnitude of $\Delta \mathbf{V}$ dispersions, or $|\Delta \mathbf{V}|$ dispersions. Unlike the B-Plane and EI mission requirements, which are defined at a particular time epoch, the $|\Delta \mathbf{V}|$ dispersions are monitored over a specified time interval. A $|\Delta \mathbf{V}|$ requirement is imposed on the lunar outbound and return trajectories.

4.3 Cislunar Analysis Assumptions

The optimal GN&C subsystem performance requirements generated from stochastic navigation implemented in the linear covariance analysis and subsequent optimization process are presented. The navigation requirements are defined at the correction burns for each scenario. The thesis presents a wide variety of data for the missions to provide a comprehensive database for reference. A sample of the data is presented in this chapter for a brief, yet insightful look at how the data are used in practice. First, a baseline case for each scenario is presented. Then, three other cases varying in survivability requirements, flight readiness, or cost function are shown in comparison to the baseline. The presentation of the data highlights the effects and sensitivity that each alteration has on the optimal requirements generation.

The baseline case evaluates each trajectory at the Preliminary Design Review (PDR) stage of flight readiness in mission planning. In essence, this means that the weights on the performance requirements are given a wide range so they can fluctuate greatly. Specifically, the lower bounds on the weights for all the error variables is 0.5. The upper bounds on the weights for each error variable is 10.0, except for the navigation error for attitude uncertainty, which is 3.0. These bounds were chosen using engineering judgment and taking into consideration empirical data for the values of the various error sources. It was determined that this range of bounds, standardized from 0.5 to 10.0 for all error sources, provides a wide range of realistic values for the derived optimal performance requirements. As the PDR stage represents the earliest design review, factors such as the expected initial conditions, environmental factors, and actuator options are most likely unknown. Using a wide range for the weights, the expected error source values can vary significantly. The baseline case uses the cost function for optimizing the sum of the weights and uses the mission requirements with a 10% margin, giving a tight tolerance.

The second case likewise simulates values at PDR and uses the cost function for optimizing the sum of the weights as well. The one alteration is the survivability requirement. For this case, the top-level requirements reflect a relaxed requirement of 2.5 times the given mission requirement without a margin.

The third case for consideration maintains the same cost function as the baseline, as well as the baseline mission requirements and margin. The bounds for the weights for IC uncertainty, system process noise, and maneuver execution error are restricted to within 5% (0.95 lower bound and 1.05 upper bound) of the initialized value. This models the Flight Readiness Review (FRR) stage of mission planning where the modeling of the system and environment is well-defined, and the thrusters and other actuators for the mission are chosen. The bounds for the weights for the navigation errors remain the same as the baseline case.

The last case will only differ from the baseline in the cost function. Instead of maximizing the sum of the weights, the cost function parameters will, in effect, de-weight the error sources that initially contribute very little to the overall error compared to those that have a significant contribution.

The remaining cases accounting for all combinations of survivability (Surv), flight readiness (FR), and cost function (CF) are included in Appendix A for reference.

4.4 Lunar Outbound Scenario

The simulated outbound trajectory is illustrated in Fig 4.5a. The four trajectory correction burns are marked by red circles, and the timeline beneath the plot displays the relative timing of each maneuver.

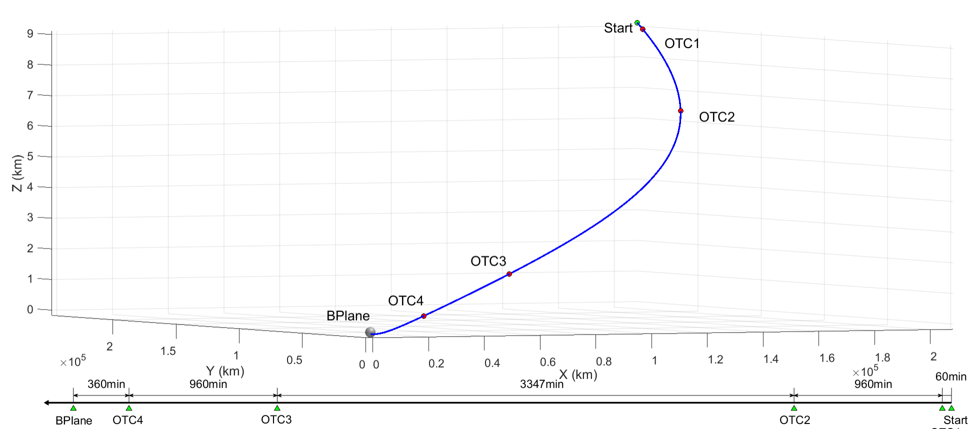

Figure 4.5 : Outbound Maneuvers

The 3-σ B-Plane dispersion mission requirements assumed for the optimal requirement generation are given in Table 4.1. The B-Plane dispersion corridor is depicted in Figs 4.6a and 4.6b, and Fig 4.7a shows the results of the sensitivity analysis of the error variables with Fig 4.7b providing the legend to interpret the individual contributions.

Rqmnt Variable	**Mission Rqmnt (3σ)**
$\mathbf{B} \cdot \mathbf{T}$ (km)	20.0
$\mathbf{B} \cdot \mathbf{R}$ (km)	10.0

Table 4.1 : B-Plane Top-Level Mission Requirements

The B-Plane dispersion corridor's location relative to the Moon is shown in Fig 4.6a. In comparison to the Moon, the corridor appears small, therefore Fig 4.6b provides a closer view of the corridor. The B-Plane dispersions represented by the total performance dispersion ellipse in blue in Fig 4.6b are less than the mission requirements represented by the requirement ellipse in black.

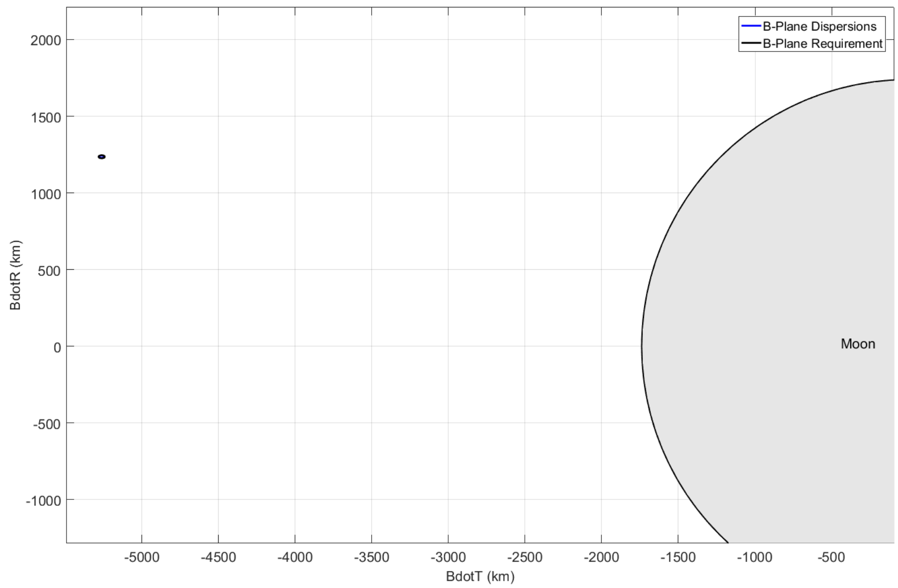

(a) Relative Location of B-Plane Corridor

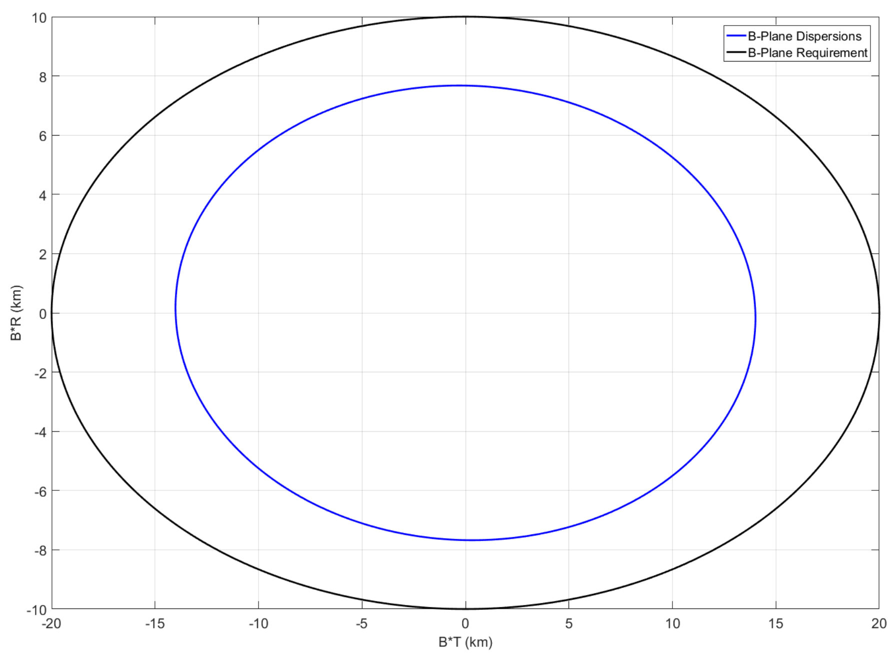

(b) B-Plane Dispersions

Figure 4.6 : Lunar B-Plane

The results of the sensitivity analysis in Fig 4.7a show the contributions of each error source to the total error. For example, the contribution of the navigation errors in position and velocity at OTC-2 ar given in the vertically-oriented, auburn colored ellipse. The largest contributions are the navigation error of the position and velocity at OTC-2 and OTC-4 and the maneuver execution error.

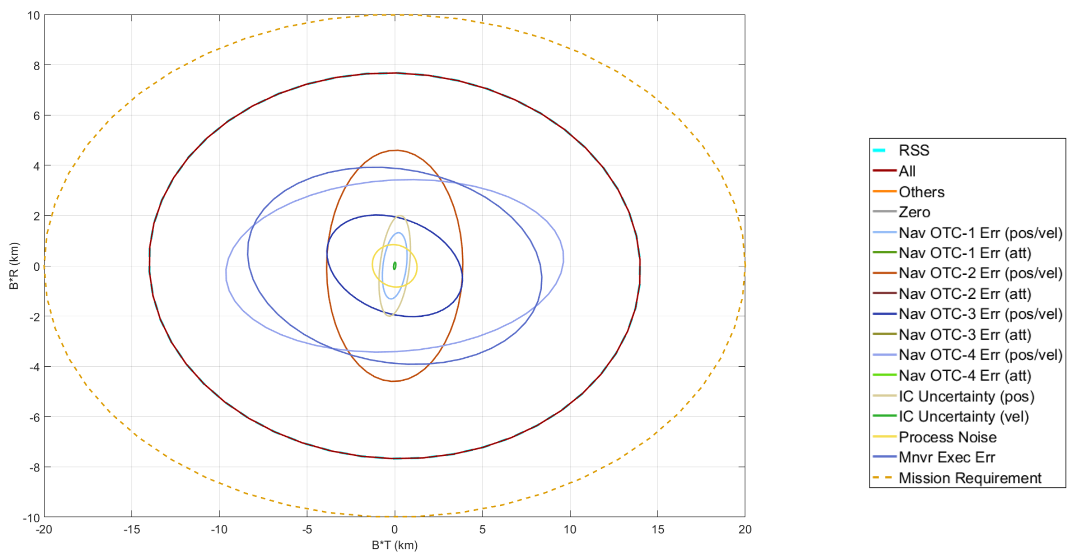

(a) Initial GN&C Subsystem Performance Sensitivity at the B-Plane **(b)** Legend

Figure 4.7 : Outbound Sensitivity Analysis Results

The contribution of the navigation error of the position and velocity at OTC-4 is large, because it is the last correction burn before the B-Plane. Therefore, significant deviations from the nominal trajectory at OTC-4 have a significant impact on the dispersions at the B-Plane, six hours later. The results of the sensitivity analysis provide the foundation upon which the optimal requirement generation is built.

4.4.1 Lunar Outbound - Baseline

Table 4.2 indicates the error contributions of each GN&C subsystem performance variable, their associated, derived optimal weight, and the GN&C subsystem performance requirement. These derived requirements help determine how accurately the navigation system must perform, what level of process noise can be tolerated, how accurately the thrusters and other actuators must perform, and how dispersed from the nominal trajectory the Orion vehicle can initially be, all without exceeding the $\Delta\mathbf{V}$ allocated for the mission.[29]

Error Variable	**Init Value (3σ)**	**Weight**	**Rqmnt (3σ)**
OTC1 Nav Err, Pos (km)	2.50	4.10	10.20
OTC1 Nav Err, Vel (m/s)	0.25	4.10	1.02
OTC1 Nav Err, Att (deg)	0.50	3.00	1.50
OTC2 Nav Err, Pos (km)	1.00	0.50	0.50
OTC2 Nav Err, Vel (m/s)	0.10	0.50	0.05
OTC2 Nav Err, Att (deg)	0.50	3.00	1.50
OTC3 Nav Err, Pos (km)	0.50	2.60	1.30
OTC3 Nav Err, Vel (m/s)	0.05	2.60	0.13
OTC3 Nav Err, Att (deg)	0.50	3.00	1.50
OTC4 Nav Err, Pos (km)	0.38	0.50	0.19
OTC4 Nav Err, Vel (m/s)	0.04	0.50	0.02
OTC4 Nav Err, Att (deg)	0.50	3.00	1.50
IC Uncertainty, Pos (km)	50.00	0.50	25.00
IC Uncertainty, Vel (m/s)	1.00	0.50	0.50
Process Noise ($m/s/\sqrt{s}$)	1.50e-4	3.81	5.72e-4
Manuever Exec Err (m/s)	0.10	0.50	0.05

Table 4.2 : Baseline GN&C Subsystem Requirements - Outbound

For example, the derived, optimal 3-σ navigation requirements for the baseline case are 10.20 km in position, 1.02 m/s in velocity, and 1.50 deg in attitude. It is easier to understand the effects of the optimal weights, by looking at the plots of the error source contributions to the B-Plane dispersions.

The qualitative results for the optimal GN&C subsystem performance requirement generation given the baseline criteria constitute Figs 4.8a - 4.8b. The legend, Fig 4.8c, describes the error source contributions, both before and after weighting. The original contributions of each error source from the sensitivity analysis are plotted with solid lines. The ellipses scaled by optimal weights are plotted in the corresponding color but with dashed lines. The original and weighted ellipses are plotted together to qualitatively show the effects of the optimal weighting. The solid black line defines the mission requirement and the solid red line represents the mission requirement with a 10% margin. The solid cyan line now represents the RSS, total error ellipse prior to applying the optimal weights. The dashed cyan line is the weighted, total error ellipse, i.e. the RSS of the individual error ellipses after they are scaled by their corresponding optimal weights. The solid cyan line approaches, but does not touch the requirement margin, however, the dashed cyan line does meet the requirements.

Fig 4.8b displays the time history requirement, $|\Delta \mathbf{V}|$ dispersions. A top-level mission requirement is imposed at each of the four navigation regions that are defined between the correction burns and after OTC-4 to the end of the simulation. The $|\Delta \mathbf{V}|$ dispersions are constrained to 3-σ values of 3.3 m/s, 3.75 m/s, 3.3 m/s, and 6 m/s, respectively with a 10% margin. Note that in addition to meeting the B-Plane dispersion requirement, the optimization also weights the error source contributions to the $|\Delta \mathbf{V}|$ dispersions in such a manner as to hit the mission requirement in the first and fourth navigation regions.

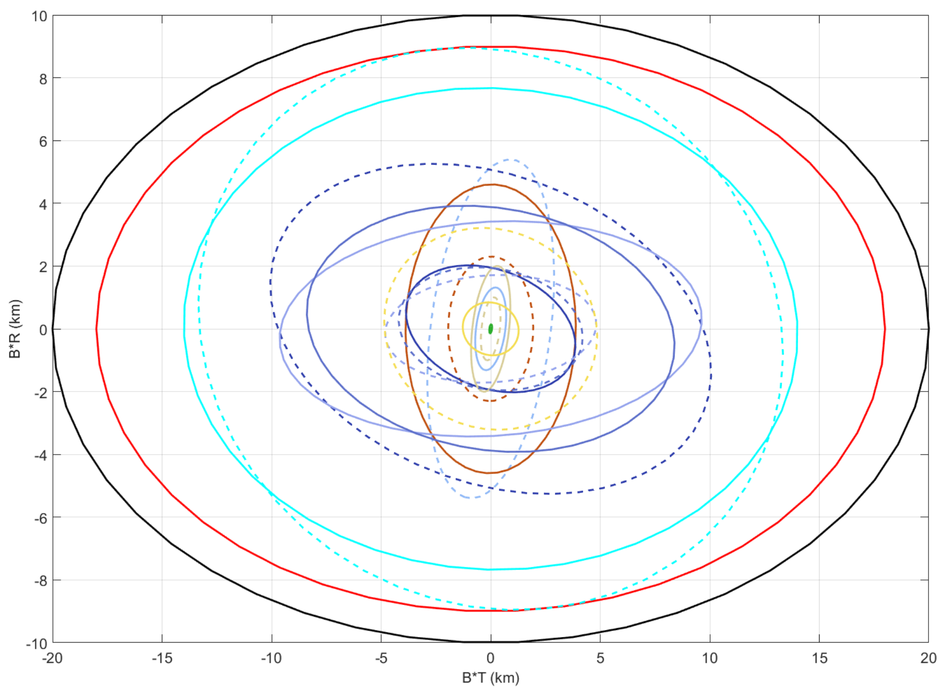

(a) B-Plane Dispersions

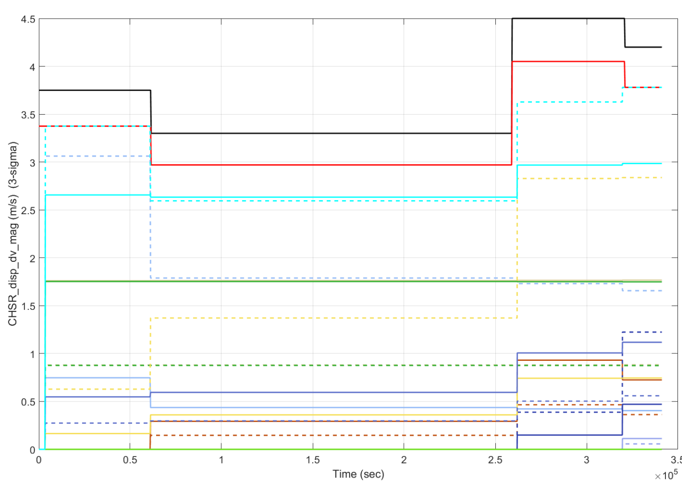

(b) Time History of $|\Delta \mathbf{V}|$ Dispersions

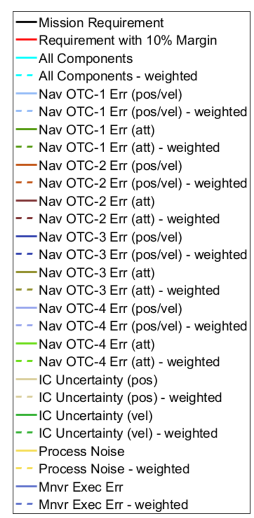

(c) Legend

Figure 4.8 : Outbound Trajectory - Baseline

4.4.2 Lunar Outbound - Survivability Altered

The survivability requirement is the same as the mission requirements multiplied by 2.5. It represents a relaxed requirement that models a requirement that solely ensures the crew's survival, disregarding any mission objectives and the condition of the spacecraft. As a result, the RSS ellipse can expand significantly. In contrast to the baseline case where error sources that initially contribute a lot to overall error are scaled down, in order to hit mission requirements, the largest contributor (the navigation error of position and velocity at OTC-4) is expanded a lot. The navigation requirement at OTC-4 for the survivability altered case is 8.03 times greater than the baseline case requirement. Once again, the $|\mathbf{\Delta V}|$ dispersion mission requirements of the first and last navigation region are met.

Error Variable	**Init Value (3σ)**	**Weight**	**Rqmnt (3σ)**
OTC1 Nav Err, Pos (km)	2.50	4.18	10.50
OTC1 Nav Err, Vel (m/s)	0.25	4.18	1.05
OTC1 Nav Err, Att (deg)	0.50	3.00	1.50
OTC2 Nav Err, Pos (km)	1.00	0.50	0.50
OTC2 Nav Err, Vel (m/s)	0.10	0.50	0.05
OTC2 Nav Err, Att (deg)	0.50	3.00	1.50
OTC3 Nav Err, Pos (km)	0.50	6.39	3.20
OTC3 Nav Err, Vel (m/s)	0.05	6.39	0.32
OTC3 Nav Err, Att (deg)	0.50	3.00	1.50
OTC4 Nav Err, Pos (km)	0.38	4.50	1.69
OTC4 Nav Err, Vel (m/s)	0.04	4.50	0.17
OTC4 Nav Err, Att (deg)	0.50	3.00	1.50
IC Uncertainty, Pos (km)	50.00	0.50	25.00
IC Uncertainty, Vel (m/s)	1.00	0.50	0.50
Process Noise ($m/s/\sqrt{s}$)	1.50e-4	0.50	7.50e-5
Manuever Exec Err (m/s)	0.10	0.50	0.05

Table 4.3 : Surv Altered GN&C Subsystem Requirements - Outbound

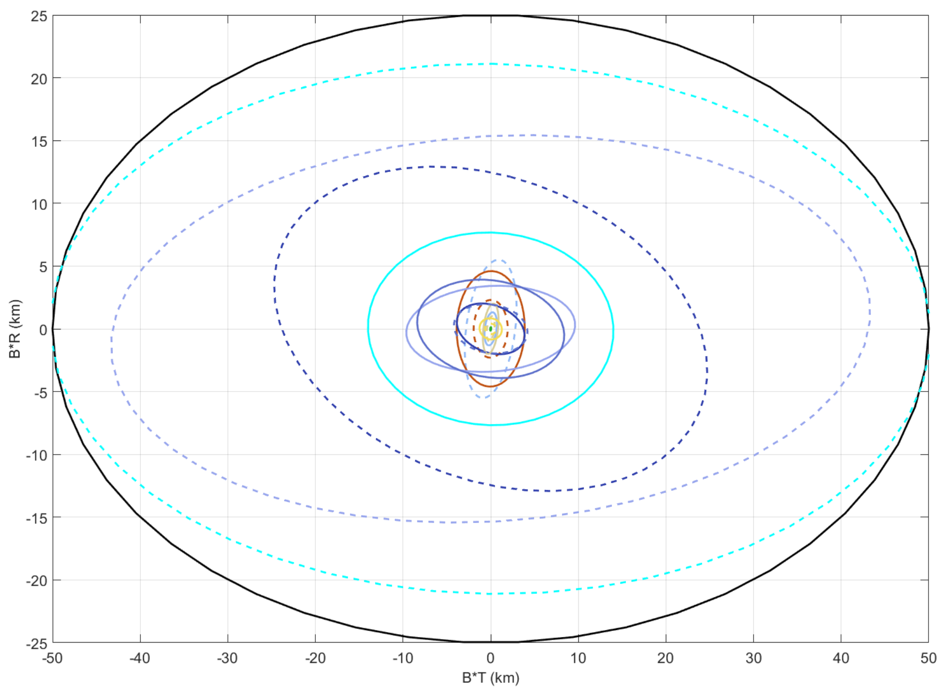

(a) B-Plane Dispersions

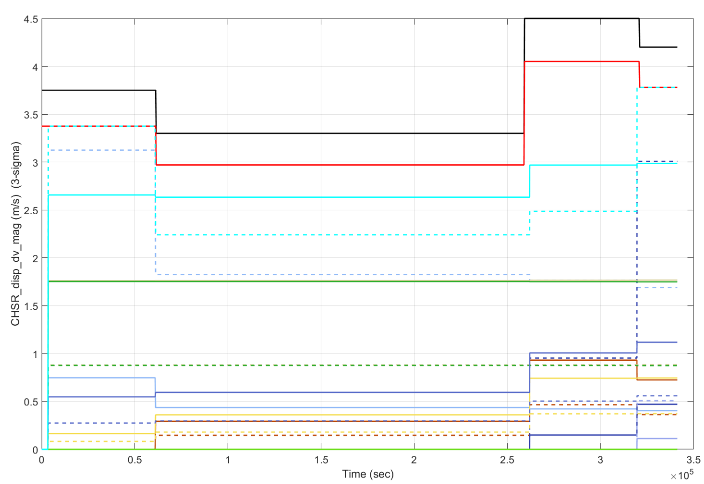

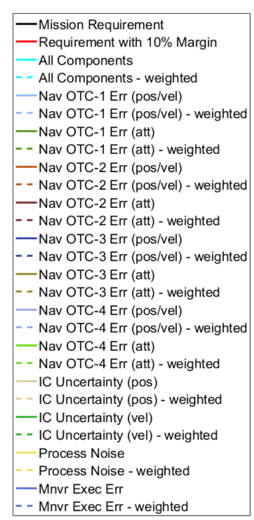

(b) Time History of $|\Delta \mathbf{V}|$ Dispersions **(c)** Legend

Figure 4.9 : Outbound Trajectory - Survivability Requirements Altered

4.4.3 Lunar Outbound - Flight Readiness Altered

The variation in flight readiness tightens the bounds on the weights for the IC uncertainty for position and velocity, system process noise, and maneuver execution error to a lower bound of 0.95 and an upper bound of 1.05. Table 4.4 summarizes the derived performance requirements for this case. Decreasing the range on the bounds of the weights for these error variables yields a 90% increase from the baseline in the derived requirements for three of these four variables. Only the performance requirement for system process noise decreases. These differences can be accounted for in the fact that in the baseline case, all four of these error sources are weighted with the lower bound weight of 0.5. The IC uncertainty for position and velocity also tends to the lower bound for this case, however, the lower bound is increased from the baseline 90%. The navigation requirements vary only slightly from the baseline, with a small decrease in the navigation requirement at OTC-1 and a small increase in the navigation requirement at OTC-3. These results show that even when the IC uncertainty, process noise, and maneuver execution error are well-known during the FRR phase, the mission planner can expect small deviations in the optimal navigation requirements for the lunar outbound trajectory.

Error Variable	**Init Value (3σ)**	**Weight**	**Rqmnt (3σ)**
OTC1 Nav Err, Pos (km)	2.50	3.14	7.86
OTC1 Nav Err, Vel (m/s)	0.25	3.14	0.79
OTC1 Nav Err, Att (deg)	0.50	3.00	1.50
OTC2 Nav Err, Pos (km)	1.00	0.50	0.50
OTC2 Nav Err, Vel (m/s)	0.10	0.50	0.050
OTC2 Nav Err, Att (deg)	0.50	3.00	1.50
OTC3 Nav Err, Pos (km)	0.50	2.94	1.47
OTC3 Nav Err, Vel (m/s)	0.05	2.94	0.15
OTC3 Nav Err, Att (deg)	0.50	3.00	1.50
OTC4 Nav Err, Pos (km)	0.38	0.50	0.19
OTC4 Nav Err, Vel (m/s)	0.04	0.50	0.02
OTC4 Nav Err, Att (deg)	0.50	3.00	1.50
IC Uncertainty, Pos (km)	50.00	0.95	47.50
IC Uncertainty, Vel (m/s)	1.00	0.95	0.95
Process Noise (m/s/$\sqrt{s}$)	1.50e-4	1.05	1.57e-4
Manuever Exec Err (m/s)	0.10	0.95	0.10

Table 4.4 : FR Altered GN&C Subsystem Requirements - Outbound

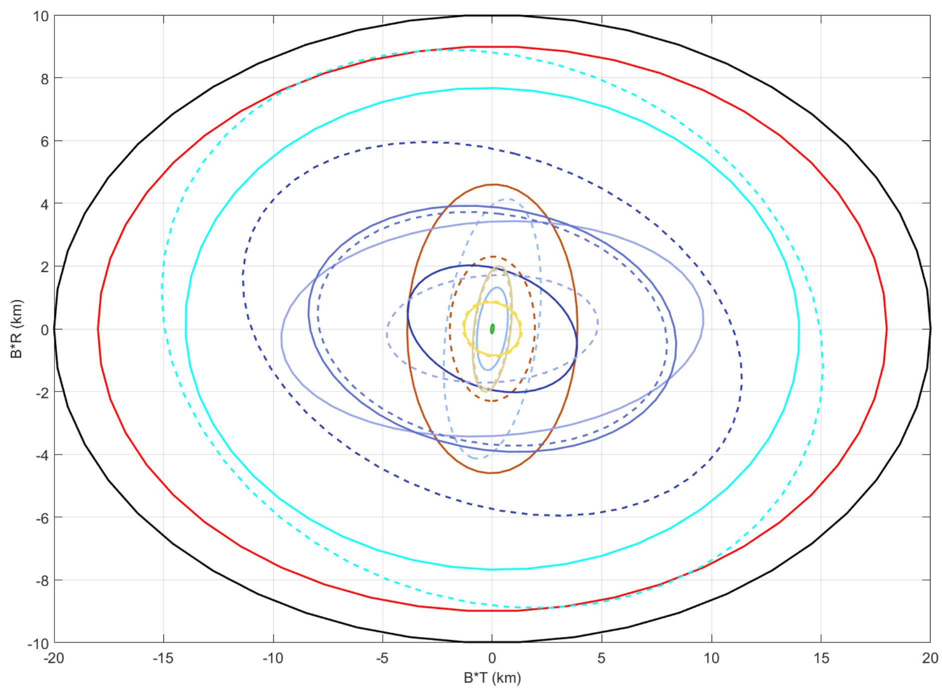

(a) B-Plane Dispersions

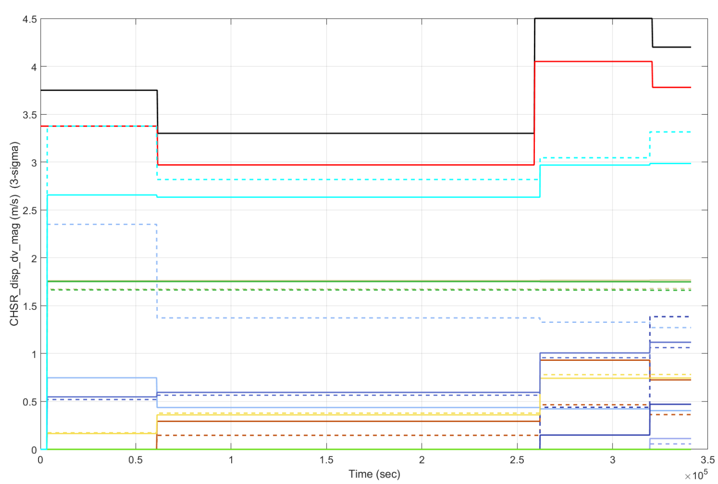

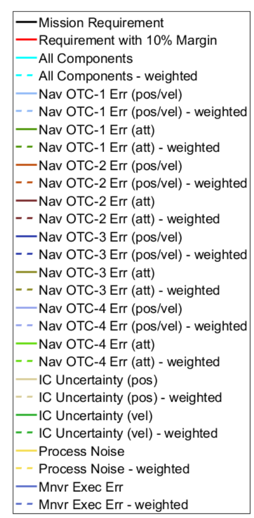

(b) Time History of $|\Delta \mathbf{V}|$ Dispersions

(c) Legend

Figure 4.10 : Outbound Trajectory - Flight Readiness Altered

4.4.4 Lunar Outbound - Cost Function Altered

Table 4.5 provides the derived navigation and other GN&C system performance requirements with a different cost function. The optimization de-weights the error sources that initially contribute a relatively small amount to the uncertainty. In this case, the different cost function yields identical results to the baseline case. Tables 4.6 and 4.7 are summary tables of all of the results, including those included in Appendix A (Table 4.7). Although only altering the cost function for this scenario yields results equivalent to the baseline, the results summarized in Table 4.7 show that the studies altering the survivability requirements and/or the flight readiness with the second cost function yield different results than altering the survivability requirements and/or flight readiness with the first cost function. For example, the navigation requirement at OTC-1 with survivability requirements and the first cost function are 10.50 km and 1.05 m/s. In contrast, the navigation requirement at OTC-1 with survivability requirements and the second cost function are 1.25 km and 0.13 m/s. Therefore, the second cost function does affect the results for equivalent outbound cases other than the baseline.

Error Variable	**Init Value (3σ)**	**Weight**	**Rqmnt (3σ)**
OTC1 Nav Err, Pos (km)	2.50	4.10	10.20
OTC1 Nav Err, Vel (m/s)	0.25	4.10	1.02
OTC1 Nav Err, Att (deg)	0.50	3.00	1.50
OTC2 Nav Err, Pos (km)	1.00	0.50	0.50
OTC2 Nav Err, Vel (m/s)	0.10	0.50	0.05
OTC2 Nav Err, Att (deg)	0.50	3.00	1.50
OTC3 Nav Err, Pos (km)	0.50	2.60	1.30
OTC3 Nav Err, Vel (m/s)	0.05	2.60	0.13
OTC3 Nav Err, Att (deg)	0.50	3.00	1.50
OTC4 Nav Err, Pos (km)	0.38	0.50	0.19
OTC4 Nav Err, Vel (m/s)	0.04	0.50	0.02
OTC4 Nav Err, Att (deg)	0.50	3.00	1.50
IC Uncertainty, Pos (km)	50.00	0.50	25.00
IC Uncertainty, Vel (m/s)	1.00	0.50	0.50
Process Noise (m/s/$\sqrt{s}$)	1.50e-4	3.81	5.72e-4
Manuever Exec Err (m/s)	0.10	0.50	0.05

Table 4.5 : CF Altered GN&C Subsystem Requirements - Outbound

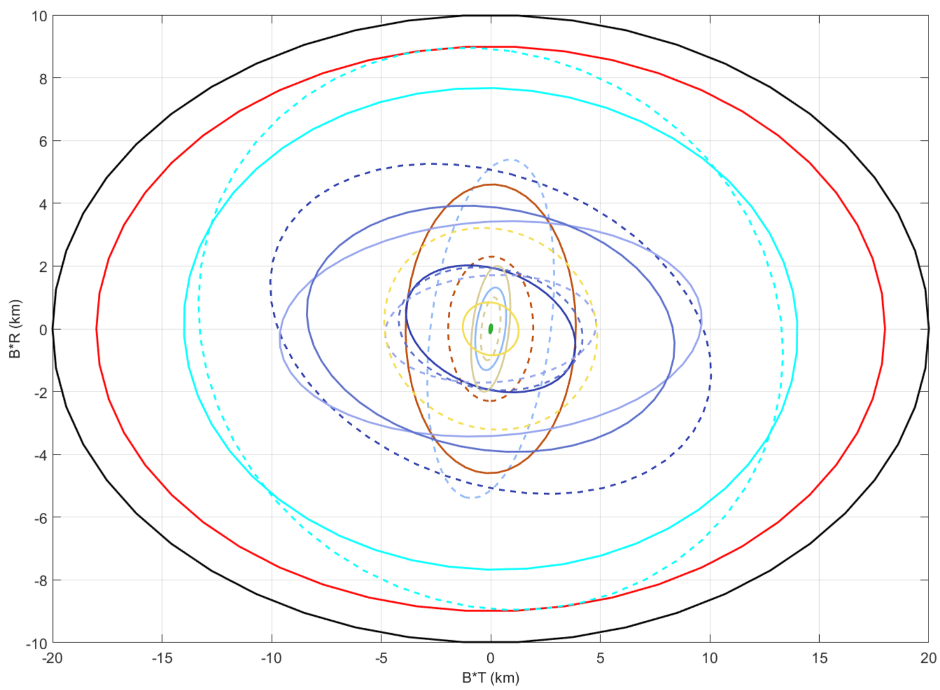

(a) B-Plane Dispersions

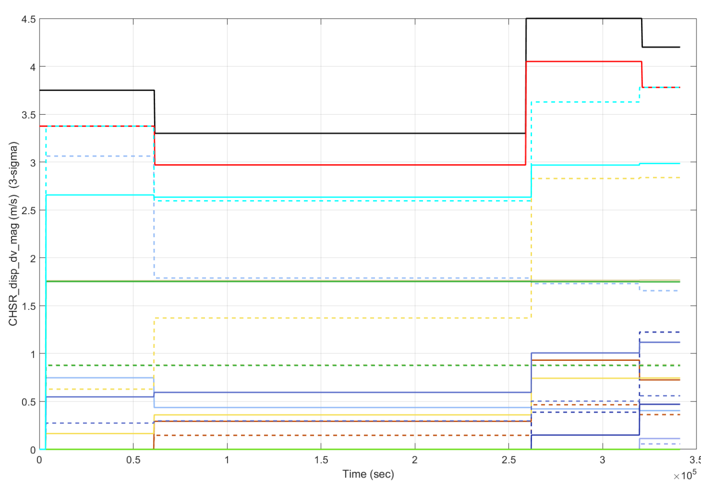

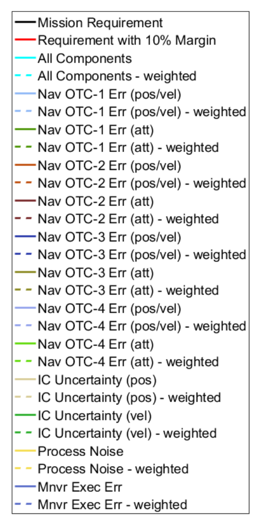

(b) Time History of $|\Delta\mathbf{V}|$ Dispersions

(c) Legend

Figure 4.11 : Outbound Trajectory - Cost Function Altered

4.4.5 Lunar Outbound - Summary

Error Variable	Baseline	Survivability Altered	Flight Readiness Altered	Cost Function Altered
OTC1 Nav Err, Pos (km)	10.20	10.50 (+2.94%)	7.86 (-22.94%)	10.20 (+0.00%)
OTC1 Nav Err, Vel (m/s)	1.02	1.05 (+2.94%)	0.79 (-22.94%)	1.02 (+0.00%)
OTC1 Nav Err, Att (deg)	1.50	1.50 (+0.00%)	1.50 (+0.00%)	1.50 (+0.00%)
OTC2 Nav Err, Pos (km)	0.50	0.50 (+0.00%)	0.50 (+0.00%)	0.50 (+0.00%)
OTC2 Nav Err, Vel (m/s)	0.05	0.05 (+0.00&)	0.05 (+0.00%)	0.05 (+0.00%)
OTC2 Nav Err, Att (deg)	1.50	1.50 (+0.00%)	1.50 (+0.00)	1.50 (+0.00%)
OTC3 Nav Err, Pos (km)	1.30	3.20 (+146.15%)	1.47 (+13.08%)	1.30 (+0.00%)
OTC3 Nav Err, Vel (m/s)	0.13	0.32 (+146..15%)	0.15 (+13.08%)	0.13 (+0.00%)
OTC3 Nav Err, Att (deg)	1.50	1.50 (+0.00%)	1.50 (+0.00%)	1.50 (+0.00%)
OTC4 Nav Err, Pos (km)	0.19	1.69 (+803.74%)	0.19 (+0.00%)	0.19 (+0.00%)
OTC4 Nav Err, Vel (m/s)	0.02	0.17 (+803.74)	0.02 (+0.00%)	0.02 (+0.00%)
OTC4 Nav Err, Att (deg)	1.50	1.50 (+0.00%)	1.50 (+0.00%)	1.50 (+0.00%)
IC Uncertainty, Pos (km)	25.00	25.00 (+0.00%)	47.50 (+90.00%)	25.00 (+0.00%)
IC Uncertainty, Vel (m/s)	0.50	0.50 (+0.00%)	0.95 (+90.00%)	0.50 (+0.00%)
Process Noise ($m/s/\sqrt{s}$)	5.72e-4	7.50e-5 (-86.89%)	1.57e-4 (-72.55%)	5.72e-4 (+0.00%)
Manuever Exec Err (m/s)	0.05	0.05 (+0.00%)	0.10 (+90.00)	0.05 (+0.00%)

Table 4.6 : Outbound Trajectory Summary Table 1 of 2

Error Variable	Baseline	Surv & FR Altered	Surv & CF Altered	FR & CF Altered	Surv, FR, and CF Altered
OTC1 Nav Err, Pos (km)	10.20	7.86 (-22.94%)	1.25 (-87.75%)	7.86 (-22.94%)	1.25 (-87.75%)
OTC1 Nav Err, Vel (m/s)	1.02	0.79 (-22.94%)	0.13 (-87.75%)	0.79 (-22.94%)	0.13 (-87.75%)
OTC1 Nav Err, Att (deg)	1.50	1.50 (+0.00%)	1.50 (+0.00%)	1.50 (+0.00%)	1.50 (+0.00%)
OTC2 Nav Err, Pos (km)	0.50	0.50 (+0.00%)	0.50 (+0.00%)	0.50 (+0.00%)	0.50 (+0.00%)
OTC2 Nav Err, Vel (m/s)	0.05	0.05 (+0.00%)	0.05 (+0.00%)	0.05 (+0.00%)	0.05 (+0.00%)
OTC2 Nav Err, Att (deg)	1.50	1.50 (+0.00%)	1.50 (+0.00%)	1.50 (+0.00%)	1.50 (+00.0%)
OTC3 Nav Err, Pos (km)	1.30	2.39 (+83.85%)	3.66 (+181.54%)	1.47 (+13.08%)	2.74 (+110.77%)
OTC3 Nav Err, Vel (m/s)	0.13	0.24 (+83.85%)	0.37 (+181.54%)	0.15 (+13.08%)	0.27 (+110.77%)
OTC3 Nav Err, Att (deg)	1.50	1.50 (+0.00%)	1.50 (+0.00%)	1.50 (+0.00%)	1.50 (+0.00%)
OTC4 Nav Err, Pos (km)	0.19	1.78 (+851.87%)	1.61 (+760.96%)	0.19 (+0.0%)	1.74 (+830.48%)
OTC4 Nav Err, Vel (m/s)	0.02	0.18 (+851.87%)	0.16 (+760.96%)	0.02 (+0.0%)	0.17 (+830.48%)
OTC4 Nav Err, Att (deg)	1.50	1.50 (+0.00%)	1.50 (+0.00%)	1.50 (+0.00%)	1.50 (+0.00%)
IC Uncertainty, Pos (km)	25.00	47.50 (+90.00%)	25.00 (+0.00%)	47.50 (+90.00%)	47.50 (+90.00%)
IC Uncertainty, Vel (m/s)	0.50	0.95 (+90.00%)	0.50 (+0.00%)	0.95 (+90.00%)	0.95 (+90.00%)
Process Noise (m/s/$\sqrt{s}$)	5.72e-4	1.42e-4 (-75.17%)	7.50e-5 (-86.89%)	1.57e-4 (-72.55%)	1.42e-4 (-75.17%)
Manuever Exec Err (m/s)	0.05	0.10 (+90.00%)	0.05 (+0.00%)	0.10 (+90.00%)	0.10 (+90.00%)

Table 4.7 : Outbound Trajectory Summary Table 2 of 2

4.5 Lunar Return Scenario

After the lunar flyby for EM1, Orion returns to the Earth by following the trajectory illustrated in Fig 4.12a. The three return trajectory correction burns are labeled by the red circles along the nominal path. The three navigation regions include the two regions between RTC-4 and RTC-5 and RTC-5 and RTC-6 and the segment after RTC-6 until EI.

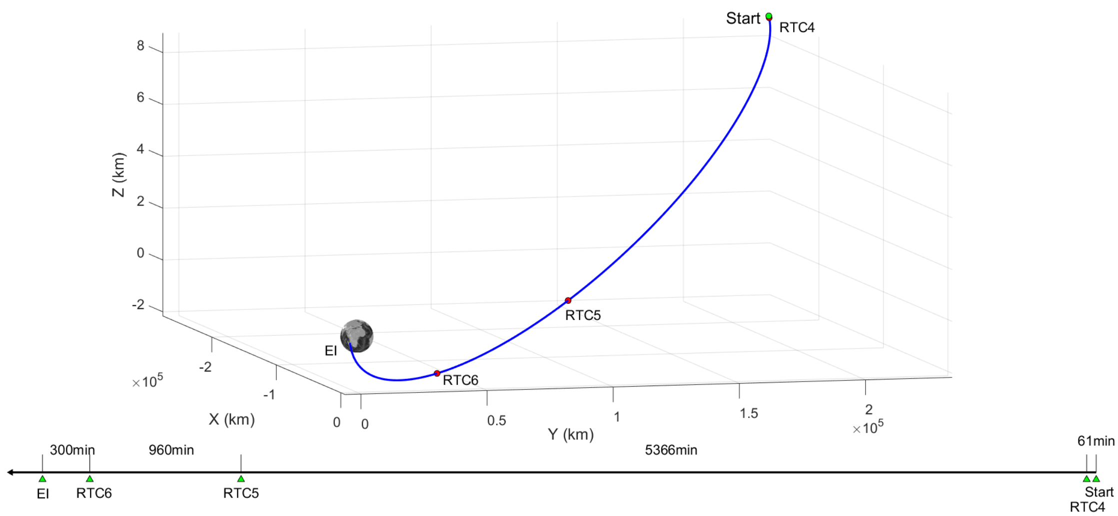

Figure 4.12 : Return Trajectory

The lunar return trajectory increases in complexity with five mission requirement parameters that must be met. They are shown in Table 4.5 with their 3-σ requirement values.[39] The EI mission requirement parameters are also correlated, and their correlation coefficients are given in Table 4.9.[39]

Rqmnt Variables	**Mission Rqmnt (3σ)**
Downtrack Position (km)	25.66
Velocity Magnitude (m/s)	5.33
Flight Path Angle (deg)	0.12
Crosstrack Position (km)	7.04
Crosstrack Velocity (m/s)	8.23

Table 4.8 : EI Top-Level Mission Requirements

Performance Constraints	**Corr Coeff**
Downtrack Position and Velocity Magnitude	-0.60
Downtrack Position and Flight Path Angle	-0.50
Crosstrack Position and Crosstrack Velocity	0.29
Velocity Magnitude and Flight Path Angle	0.55

Table 4.9 : Correlation Coefficients for Performance Constraints

Figs 4.13a - 4.14c display the sensitivity analysis information used for the optimal GN&C performance requirement generation at EI. The multiple mission requirements and multiple constraints would increase the difficulty of deriving the performance requirements with a traditional engineering heuristics approach. However, with the systematic approach demonstrated in this research, the performance requirements are derived in the same way regardless of the complexity of the problem. Each error source contributes uniquely to each of the mission requirement ellipses, however maneuver execution error and the position and velocity navigation error at RTC-6 consistently contribute significantly to the dispersions of the mission requirement parameters.

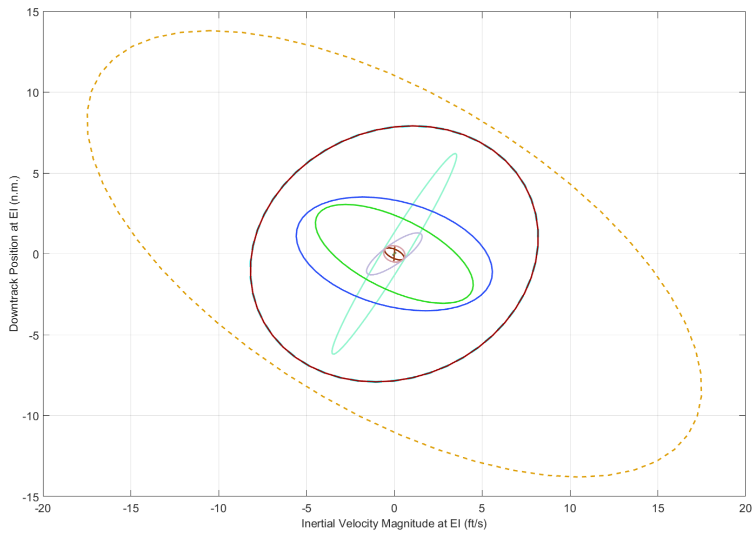

(a) Initial GN&C Subsystem Performance Sensitivity at EI: Downtrack Position v. Velocity Magnitude

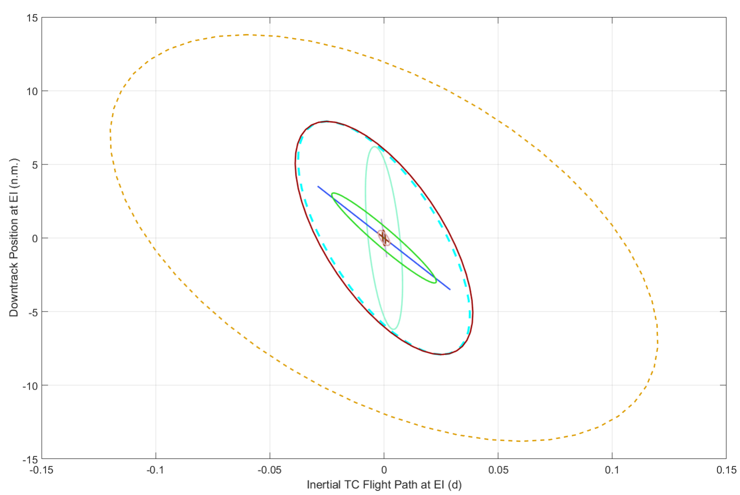

(b) Initial GN&C Subsystem Performance Sensitivity at EI: Downtrack Position v. Flight Path Angle

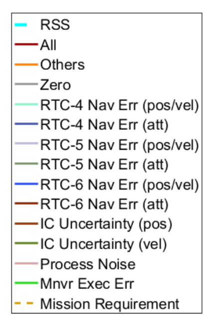

(c) Legend

Figure 4.13 : Return Sensitivity Analysis Results 1 of 2

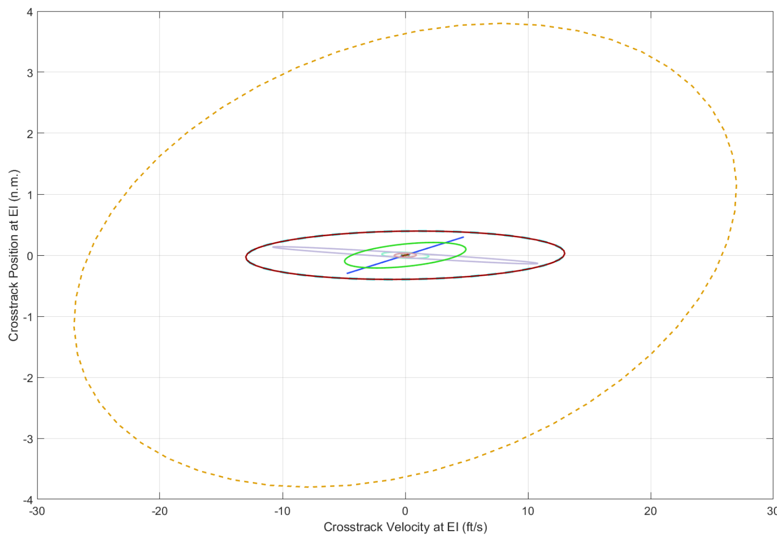

(a) Initial GN&C Subsystem Performance Sensitivity at EI: Crosstrack Position v. Crosstrack Velocity

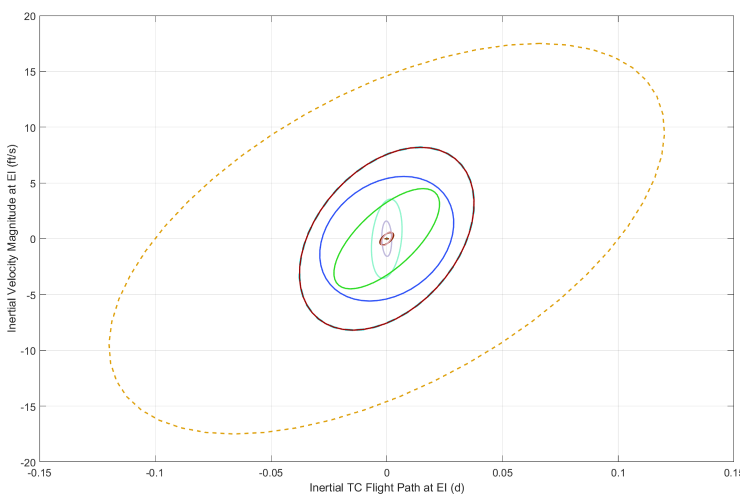

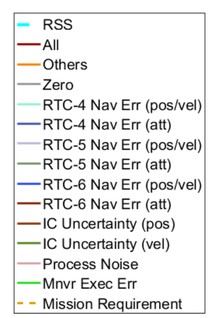

(b) Initial GN&C Subsystem Performance Sensitivity at EI: Velocity Magnitude v. Flight Path Angle

(c) Legend

Figure 4.14 : Return Sensitivity Analysis Results 2 of 2

4.5.1 Lunar Return - Baseline

Referencing Table 4.10, in a similar manner to the lunar outbound baseline case, the return baseline case scales down the error variables that initially contribute a lot to overall error in the sensitivity study. The position and velocity navigation error at RTC-6 are scaled down by a factor of 0.59, approaching the lower bound. The derived navigation requirement at RTC-6 is 0.29 km, 0.03 m/s, with an attitude uncertainty of 1.50 degrees. Analyzing Figs 4.15a - 4.15e, the optimization allows the requirements for downtrack position and velocity magnitude dispersions and crosstrack position and crosstrack velocity dispersions to be met in addition to the $|\mathbf{\Delta V}|$ dispersions in the first navigation region.

Error Variable	**Init Value (3σ)**	**Weight**	**Rqmnt (3σ)**
RTC4 Nav Err, Pos (km)	2.50	0.50	1.25
RTC4 Nav Err, Vel (m/s)	0.25	0.50	0.13
RTC4 Nav Err, Att (deg)	0.50	3.00	1.50
RTC5 Nav Err, Pos (km)	1.00	1.91	1.91
RTC5 Nav Err, Vel (m/s)	0.10	1.91	0.19
RTC5 Nav Err, Att (deg)	0.50	3.00	1.50
RTC6 Nav Err, Pos (km)	0.50	0.59	0.29
RTC6 Nav Err, Vel (m/s)	0.05	0.59	0.03
RTC6 Nav Err, Att (deg)	0.50	3.00	1.50
IC Uncertainty, Pos (km)	50.00	9.55	477.00
IC Uncertainty, Vel (m/s)	1.00	0.50	0.50
Process Noise ($m/s/\sqrt{s}$)	1.50e-4	10.00	1.50e-3
Manuever Exec Err (m/s)	0.10	0.50	0.05

Table 4.10 : Baseline GN&C Subsystem Requirements - Return

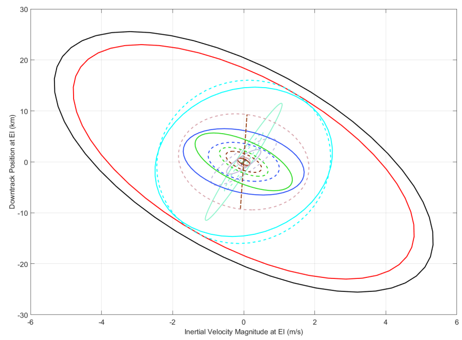

(a) Downtrack Position v. Velocity Magnitude

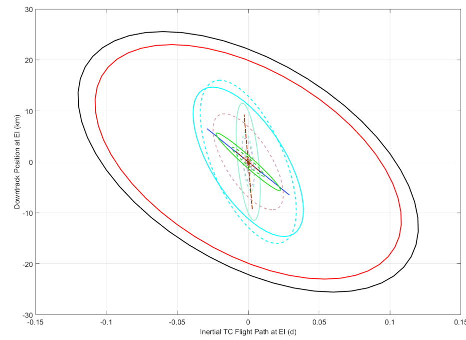

(b) Downtrack Position v. Flight Path Angle

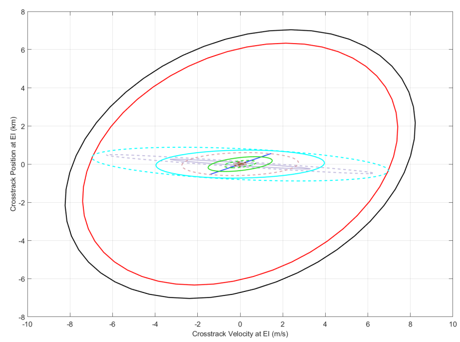

(c) Crosstrack Position v. Crosstrack Velocity

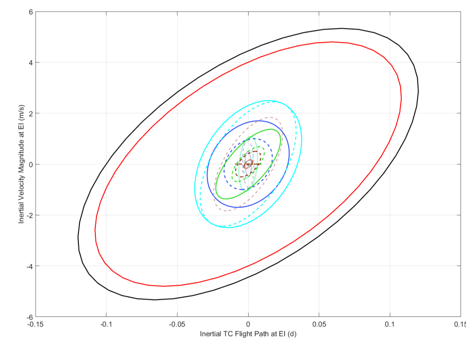

(d) Velocity Magnitude v. Flight Path Angle

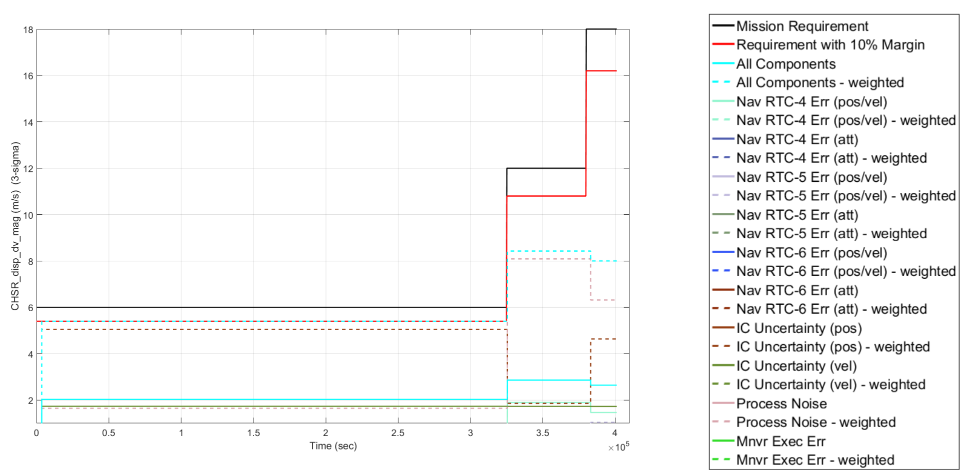

(e) Time History of $|\mathbf{\Delta V}|$ Dispersions

Figure 4.15 : Return Trajectory - Baseline

4.5.2 Lunar Return - Survivability Altered

The relaxed mission requirements for the survivability altered case allows the optimization to weight the contribution of the position and velocity navigation error at RTC-6 resulting in a derived navigation requirement at RTC-6 over 8 times the baseline value. All of the other error variables are weighted the same as in the baseline case except the position and velocity navigation error at RTC-5. Figs 4.16a, 4.16c, and 4.16e show that the correlated performance parameter dispersions of downtrack position and inertial velocity magnitude and crosstrack position and crosstrack velocity, as well as $|\Delta \mathbf{V}|$ dispersions in the first navigation region limit the GN&C system performance.

Error Variable	**Init Value (3σ)**	**Weight**	**Rqmnt (3σ)**
RTC4 Nav Err, Pos (km)	2.50	0.50	1.25
RTC4 Nav Err, Vel (m/s)	0.25	0.50	0.13
RTC4 Nav Err, Att (deg)	0.50	3.00	1.50
RTC5 Nav Err, Pos (km)	1.00	5.40	5.40
RTC5 Nav Err, Vel (m/s)	0.10	5.40	0.54
RTC5 Nav Err, Att (deg)	0.50	3.00	1.50
RTC6 Nav Err, Pos (km)	0.50	5.35	2.67
RTC6 Nav Err, Vel (m/s)	0.05	5.35	0.27
RTC6 Nav Err, Att (deg)	0.50	3.00	1.50
IC Uncertainty, Pos (km)	50.00	9.55	477.00
IC Uncertainty, Vel (m/s)	1.00	0.50	0.50
Process Noise (m/s/$\sqrt{s}$)	1.50e-4	10.00	1.50e-3
Manuever Exec Err (m/s)	0.10	0.50	0.05

Table 4.11 : Survivability Altered GN&C Subsystem Requirements - Return

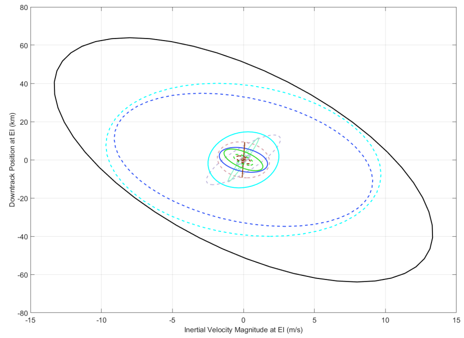

(a) Downtrack Position v. Velocity Magnitude

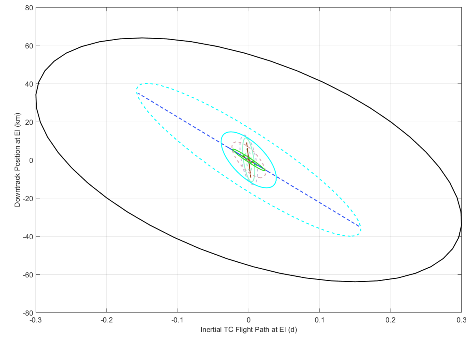

(b) Downtrack Position v. Flight Path Angle

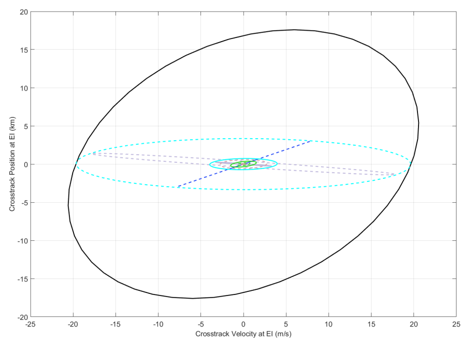

(c) Crosstrack Position v. Crosstrack Velocity

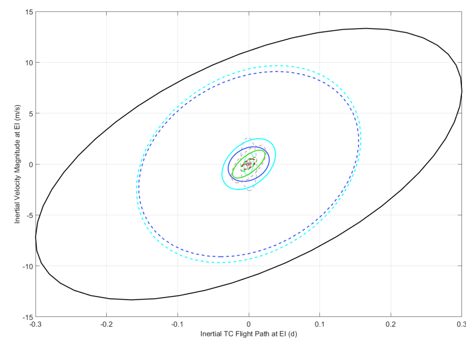

(d) Velocity Magnitude v. Flight Path Angle

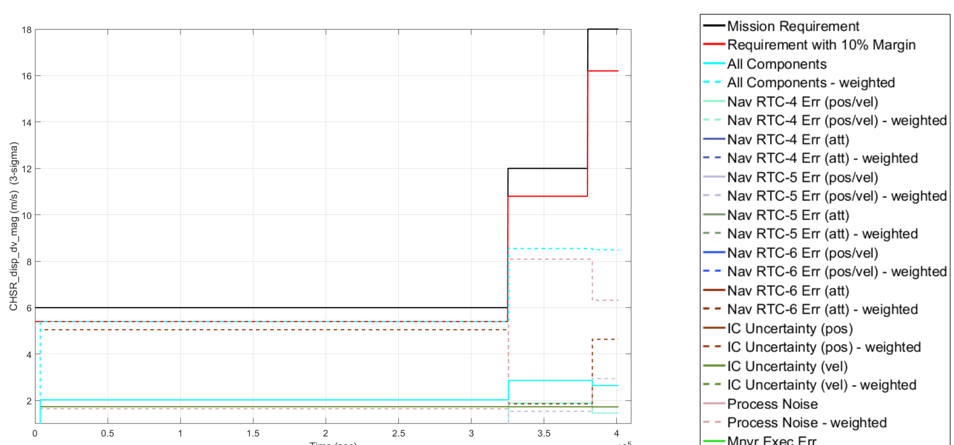

(e) Time History of $|\Delta \mathbf{V}|$ Dispersions

Figure 4.16 : Return Trajectory - Survivability Altered

4.5.3 Lunar Return - Flight Readiness Altered

In the variation for FRR, all of the error sources that are not navigation errors are scaled by the upper bound of the weights, as the cost function maximizes the sum of the weights. Another notable difference from the baseline, and the other variations is that contributions of all the error sources are not capped by the $|\Delta \mathbf{V}|$ dispersion requirements. In fact, the weighted RSS contributions are less than or equal to the original sensitivity study values. This is likely caused by the decreased value of the IC uncertainty for position. The optimal performance requirement for this error variable is 88.99% less than the baseline and the other primary variations.

Error Variable	**Init Value (3σ)**	**Weight**	**Rqmnt (3σ)**
RTC4 Nav Err, Pos (km)	2.50	0.50	1.25
RTC4 Nav Err, Vel (m/s)	0.25	0.50	0.125
RTC4 Nav Err, Att (deg)	0.50	3.00	1.50
RTC5 Nav Err, Pos (km)	1.00	1.50	1.50
RTC5 Nav Err, Vel (m/s)	0.10	1.50	0.15
RTC5 Nav Err, Att (deg)	0.50	3.00	1.50
RTC6 Nav Err, Pos (km)	0.50	1.69	0.85
RTC6 Nav Err, Vel (m/s)	0.05	1.69	0.09
RTC6 Nav Err, Att (deg)	0.50	3.0	1.50
IC Uncertainty, Pos (km)	50.00	1.05	52.50
IC Uncertainty, Vel (m/s)	1.00	1.05	1.05
Process Noise (m/s/$\sqrt{s}$)	1.50e-4	1.05	1.57e-4
Manuever Exec Err (m/s)	0.10	1.05	0.11

Table 4.12 : Flight Readiness Altered GN&C Subsystem Requirements - Return

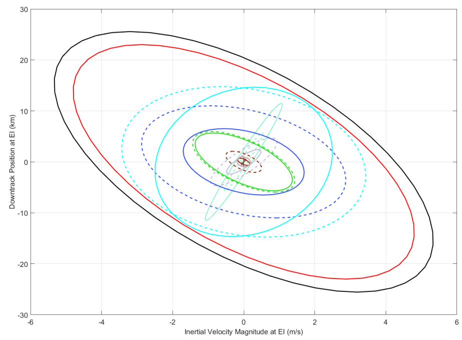

(a) Downtrack Position v. Velocity Magnitude

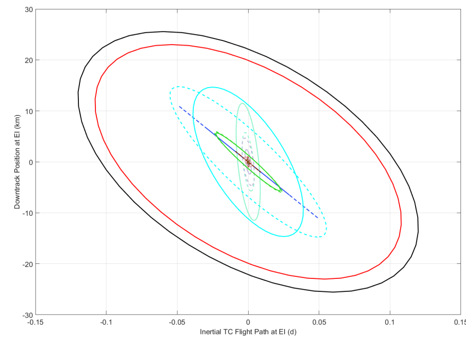

(b) Downtrack Position v. Flight Path Angle

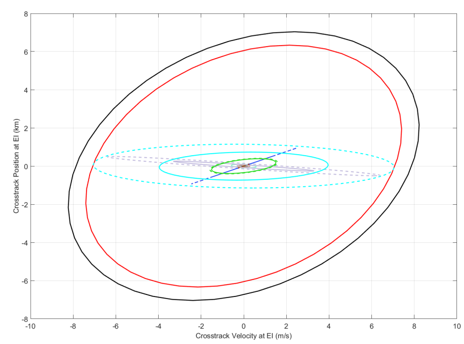

(c) Crosstrack Position v. Crosstrack Velocity

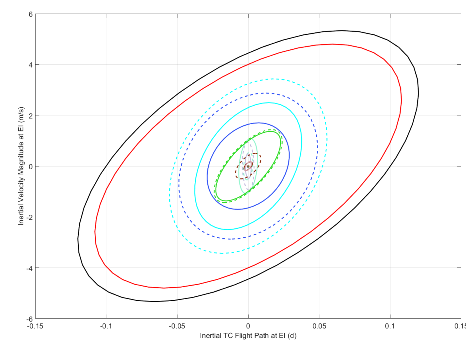

(d) Velocity Magnitude v. Flight Path Angle

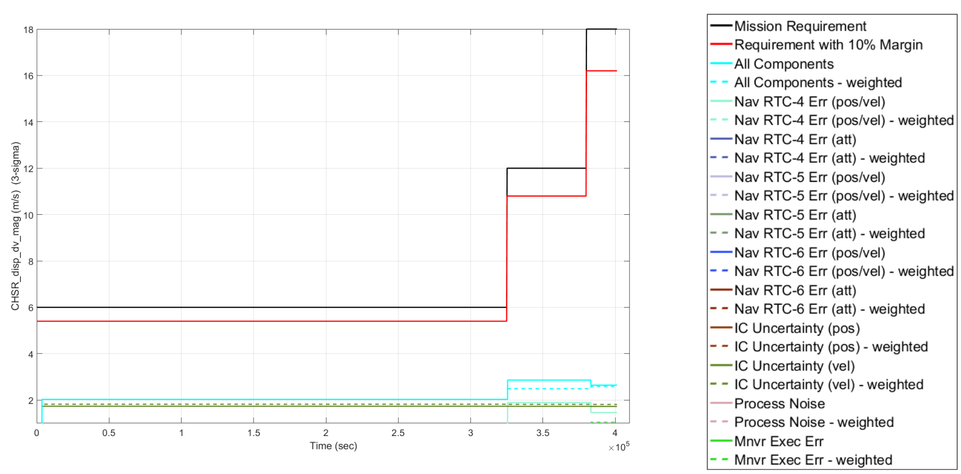

(e) Time History of $|\Delta \mathbf{V}|$ Dispersions

Figure 4.17 : Return Trajectory - Flight Readiness Altered

4.5.4 Lunar Return - Cost Function Altered

The same trends for the optimal GN&C subsystem performance requirements exist between the baseline and cost function altered cases for the lunar return trajectory as for the lunar outbound case. Principally, there is no difference between the derived requirements for the baseline and cost function altered cases. Additionally the survivability altered and flight readiness altered cases for both cost functions yield the same GN&C performance requirements. The only indication that the second cost function has a unique affect on the derivation of optimal performance requirements is observed when survivability and flight readiness conditions are altered simultaneously. The differences are minimal and only affect the maneuver execution error requirement and the position and velocity navigation requirements at RTC-5.

Error Variable	**Init Value (3σ)**	**Weight**	**Rqmnt (3σ)**
RTC4 Nav Err, Pos (km)	2.50	0.50	1.25
RTC4 Nav Err, Vel (m/s)	0.25	0.50	0.13
RTC4 Nav Err, Att (deg)	0.50	3.00	1.50
RTC5 Nav Err, Pos (km)	1.00	1.91	1.91
RTC5 Nav Err, Vel (m/s)	0.10	1.91	0.19
RTC5 Nav Err, Att (deg)	0.50	3.00	1.50
RTC6 Nav Err, Pos (km)	0.50	0.59	0.29
RTC6 Nav Err, Vel (m/s)	0.05	0.59	0.03
RTC6 Nav Err, Att (deg)	0.50	3.00	1.50
IC Uncertainty, Pos (km)	50.00	9.55	477.00
IC Uncertainty, Vel (m/s)	1.00	0.50	0.50
Process Noise (m/s/$\sqrt{s}$)	1.50e-4	10	1.50e-3
Manuever Exec Err (m/s)	0.10	0.50	0.05

Table 4.13 : Cost Function Altered GN&C Subsystem Requirements - Return

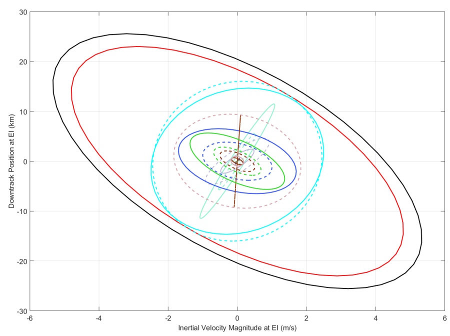

(a) Downtrack Position v. Velocity Magnitude

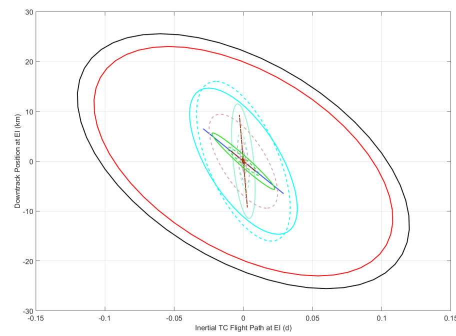

(b) Downtrack Position v. Flight Path Angle

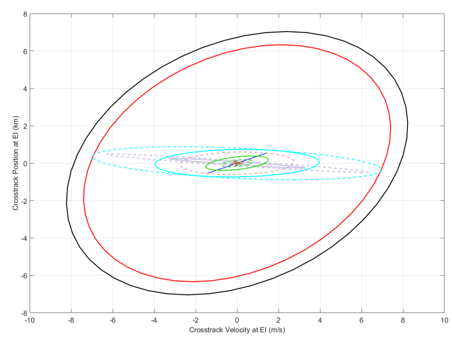

(c) Crosstrack Position v. Crosstrack Velocity

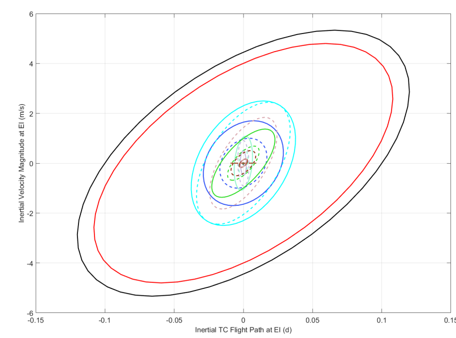

(d) Velocity Magnitude v. Flight Path Angle

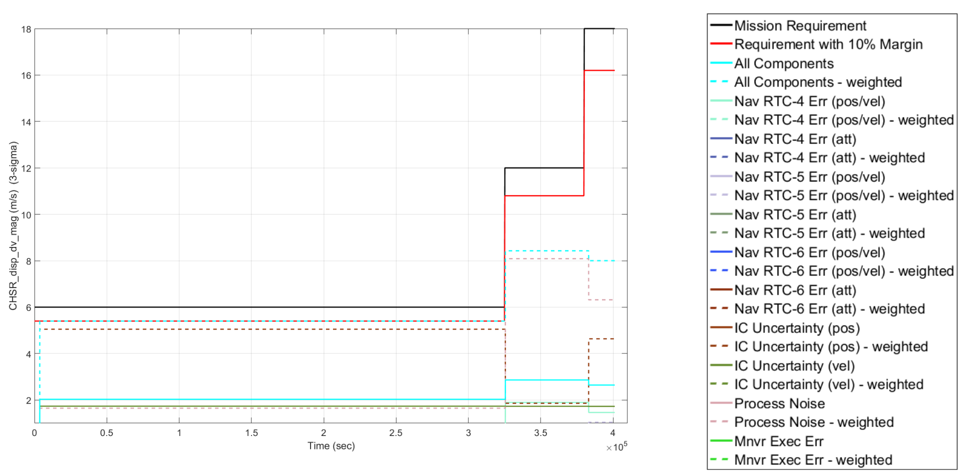

(e) Time History of $|\Delta \mathbf{V}|$ Dispersions

Figure 4.18 : Return Trajectory - Cost Function Altered

4.5.5 Lunar Return - Summary

The summary Tables 4.14 and 4.15 provide a quick reference to compare the derived requirements from one case to another. They give an idea of the sensitivity that each alteration has in the process of optimizing the GN&C subsystem performance requirements.

Error Variable	**Baseline**	**Survivability Altered**	**Flight Readiness Altered**	**Cost Function Altered**
RTC4 Nav Err, Pos (km)	1.25	1.25 (+0.00%)	1.25 (+0.00%)	1.25 (+0.00%)
RTC4 Nav Err, Vel (m/s)	0.13	0.13 (+0.00%)	0.13 (+0.00%)	0.13 (+0.00%)
RTC4 Nav Err, Att (deg)	1.50	1.50 (+0.00%)	1.50 (+0.00%)	1.50 (+0.00%)
RTC5 Nav Err, Pos (km)	1.91	5.40 (+182.72%)	1.94 (+1.57%)	1.91 (+0.00%)
RTC5 Nav Err, Vel (m/s)	0.19	0.54 (+182.72%)	0.19 (+1.57%)	0.19 (+0.00%)
RTC5 Nav Err, Att (deg)	1.50	1.50 (+0.00%)	1.50 (+0.0%)	1.50 (+0.00%)
RTC6 Nav Err, Pos (km)	0.29	2.67 (+808.16%)	0.85 (+187.41%)	0.29 (+0.00%)
RTC6 Nav Err, Vel (m/s)	0.03	0.27 (+808.16%)	0.09 (+187.41%)	0.03 (+0.00%)
RTC6 Nav Err, Att (deg)	1.50	1.50 (+0.00%)	1.50 (+0.00%)	1.50 (+0.00%)
IC Uncertainty, Pos (km)	477.00	477.00 (+0.00%)	52.50 (-88.99%)	477.00 (+0.00%)
IC Uncertainty, Vel (m/s)	0.50	0.50 (+0.00%)	1.05 (+110.00%)	0.50 (+0.00%)
Process Noise (m/s/$\sqrt{s}$)	1.50e-3	1.50e-3 (+0.00%)	1.57e-4 (-89.53%)	1.50e-3 (+0.00%)
Manuever Exec Err (m/s)	0.05	0.05 (+0.00%)	0.11 (+110.00%)	0.05 (+0.00%)

Table 4.14 : Return Trajectory Summary Table 1 of 2

Error Variable	Baseline	Surv & FR Altered	Surv & CF Altered	FR & CF Altered	Surv, FR, and CF Altered
RTC4 Nav Err, Pos (km)	1.25	1.25 (+0.00%)	1.25 (+0.00%)	1.25 (+0.00%)	1.25 (+0.00%)
RTC4 Nav Err, Vel (m/s)	0.13	0.13 (+0.00%)	0.13 (+0.00%)	0.13 (+0.00%)	0.13 (+0.00%)
RTC4 Nav Err, Att (deg)	1.50	1.50 (+0.00%)	1.50 (+0.00%)	1.50 (+0.00%)	1.50 (+0.00%)
RTC5 Nav Err, Pos (km)	1.91	5.41 (+183.25%)	5.40 (+182.72%)	1.94 (+1.57%)	5.42 (+183.77%)
RTC5 Nav Err, Vel (m/s)	0.19	0.54 (+183.25%)	0.54 (+182.72%)	0.19 (+1.57%)	0.54 (+183.77%)
RTC5 Nav Err, Att (deg)	1.50	1.50 (+0.00%)	1.50 (+0.00%)	1.50 (+0.00%)	1.50 (+0.00%)
RTC6 Nav Err, Pos (km)	0.29	2.79 (+848.98%)	2.67 (+808.16%)	0.85 (+187.41%)	2.79 (+848.98%)
RTC6 Nav Err, Vel (m/s)	0.03	0.28 (+848.98%)	0.27 (+808.16%)	0.09 (+187.41%)	0.28 (+848.98%)
RTC6 Nav Err, Att (deg)	1.50	1.50 (+0.00%)	1.50 (+0.00%)	1.50 (+0.00%)	1.50 (+0.00%)
IC Uncertainty, Pos (km)	477.00	52.50 (-88.99%)	477.00 (+0.00%)	52.50 (-88.99%)	52.50 (-88.99%)
IC Uncertainty, Vel (m/s)	0.50	1.05 (+110.00%)	0.50 (+0.00%)	1.05 (+110.00%)	1.05 (+110.00%)
Process Noise (m/s/$\sqrt{s}$)	1.50e-3	1.57e-4 (-89.53%)	1.5-0e-3 (+0.00%)	1.57e-4 (-89.53%)	1.57e-4 (-89.53%)
Manuever Exec Err (m/s)	0.05	0.11 (+110.00%)	0.05 (+0.00%)	0.11 (+110.00%)	0.10 (+90.00%)

Table 4.15 : Return Trajectory Summary Table 2 of 2

Chapter 5

Concluding Remarks

5.1 Overview

This thesis has demonstrated the versatility of a novel, systematic approach for deriving optimal GN&C subsystem performance requirements for both a lunar outbound and a lunar return flight segment. These performance requirements have been generated given multiple mission requirements and performance constraints, different optimization criteria, and varying phases in the design process. Specifically, eight different combinations of altering the survivability requirements, the flight readiness of the simulated system, and the optimization cost function have been analyzed and compared. The database of optimal GN&C performance requirements that have been created provides an in-depth analysis of the effect and sensitivity of tweaking various parameters for the optimal derivation.

5.2 Potential for Future Work

The next step in the discussed work may be to use the optimally derived GN&C performance requirements to choose an optimal sensor suite for the mission profiles. These performance requirements indicate how accurately the GN&C system must perform to ultimately meet mission requirements. Therefore, the user can match the expected performance of a given sensor suite to the derived requirement.

To further increase the versatility of this approach, it can be applied to mission requirements other than ellipses and time histories. Specifically, the capability of using polygon requirements for square, rectangular, or other shaped corridors is desired.

A third consideration for future study of this concept is to optimize the design space. Ideally, the error source ellipse fills the entire mission requirement ellipse. This can be done through linearizing the problem introduced in Chapter 3 of using the eigenvalues of the transformed, rotated performance ellipse in the optimization $\mathbf{A}$ matrix. Other methods, including exploring different cost functions, can be pursued to increase the area of the RSS, performance ellipse within the mission requirements, optimizing the design space.

Appendix A

5.3 Additional Cases Run for Reference

5.3.1 Lunar Outbound Scenario

Survivability and Flight Readiness Altered

Error Variable	Init Value (3σ)	Weight	Rqmnt (3σ)
OTC1 Nav Err, Pos (km)	2.50	3.15	7.86
OTC1 Nav Err, Vel (m/s)	0.25	3.15	0.79
OTC1 Nav Err, Att (deg)	0.50	3.00	1.50
OTC2 Nav Err, Pos (km)	1.00	0.50	0.50
OTC2 Nav Err, Vel (m/s)	0.10	0.50	0.05
OTC2 Nav Err, Att (deg)	0.50	3.00	1.50
OTC3 Nav Err, Pos (km)	0.50	4.77	2.39
OTC3 Nav Err, Vel (m/s)	0.05	4.77	0.24
OTC3 Nav Err, Att (deg)	0.50	3.00	1.50
OTC4 Nav Err, Pos (km)	0.38	4.74	1.78
OTC4 Nav Err, Vel (m/s)	0.04	4.74	0.18
OTC4 Nav Err, Att (deg)	0.50	3.00	1.50
IC Uncertainty, Pos (km)	50.00	0.95	47.50
IC Uncertainty, Vel (m/s)	1.00	0.95	0.95
Process Noise (m/s/$\sqrt{s}$)	1.50e-4	0.95	1.42e-4
Manuever Exec Err (m/s)	0.10	0.95	0.10

Table 5.1 : Surv and FR Altered GN&C Subsystem Requirements - Outbound

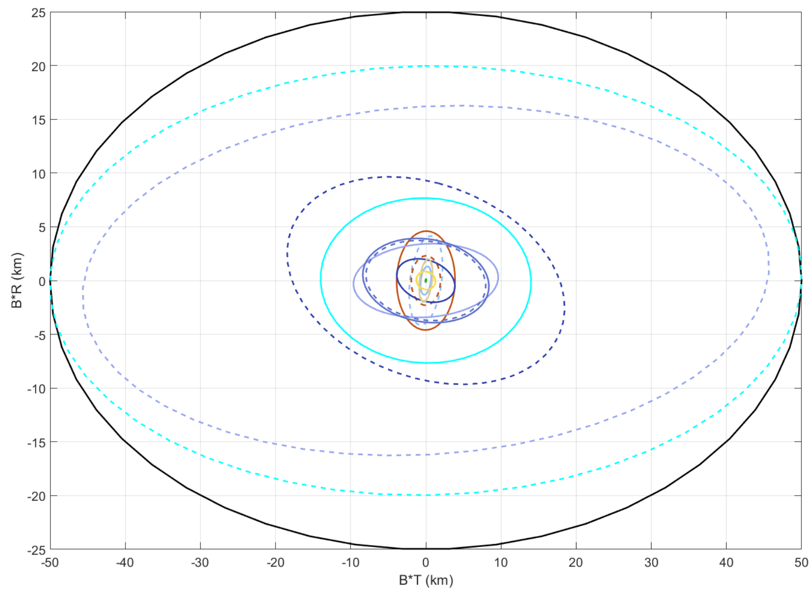

(a) B-Plane Dispersions

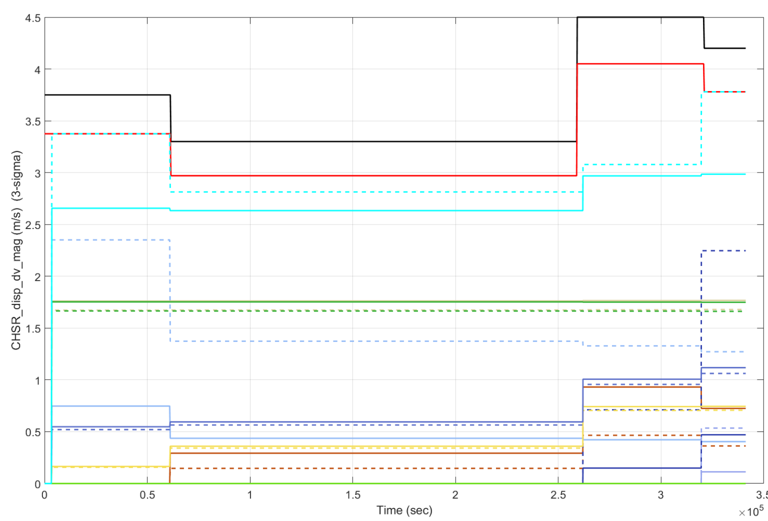

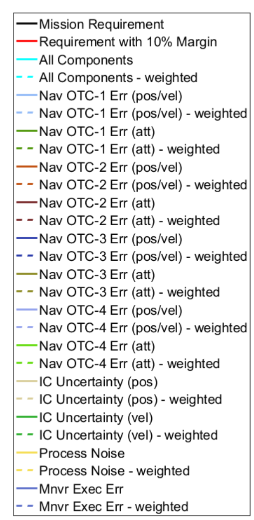

(b) Time History of $|\Delta \mathbf{V}|$ Dispersions **(c)** Legend

Figure 5.1 : Outbound Trajectory - Surv and FR Altered

Survivability and Cost Function Altered

Error Variable	Init Value (3σ)	Weight	Rqmnt (3σ)
OTC1 Nav Err, Pos (km)	2.50	0.50	1.25
OTC1 Nav Err, Vel (m/s)	0.25	0.50	0.13
OTC1 Nav Err, Att (deg)	0.50	3.00	1.50
OTC2 Nav Err, Pos (km)	1.00	0.50	0.50
OTC2 Nav Err, Vel (m/s)	0.10	0.50	0.05
OTC2 Nav Err, Att (deg)	0.50	3.00	1.50
OTC3 Nav Err, Pos (km)	0.50	7.33	3.66
OTC3 Nav Err, Vel (m/s)	0.05	7.33	0.37
OTC3 Nav Err, Att (deg)	0.50	3.00	1.50
OTC4 Nav Err, Pos (km)	0.38	4.29	1.61
OTC4 Nav Err, Vel (m/s)	0.04	4.29	0.16
OTC4 Nav Err, Att (deg)	0.50	3.00	1.50
IC Uncertainty, Pos (km)	50.00	0.50	25.00
IC Uncertainty, Vel (m/s)	1.00	0.50	0.50
Process Noise (m/s/$\sqrt{s}$)	1.50e-4	0.50	7.50e-5
Manuever Exec Err (m/s)	0.10	0.50	0.05

Table 5.2 : Surv and CF Altered GN&C Subsystem Requirements - Outbound

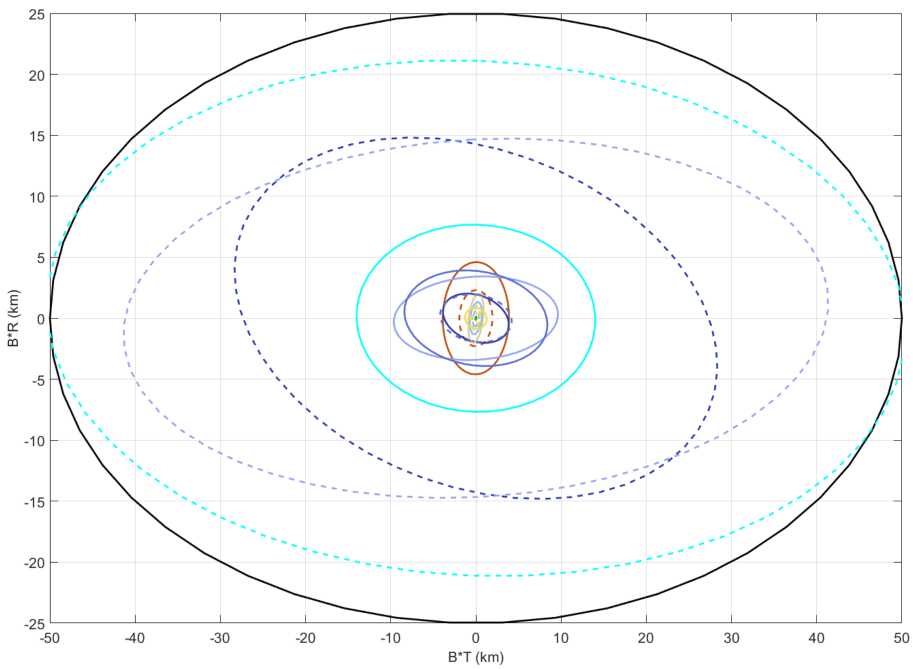

(a) B-Plane Dispersions

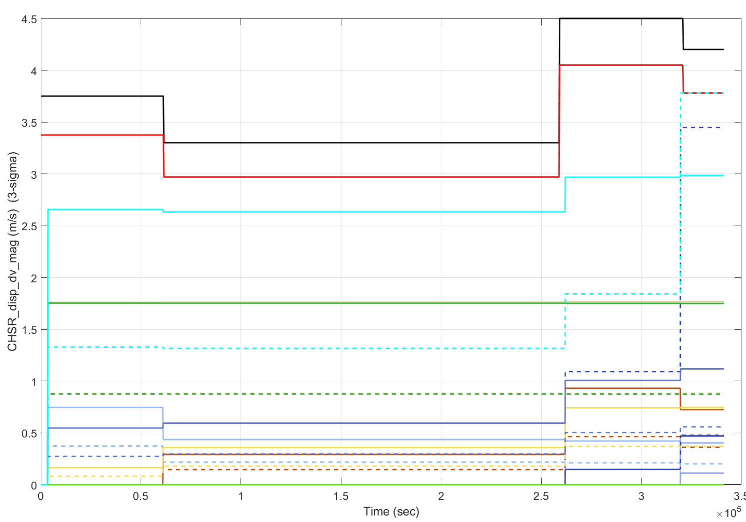

(b) Time History of $|\Delta \mathbf{V}|$ Dispersions

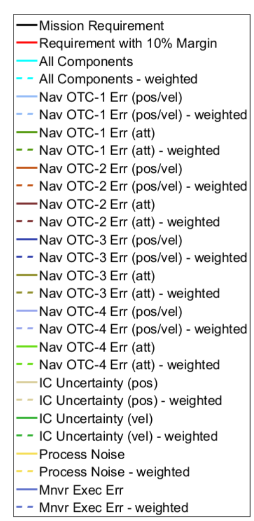

(c) Legend

Figure 5.2 : Outbound Trajectory - Surv and CF Altered

Flight Readiness and Cost Function Altered

Error Variable	Init Value (3σ)	Weight	Rqmnt (3σ)
OTC1 Nav Err, Pos (km)	2.50	3.14	7.86
OTC1 Nav Err, Vel (m/s)	0.25	3.14	0.79
OTC1 Nav Err, Att (deg)	0.50	3.00	1.50
OTC2 Nav Err, Pos (km)	1.00	0.50	0.50
OTC2 Nav Err, Vel (m/s)	0.10	0.50	0.05
OTC2 Nav Err, Att (deg)	0.50	3.00	1.50
OTC3 Nav Err, Pos (km)	0.50	2.94	1.47
OTC3 Nav Err, Vel (m/s)	0.05	2.94	0.14
OTC3 Nav Err, Att (deg)	0.50	3.00	1.50
OTC4 Nav Err, Pos (km)	0.38	0.50	0.19
OTC4 Nav Err, Vel (m/s)	0.04	0.50	0.02
OTC4 Nav Err, Att (deg)	0.50	3.00	1.50
IC Uncertainty, Pos (km)	50.00	0.95	47.50
IC Uncertainty, Vel (m/s)	1.00	0.95	0.95
Process Noise (m/s/$\sqrt{s}$)	1.50e-4	1.05	1.57e-4
Manuever Exec Err (m/s)	0.10	0.95	0.10

Table 5.3 : FR and CF Altered GN&C Subsystem Requirements - Outbound

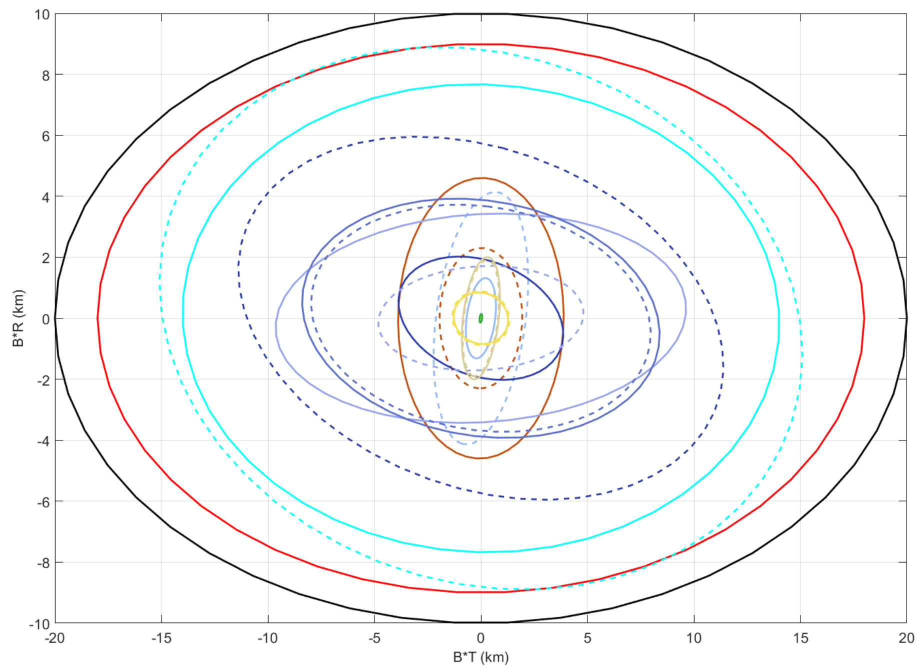

(a) B-Plane Dispersions

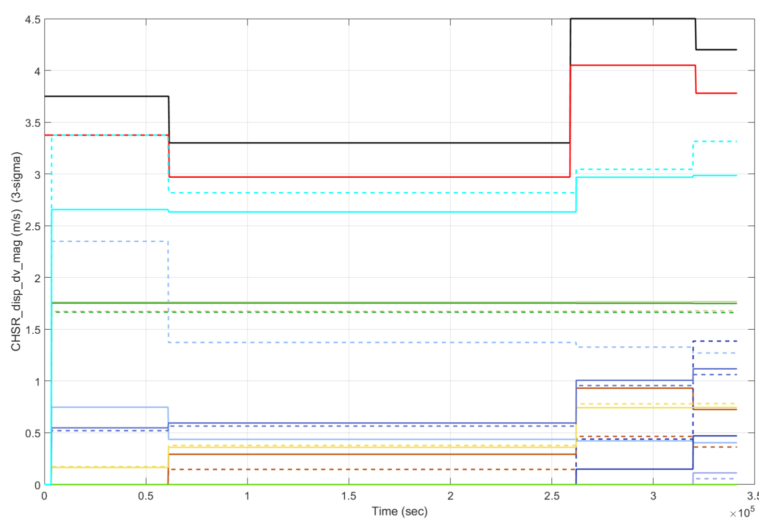

(b) Time History of $|\Delta \mathbf{V}|$ Dispersions

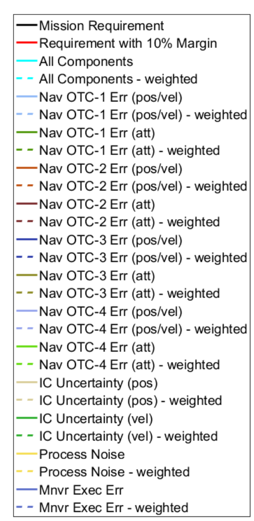

(c) Legend

Figure 5.3 : Outbound Trajectory - FR and CF Altered

Survivability, Flight Readiness, and Cost Function Altered

Error Variable	**Init Value (3σ)**	**Weight**	**Rqmnt (3σ)**
OTC1 Nav Err, Pos (km)	2.50	0.50	1.25
OTC1 Nav Err, Vel (m/s)	0.25	0.50	0.13
OTC1 Nav Err, Att (deg)	0.50	3.00	1.50
OTC2 Nav Err, Pos (km)	1.00	0.50	0.50
OTC2 Nav Err, Vel (m/s)	0.10	0.50	0.05
OTC2 Nav Err, Att (deg)	0.50	3.00	1.50
OTC3 Nav Err, Pos (km)	0.50	5.47	2.74
OTC3 Nav Err, Vel (m/s)	0.05	5.47	0.27
OTC3 Nav Err, Att (deg)	0.50	3.00	1.50
OTC4 Nav Err, Pos (km)	0.38	4.63	1.74
OTC4 Nav Err, Vel (m/s)	0.04	4.63	0.17
OTC4 Nav Err, Att (deg)	0.50	3.00	1.50
IC Uncertainty, Pos (km)	50.00	0.95	47.50
IC Uncertainty, Vel (m/s)	1.00	0.95	0.95
Process Noise (m/s/$\sqrt{s}$)	1.50e-4	0.95	1.42e-4
Manuever Exec Err (m/s)	0.10	0.95	0.10

Table 5.4 : Surv, FR, and CF Altered GN&C Subsystem Requirements - Outbound

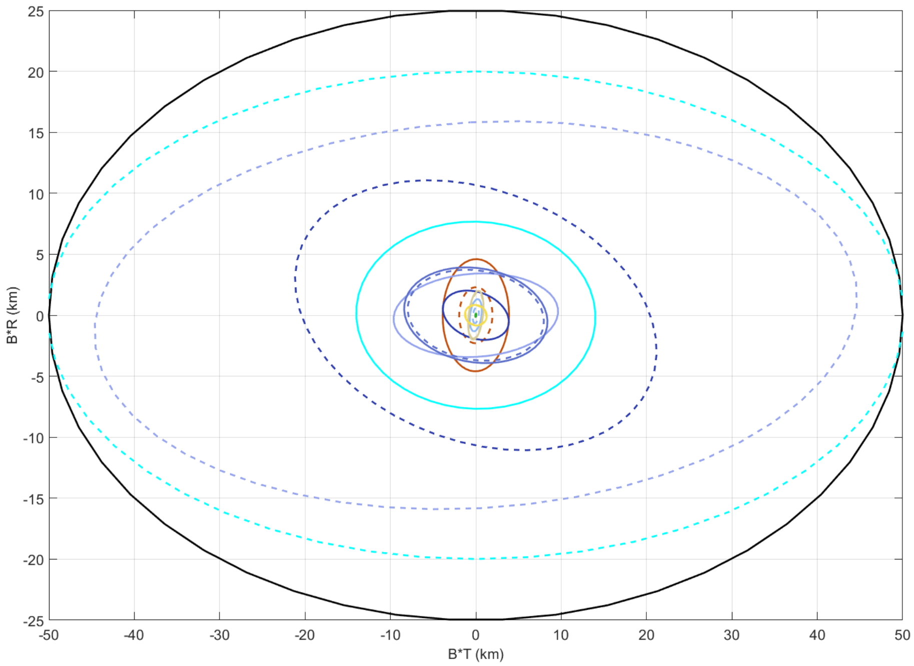

(a) B-Plane Dispersions

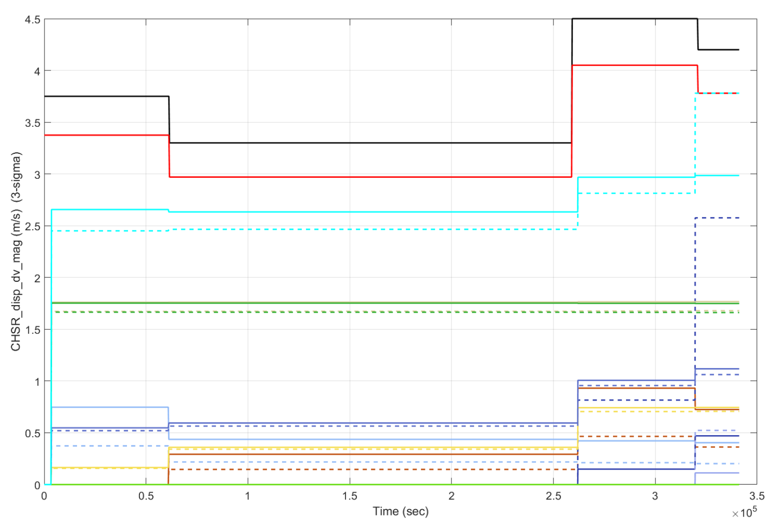

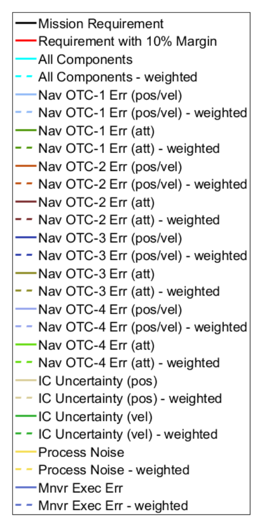

(b) Time History of $|\Delta \mathbf{V}|$ Dispersions **(c)** Legend

Figure 5.4 : Outbound Trajectory - Surv, FR, and CF Altered

5.3.2 Lunar Return Scenario

Survivability and Flight Readiness Altered

Error Variable	Init Value (3σ)	Weight	Rqmnt (3σ)
RTC4 Nav Err, Pos (km)	2.50	0.50	1.25
RTC4 Nav Err, Vel (m/s)	0.25	0.50	0.13
RTC4 Nav Err, Att (deg)	0.50	3.00	1.50
RTC5 Nav Err, Pos (km)	1.00	5.41	5.41
RTC5 Nav Err, Vel (m/s)	0.10	5.41	0.54
RTC5 Nav Err, Att (deg)	0.50	3.00	1.50
RTC6 Nav Err, Pos (km)	0.50	5.58	2.79
RTC6 Nav Err, Vel (m/s)	0.05	5.58	0.28
RTC6 Nav Err, Att (deg)	0.50	3.00	1.50
IC Uncertainty, Pos (km)	50.00	1.05	52.50
IC Uncertainty, Vel (m/s)	1.00	1.05	1.05
Process Noise (m/s/$\sqrt{s}$)	1.50e-4	1.05	1.57e-4
Manuever Exec Err (m/s)	0.10	1.05	0.11

Table 5.5 : Surv and FR Altered GN&C Subsystem Requirements - Return

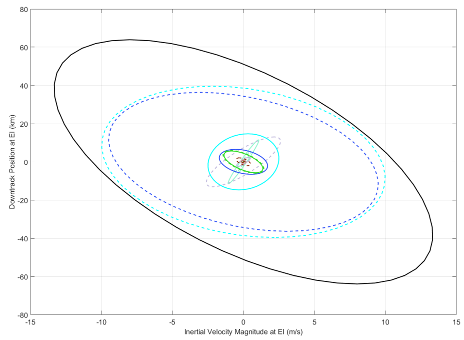

(a) Downtrack Position v. Velocity Magnitude

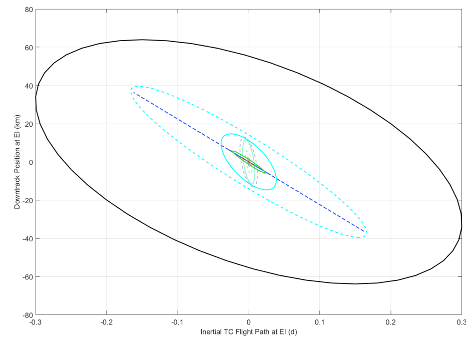

(b) Downtrack Position v. Flight Path Angle

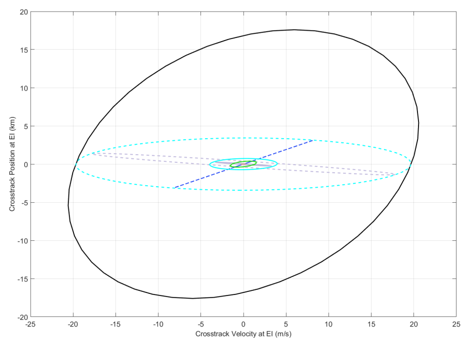

(c) Crosstrack Position v. Crosstrack Velocity

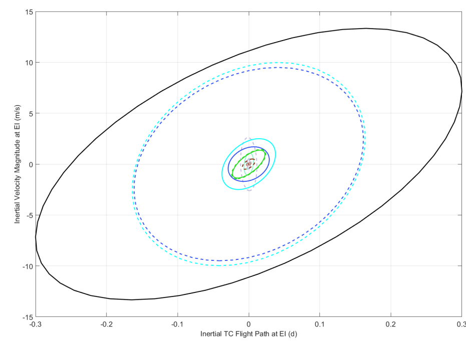

(d) Velocity Magnitude v. Flight Path Angle

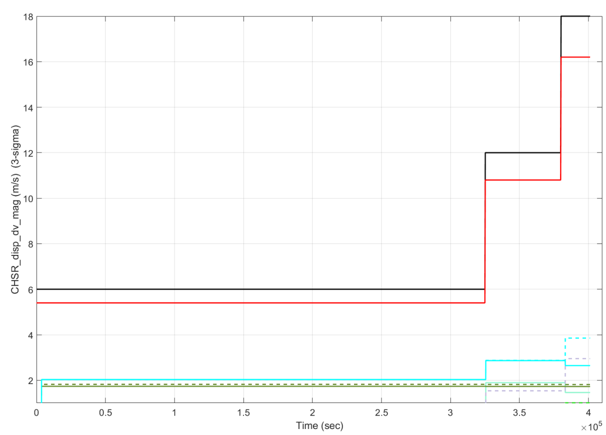

(e) Time History of $|\Delta\mathbf{V}|$ Dispersions

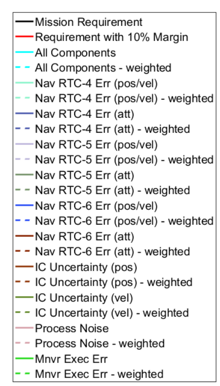

(f) Legend

Figure 5.5 : Return Trajectory - Surv and FR Altered

Survivability and Cost Function Altered

Error Variable	**Init Value (3σ)**	**Weight**	**Rqmnt (3σ)**
RTC4 Nav Err, Pos (km)	2.50	0.50	1.25
RTC4 Nav Err, Vel (m/s)	0.25	0.50	0.13
RTC4 Nav Err, Att (deg)	0.50	3.00	1.50
RTC5 Nav Err, Pos (km)	1.00	5.40	5.40
RTC5 Nav Err, Vel (m/s)	0.10	5.40	0.54
RTC5 Nav Err, Att (deg)	0.50	3.00	1.50
RTC6 Nav Err, Pos (km)	0.50	5.35	2.67
RTC6 Nav Err, Vel (m/s)	0.05	5.35	0.27
RTC6 Nav Err, Att (deg)	0.50	3.00	1.50
IC Uncertainty, Pos (km)	50.00	9.55	477.00
IC Uncertainty, Vel (m/s)	1.00	0.50	0.50
Process Noise (m/s/$\sqrt{s}$)	1.50e-4	10.00	1.50e-3
Manuever Exec Err (m/s)	0.10	0.50	0.05

Table 5.6 : Surv and CF Altered GN&C Subsystem Requirements - Return

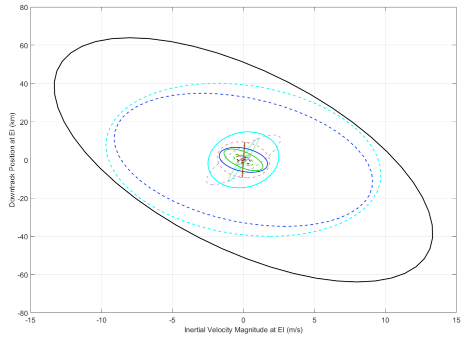

(a) Downtrack Position v. Velocity Magnitude

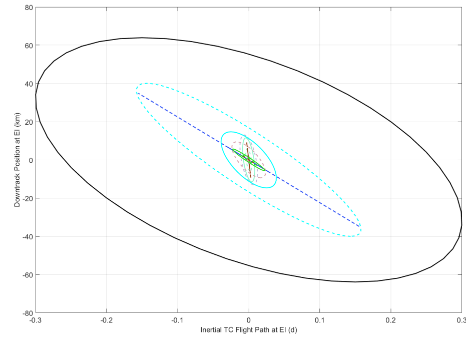

(b) Downtrack Position v. Flight Path Angle

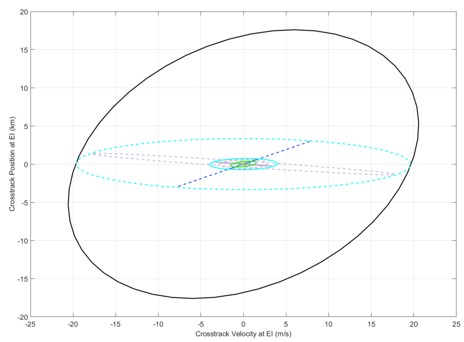

(c) Crosstrack Position v. Crosstrack Velocity

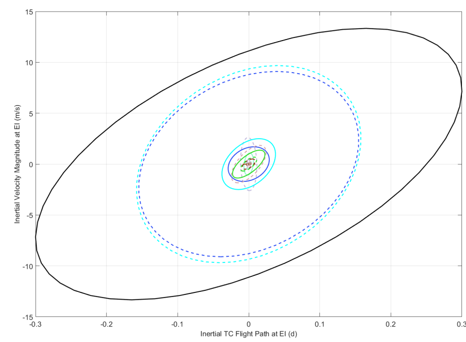

(d) Velocity Magnitude v. Flight Path Angle

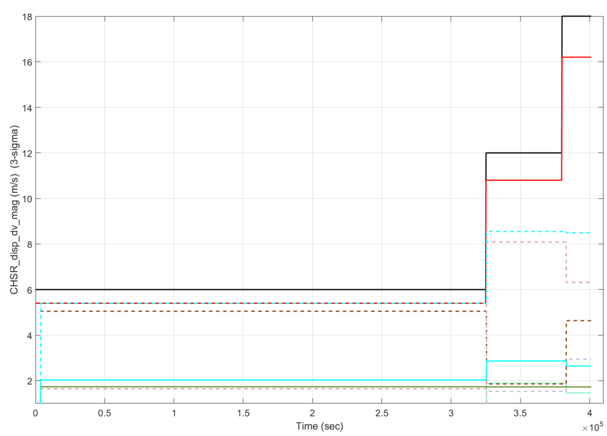

(e) Time History of $|\Delta \mathbf{V}|$ Dispersions

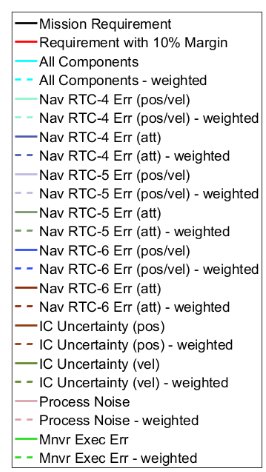

(f) Legend

Figure 5.6 : Return Trajectory - Surv and CF Altered

Flight Readiness and Cost Function Altered

Error Variable	Init Value (3σ)	Weight	Rqmnt (3σ)
RTC4 Nav Err, Pos (km)	2.50	0.50	1.25
RTC4 Nav Err, Vel (m/s)	0.25	0.50	0.13
RTC4 Nav Err, Att (deg)	0.50	3.00	1.50
RTC5 Nav Err, Pos (km)	1.00	1.94	1.94
RTC5 Nav Err, Vel (m/s)	0.10	1.94	0.19
RTC5 Nav Err, Att (deg)	0.50	3.00	1.50
RTC6 Nav Err, Pos (km)	0.50	1.69	0.85
RTC6 Nav Err, Vel (m/s)	0.05	1.69	0.09
RTC6 Nav Err, Att (deg)	0.50	3.00	1.50
IC Uncertainty, Pos (km)	50.00	1.05	52.50
IC Uncertainty, Vel (m/s)	1.00	1.05	1.05
Process Noise (m/s/$\sqrt{s}$)	1.50e-4	1.05	1.57e-4
Manuever Exec Err (m/s)	0.10	1.05	0.11

Table 5.7 : FR and CF Altered GN&C Subsystem Requirements - Return

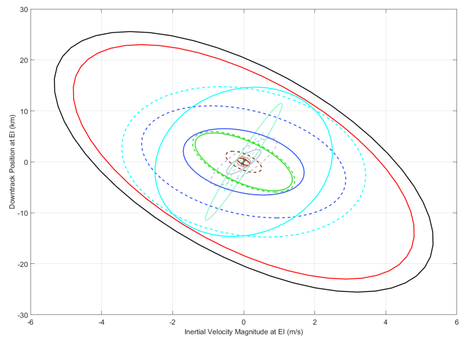

(a) Downtrack Position v. Velocity Magnitude

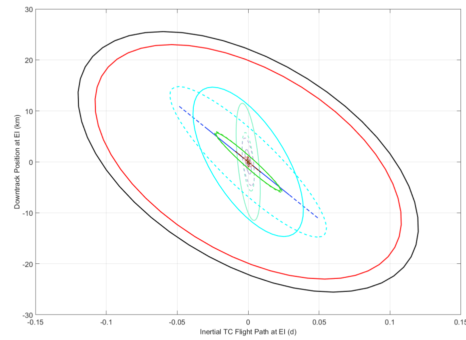

(b) Downtrack Position v. Flight Path Angle

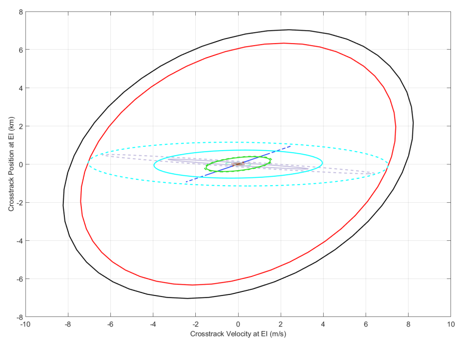

(c) Crosstrack Position v. Crosstrack Velocity

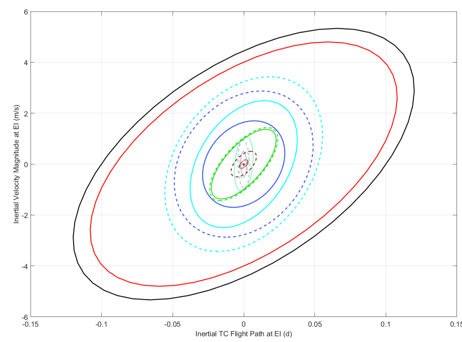

(d) Velocity Magnitude v. Flight Path Angle

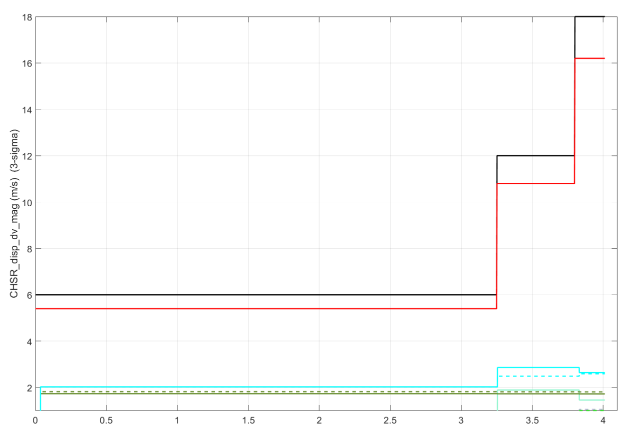

(e) Time History of $|\Delta \mathbf{V}|$ Dispersions

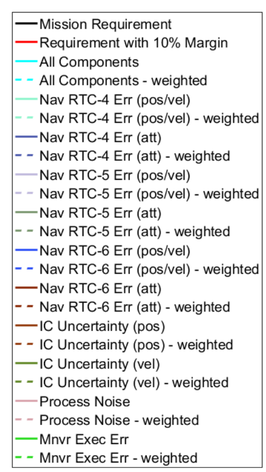

(f) Legend

Figure 5.7 : Return Trajectory - FR and CF Altered

Survivability, Flight Readiness, and Cost Function Altered

Error Variable	**Init Value (3σ)**	**Weight**	**Rqmnt (3σ)**
RTC4 Nav Err, Pos (km)	2.50	0.50	1.25
RTC4 Nav Err, Vel (m/s)	0.25	0.50	0.13
RTC4 Nav Err, Att (deg)	0.50	3.00	1.05
RTC5 Nav Err, Pos (km)	1.00	5.42	5.42
RTC5 Nav Err, Vel (m/s)	0.10	5.42	0.54
RTC5 Nav Err, Att (deg)	0.50	3.00	1.50
RTC6 Nav Err, Pos (km)	0.50	5.59	2.79
RTC6 Nav Err, Vel (m/s)	0.05	5.59	0.28
RTC6 Nav Err, Att (deg)	0.50	3.00	1.50
IC Uncertainty, Pos (km)	50.00	1.05	52.50
IC Uncertainty, Vel (m/s)	1.00	1.05	1.05
Process Noise (m/s/$\sqrt{s}$)	1.50e-4	1.05	1.57e-4
Manuever Exec Err (m/s)	0.10	0.95	0.10

Table 5.8 : Surv, FR, and CF Altered GN&C Subsystem Requirements - Return

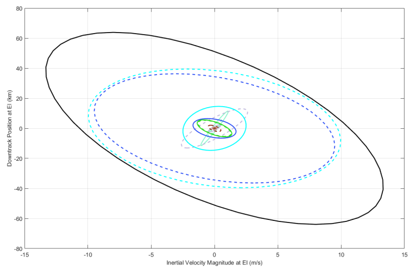

(a) Downtrack Position v. Velocity Magnitude

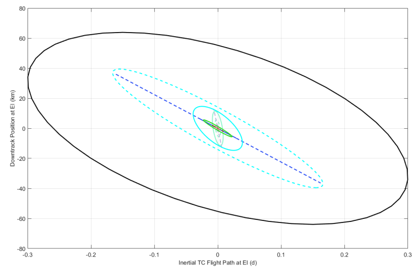

(b) Downtrack Position v. Flight Path Angle

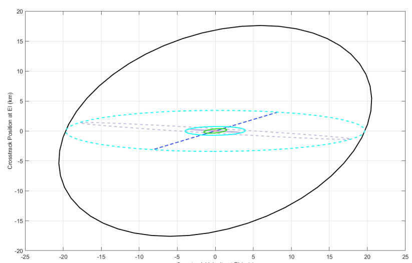

(c) Crosstrack Position v. Crosstrack Velocity

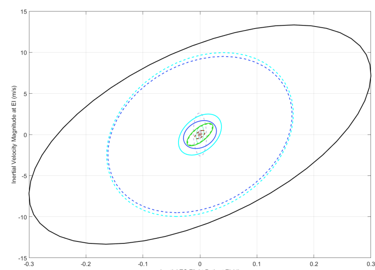

(d) Velocity Magnitude v. Flight Path Angle

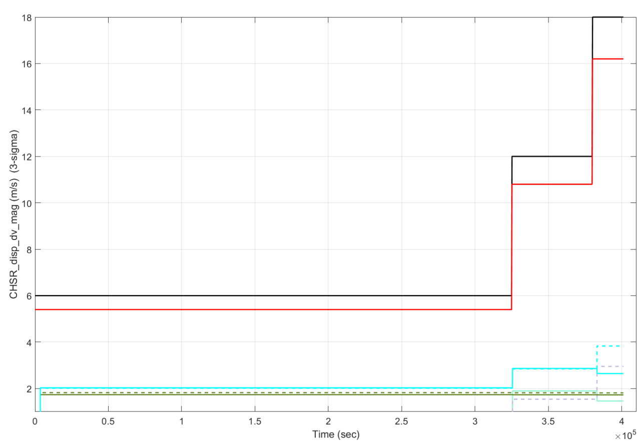

(e) Time History of $|\Delta \mathbf{V}|$ Dispersions

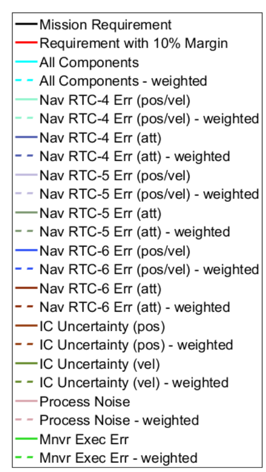

(f) Legend

Figure 5.8 : Return Trajectory - Surv, FR, and CF Altered

Bibliography

[1] W. J. Larson, et al., *Applied Space Systems Engineering.* The McGraw-Hill Companies, Inc., Boston: 2009.

[2] D. C. Woffinden and L. Breger, "Automated Derivation and Verification of Navigation Requirements for On-orbit Rendezvous," *AIAA Conference*, August 2013.

[3] J. J. Sellers et al, *Understanding Space.* The McGraw-Hill Companies, Inc., New York: 2005.

[4] *NASA Systems Engineering Handbook*, NASA, NASA/SP-2016-6105 Rev 2, 2017.

[5] D. G. Hoag, "The History of Apollo Onboard Guidance, Navigation and Control," *Journal of Guidance, Control, and Dynamics*, Vol. 6, January 1983.

[6] J. L. Goodman, "Space Shuttle Navigation in the GPS Era," United Space Alliance, LLC, 2000.

[7] H. Mamich and C. N. D'Souza, "Orion Preliminary Navigation System Design," *AIAA Conference*, August 2008.

[8] R. S. Gay, G. N. Holt, and R. Zanetti, "Orion Exploration Flight Test-1 Post-Flight Navigation Performance Assessment Relative to the Best Estimated Trajectory," AAS, 2016.

[9] J. Lazio and L. Deutsch, "The Deep Space Network at 50," *Physics Today*, American Institute of Physics, December 2014.

[10] D. M. Velez, "System Level Dispersion Analysis Examining Program Benefits to a Low-Thrust Interplanetary CubeSat from Autonomous Guidance and Navigation," Master's Thesis, MIT, August 2016.

[11] N. A. Bader "Autonomous Vision Navigation for Spacecraft in Lunar Orbit," Master's thesis, Rice University, April 2016.

[12] D. C. Woffinden, "Angles Only Navigation for Autonomous Orbital Rendezvous," Doctoral Dissertation, Utah State University, December 2008.

[13] N. Barbour and W. Howell, "Inertial Navigation System," Draper Laboratory, CSDL-P-4475, January 2007.

[14] C. S. Draper et al. "Apollo Guidance and Navigation," *Space Navigation Guidance and Control*, Vol. 1, MIT, June 1965.

[15] D. K. Geller, "Linear Covariance Techniques for Orbital Rendezvous Analysis and Autonomous Onboard Mission Planning," *Journal of Guidance, Control, and Dynamics*, Vol. 29, No. 6, November - December 2006.

[16] C. D'Souza, *Stochastic Estimation in Aerospace Navigation*. NASA JSC, December 2013.

[17] A. S. Kremer, "Linear Covariance Analysis Trade Study of Autonomous Navigation Schemes for Cislunar Missions," Master's Thesis, MIT, May 2007.

[18] K. Mand, "Rendezvous and Proximity Operations at the Earth-Mnnoon L2 Lagrange Point: Navigation Analysis for Preliminary Trajectory Design," Master's Thesis, Rice University, May 2014.

[19] C. D'Souza, G. Holt, R. Zanetti, and B. Wood, "Ground-based navigation and dispersion analysis for the Orion Exploration Mission 1," AAS 16-235, 2016.

[20] J. B. Roberts and P. D. Spanos, *Random Vibrations and Statistical Linearization*. Dover Publications, 2003.

[21] I. M. Sobol, *A Primer for the Monte Carlo Method*. CRC PRess, 1994.

[22] J. M. Hammersly and D. C. Handscomb, *Monte Carlo Methods*. Methuen & Co. Ltd., London: 1964.

[23] P. S. Maybeck, *Stochastic Models, Estimation and Control*. New York: Academic Press, August 1979.

[24] "Guidance, Navigation and Control," CBAerospace. 2014. Accessed February 27, 2018. http://www.cbaerospace.com.au.

[25] B. G. Marchand, M. W. Weeks, et al, "Onboard Autonomous Targeting for the Trans-Earth Phase of Orion," *Journal of Guidance, Control, and Dynamics*, Vol. 33, No. 3, May - June 2010.

[26] S. K. Scarritt and B. G. Marchand et al., "Finite-Burn Linear Targeting Algorithm for Autonomous Path Planning and Guidance," *Journal of Guidance, Control, and Dynamics*, Vol. 35, No. 5, September - October 2012.

[27] S. K. Scarritt, T. Fill, and S. Robinson, "Advances in Orion's On-Orbit Guidance and Targeting System Architecture," *AAS GN&C Conference*, January 2018.

[28] Y. Chou, *Statistical Analysis*, 2nd ed. Holt, Rinehart and Winston, New York: 1975.

[29] D. Woffinden, S. Bhatt, D. Kirkpatrick, and P. Spanos, "Optimal Multi-Variable Mult-Constraint Spacecraft GN&C Requirement Derivation," *AAS Conference*, January 2018.

[30] B. Noble and J. W. Daniel, *Applied Linear Algebra*, 2nd ed. Prentice-Hall, Inc., New Jersey: 1977.

[31] Y. Sisman, “A Full-Factorial Design Approach for Coordinate Transformation,” *Arabian Journal for Science & Engineering*, Vol. 39, January 2014.

[32] D. Eberly, “Intersection of Ellipses,” *Geometric Tools, LLC*, Vol. 37, No. 4, pp. 1250-1259, October 10, 2000.

[33] R. F. Stengel, *Optimal Control and Estimation*. Dover Publications Inc.: New York, 1994.

[34] A. E. Bryson, Jr., Y. Ho, *Applied Optimal Control: Optimization, Estimation, and Control*. USA: Hemisphere Publishing Corporation, 1975.

[35] “Orion System Timeline Exploration Mission Edition,” Lockheed Martin Space Systems Company, May 19, 2016.

[36] D.-H. Cho, Y. Chung, and H. Bang, “Trajectory Correction Maneuver Design Using an Improved B-Plane Targeting Method,” *Acta Astronautica*, Elsevier Ltd., 2011.

[37] “B-Plane Targeting,” Systems Tool Kit (STK). February 2018. Accessed April 3, 2018. http://help.agi.com/stk/index.htm#gator/eq-bplane.htm.

[38] C. D’Souza, “Hyperbolic (B-Plane) Parameters and Paritials for the Orion Earth-Moon Missions,” Tech. Rep. FlyDyn-CEV-15-27, National Aeronautics and Space Administration, Johnson Space Center, Engineering Directorate, July 2015.

[39] J. Rea, ”Entry Interface Accuracy Requirements for Exploration Mission Critical Design Review,” Tech. Rep. FltDyn-CEV-15-28, National Aeronautics and Space Administration, Johnson Space Center, Engineering Directorate, July 2015.